Università degli Studi di Padova

Universitá degli Studi di Padova

Dipartimento di Ingegneria Industriale

SCUOLA DI DOTTORATO DI RICERCA IN INGEGNERIA INDUSTRIALE
INDIRIZZO IN INGEGNERIA DELL'ENERGIA
CICLO XXIX

Islanded Distribution Networks Supplied by Distributed Generation

Direttore della scuola: Ch.mo Prof. Paolo Colombo
Coordinatore d'indirizzo: Ch.ma Prof.ssa Luisa Rossetto
Supervisore: Ch.mo Prof. Roberto Caldon
Co-Supervisore: Ch.mo Prof. Roberto Turri

Dottorando: Fatihe Ramadan Abusief

31 Gennaio 2017

Abstract

The modern power systems have recently increased the interest in distributed generation (DG) technologies due to, fuel cost uncertainties, environmental constraints, and increasing power consumption with shortage of transmission capacities. Distributed generation (DG) using clean and renewable energy in power supply system have attracted serious attention. Many developing countries are adopting distributed generation (DG) technologies for their power systems expansion planning. Solar Energy is one of the most promising, nonpolluting, free source of energy. The enormous development of the exploitation of renewable energy throughout the territory leads to rethink the paradigm of traditional power grid. In particular, the possibility of operating of small networks in islanded configuration in remote villages, along with several benefits that we can glimpse. In some countries, electrical distribution lines have to cross areas where the installation cost could be very high and carrying out maintenance could become extremely difficult (e.g. desert areas). As a result, frequent power disconnections and blackout heavily affect the quality of supply of end-users. Conversely, the renewable energy sources exploitation in supplying portions of the distribution network during system disconnections is very interesting, both for reducing fossil fuel use and as backup power generator. In case the islanded local electrification makes use of discontinuous and unpredictable energy sources such as photovoltaic, a Battery Energy Storage System is required to regulate the system, supplying power balance and voltage stability. This requires, however, the development of appropriate control strategies to allow a continuous balance between the load and the generation. In this thesis, a control strategy implementing Battery Energy Storage System (BESS) and PV generation plants has been developed and tested for electrification of modeled remote distribution network. In the proposed (SMO) master/slave control strategy, the BESS operates as a slack node, while PV are controlled as PQ generators. The ability of the developed control strategy to preserve energy balance and system stability was extensively investigated. To minimize the BESS size, a use of Synchronous Generators was introduced to supply base load during night period. Furthermore, for efficiency improvement of the BESS and further reduction in batteries size especially under peak load conditions, a Battery Supercapacitor Hybrid Energy Storage System (ESS) was developed and investigated.

Acknowledgements

Thank God for helping me achieve this work.
I then would like to express my sincere gratitude to my supervisors, Professor Roberto Caldon and Professor Roberto Turri for their continued guidance and encouragement throughout the period of my PhD studies. I appreciate their valuable suggestions and comments. This thesis would not be possible without their support and advice.
My appreciation is also extended to Dr. Fabio Bignucolo for his valuable suggestions.
I would like to sincerely thank my colleagues especially Massimiliano who is usually there for assistance. I would also like to thank my other colleagues, Antonino, Andrea and Riccardo for their support and valuable discussions.
I would like to express my deepest gratitude and love to my dear parents for their unlimited love and support. I pray God to bless them and reward them.
I would like to extend my gratitude to my brothers and sisters for their moral support and consistent motivation.
Finally, words alone cannot express the thanks I owe to my wife and children, their ceaseless encouragement and assistance were always a source of strength for me. To them I dedicate this work and wish them all the best.

Contents

List of Figures

List of Tables

Chapter 1

Introduction

1.1 Background and Motivation

The global population growth and industrialization lead to a rapid increase in the demand for electric energy. The IEO2016 expects a growth in global energy demand of 629 quadrillion Btu in 2020 and 815 quadrillion Btu in 2040 and an increase of 48% from 2012 to 2040. This forces the electric utilities to dramatically rise their energy generation to fulfil these requirements.
The traditional power systems comprise generation systems which utilize large centrally located power plants, transmission and sub-transmission systems to transmit bulk power quantities for long distances from generating plants to load centers, and the distribution system to feed different load types as industrial, commercial and residential loads with unidirectional power flow from generation systems to load centers. Most of the centralized power plants make use of fossil fuel to generate electricity, 70% of the generated electricity in 2012 was from fossil fuel generation technologies [1]. Only one third of the fuel energy is converted into electricity, with 20% of the generation capacity is reserved for peak demand which may be used only 5% of the time [2]. The existing transmission and distribution networks are aged and overburdened and need to be upgraded to meet growth demand requirements. Electricity generated from fossil fuel can be considered as a significant contributor in greenhouse gas emission and environment pollution. As a result of the growth of generated electricity by 2020, carbon dioxide emission is expected to increase by 35% [3]. The world today is at turn point, fossil fuel is highly consumed while reserves are depleting, oil prices are unstable and greenhouse gas pollution, which has a harmful effect on the ozone layer, is increasing along with continuous growth in energy demand. In order to overcome the negative impacts associated with the use of fossil fuel and to guarantee growth on long term bases, alternative energy sources have to be participated in the energy mix. Modern technologies provide us with distributed generation (DG) utilizing renewable energy resources.

1.2 Stand-alone Systems

Electrification of remote areas or islands through a power grid, in some cases, can be technically either impossible or extremely costly. Islanded systems making use of distributed generations (DGs) utilizing local available renewable energy sources can be a promising approach from both economic and environmental points of view. Generally, a stand-alone system may operate in grid connected or in islanded mode. In grid connected mode, the grid provides operating voltage and frequency regulation while all the DGs are called to work as grid following units to exchange power with main grid. However, in islanded mode the system control is more challenging. The system must be equipped with the suitable controllers for proper system voltage and frequency regulation. Developing and implementation of appropriate control strategy is a key factor for an islanded system operation. In case the islanded system makes use of intermitted energy sources such as photovoltaic (PV), a Battery Energy Storage System is essential for preserving system stability and balance of generation and load power. Master-slave control strategy can be considered as one of the most commonly used schemes to manage PVs integrated battery energy storage in stand-alone systems.

1.3 The case study of Libya

In this thesis, a MV distribution network for a remote typical Libyan oasis town (Al-Kufra) is addressed as a case study.
Libya is a developing country located in the middle of North Africa along a coast of $\sim 2000km$ with a population of 6.5 millions, most of them live along the coast. As many other developing countries Libya intends to implement DG technologies using renewable resources for its generation expansion planning, especially solar energy which has large availability. The entire area is $1,750,000km^2$, large part of it located in the Sahara desert which has a great rate of solar radiation [4]. According to EU scientists, because the sunlight in this area is more intense, solar photovoltaic (PV) panels in northern Africa could generate up to three times the electricity compared with similar panels in northern Europe. Figure 1.1 shows the Annual Direct Solar Irradiance in the southern EU-MENA Region. The primary energy received by each square meter of land equals $1-2$ barrels of oil per year [5].
Libya is wealthy in solar radiation income with the daily average radiation on a horizontal plane being $8.1kWh/m^2/day$ in the southern region in Al-Kufra and $7.1kWh/m^2/day$ in the coastal region [6].

1.3.1 Libyan Electricity Network Overview

The entire power sector in Libya is operated by GECOL. The General Electric Company of Libya (GECOL) is a totally government owned corporation. Most of the fossil-fuelled

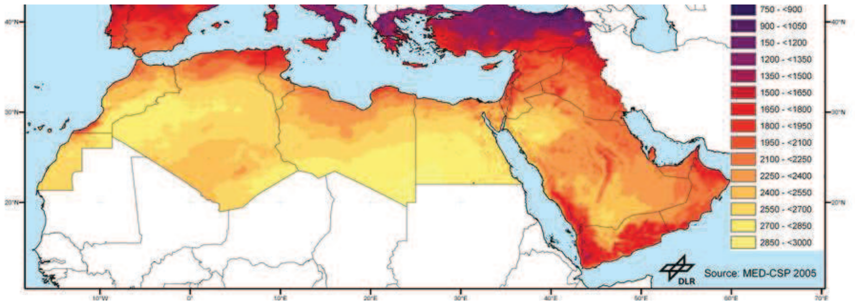

Figure 1.1: Annual Direct Solar Irradiance in the southern EU-MENA Region.

generation power plants are located along the coast as shown in figure 1.2 [4], [7].

The last registered data about the Libyan national electric grid was in 2012 listed in

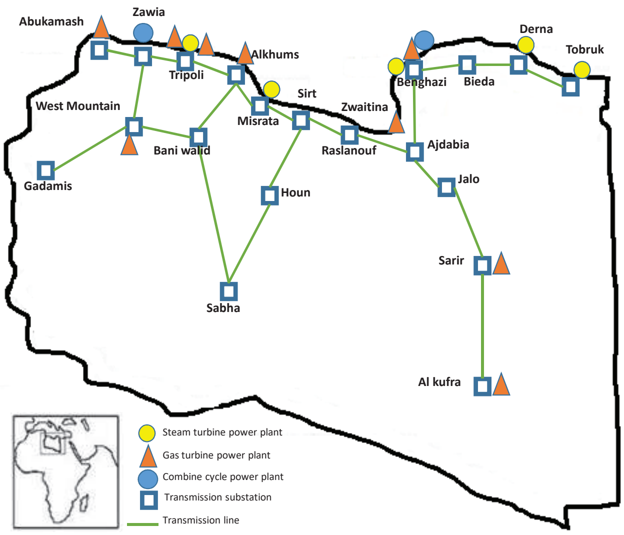

Figure 1.2: Generation power plants and Transmission lines.

GECOL's (statistics 2012) report. The number of power plants classified by type of production technology along with their installed and available capacities are listed in table 1.1.

The total energy production in 2012 was $33,980GWh$ while the percentage of fuel types utilized for energy production is shown in figure 1.3 [7].

Table 1.1: Production capacities and used technology [7].

Production Technology	**Number of Units**	**Installed Capacity (MW)**	**Available Capacity (MW)**
Steam	14	1,240	590
Gas	32	4,611	3,487
Group	15	2,355	2,055
Group	12	582	225
Total	71	8,788	6,798

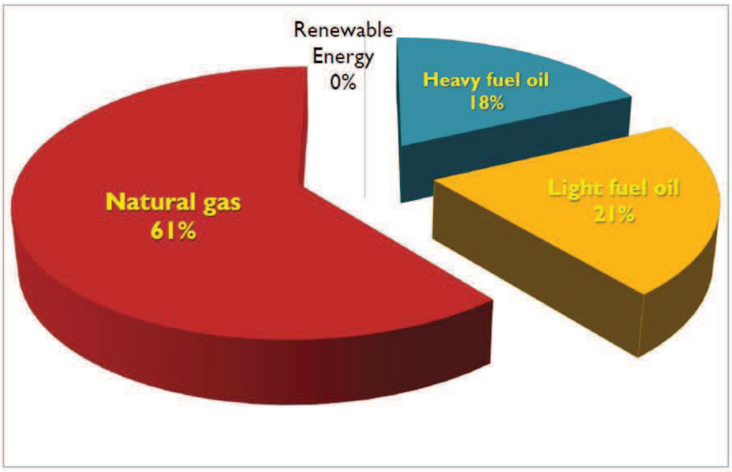

Figure 1.3: Fuel types utilized for energy production.

The transmission networks are categorized according to voltage levels into 400kV, 220kV and 132kV while the sub transmission voltage level is 66kV and the distribution systems have medium voltages of 30kV and 11kV. According to voltage levels, the total lengths and types of the lines in addition to the number of the substations and their installed capacities are listed in table 1.2.

Table 1.2: Transmission networks lines and substations [7].

Voltage Level (kV)	Overhead line (km)	Cables (km)	Number of Substations	Substations' Installed capacity (MW)
400	2290	-	13	9,600
220	13,706	154	87	19,006
66	14,311	165	195	4,359
30	11,142	5,084	461	13,914

On the other hand, the maximum load in 2012 was $5,981MW$ with electricity consumption per capita of $4,850kWh$. The electricity demand is growing rapidly with an expected peak load to be more than $8MW$ in 2020 as shown in figure 1.4 [8]. The total number of customers are categorized into five main groups with the electricity consumption per sector as reported in Figure 1.5.

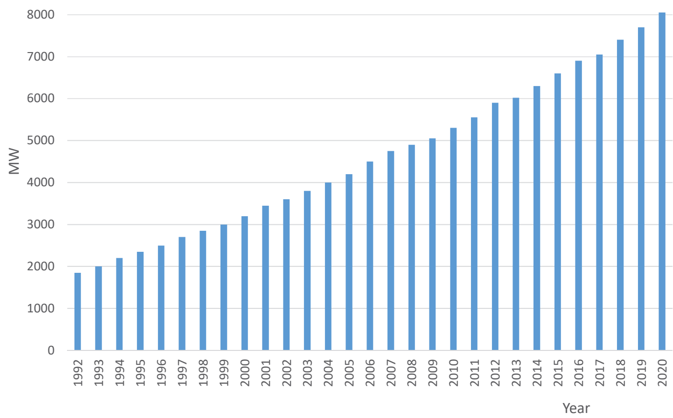

Figure 1.4: The Growth Of Peak Load from 1992-2020.

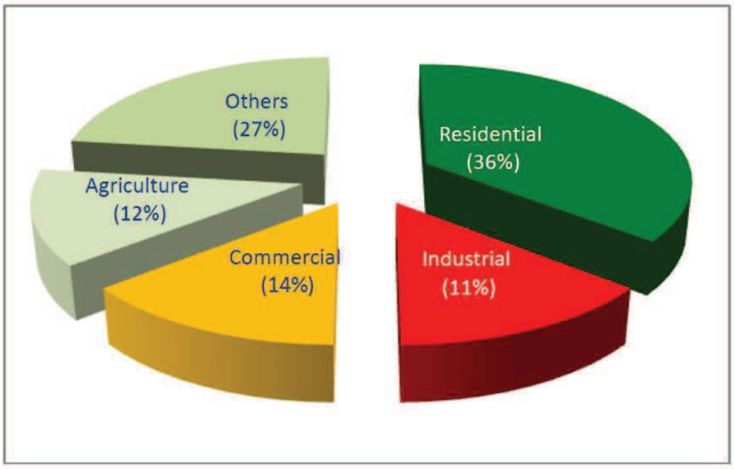

Source: General electric company of Libya (GECOL)

Figure 1.5: Electricity consumption per sector (2012).

Energy related emissions can be considered as the source of almost the total CO_2 emissions in Libya. Figure 1.6 illustrages the main sectors and their contributions in CO_2 emission.

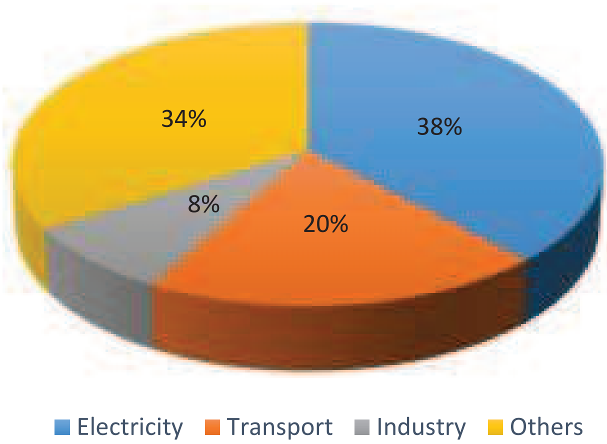

Figure 1.6: CO2 Emission by sectors.

In order to cover the growth energy demand within the environmental constraints related to greenhouse gas emissions, the Renewable Energy Authority of Libya (REAOL) has proposed the strategic plan shown in figure 1.7 [9] for developing the renewable energy utilizations in Libya (2013-2025) [9].

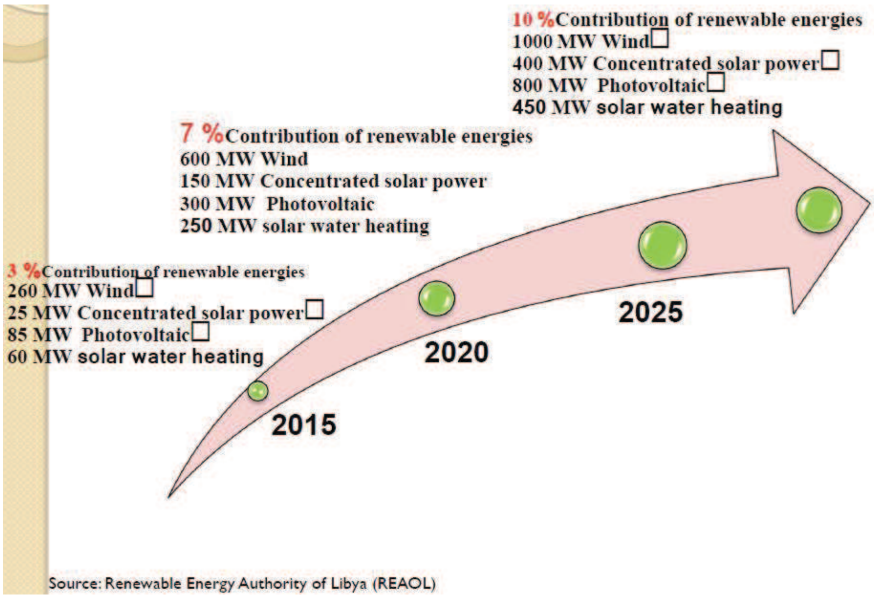

Figure 1.7: Strategic Plan for developing the Renewable Energy in Libya (2013-2025).

1.4 Aims and objectives

The objective of the thesis is to study and investigate the exploitation of renewable energy sources in supplying portions of the distribution network in grid connected mode or in islanded mode during system disconnections.

Implementation of Distributed Generation Technologies and the electrical system behavior in steady-state conditions are investigated focusing on the improvement of the network power quality levels in both grid connected and islanded modes.

A single master/slave control strategy, implementing BESS and PV generating plants, is proposed to regulate frequency and voltage in islanded mode.

The control schemes (control frames, control models and model parameters) are developed, in DIgSILENT (Power Factory) environment, both for the storage system operating as slack node and for the slave PV generator plants.

In the proposed control strategy, the BESS modulates the voltage and frequency at its point of common coupling (PCC) in order to indirectly control the PVs reference signals. The PV generation plants regulate their active power outputs depending on the reference

signal provided by the master (BESS) to bring back, within proper time response, the system frequency to its rated value after any load perturbation. On the other hand, the PV reactive power is evaluated according the reference signal provided by the BESS aiming to keep the system voltage closed to 1p.u. and reducing reactive power of the BESS to zero at steady state.
In the proposed control strategy, the BESS active power exchange with network is minimized in order to preserve BESS ability in system stabilization, also the number of charge and discharge cycles of the batteries is reduced for improvement of their life span. The proposed control strategy does not require communication channels between the master and slaves for the optimal operation of the stand-alone system since system voltage and frequency are used to coordinate BESS power exchange with PVs outputs.
In MV islanded networks the size of BESS can be relatively large and have heavily impact on the total installation cost of the system. Aiming to reduce the size of the BESS and consequently the overall installation cost, synchronous generators are introduced as another group of slaves to the proposed control strategy for supplying the base load, especially during night. The required control models are developed for the diesel generators to regulate their active and reactive power according to the frequency and voltage imposed by BESS.
In order to limit batteries' discharge under peak load conditions, getting benefit from high power density characteristic of supercapacitors, a battery-supercapacitor hybrid EES is introduced to the proposed control strategy. The hybrid EES is modeled in DIgSILENT power factory to investigate the contribution of each of the battery and supercapacitor in active power provided by the EES, where the supercapacitor provides the major part of the peak power while the battery supplies the low continuous power.
The simulations performed throughout this thesis has been carried out using the commercial software DIgSILENT power factory to demonstrate validity of the developed control models and to confirm the ability of the proposed control strategy.

1.5 The structure of the thesis

The thesis comprises six chapters. The next two chapters present literature to get the state of art of the main components and systems required for stand-alone systems making use of renewable energy sources. The later chapters provide design of the proposed control scheme, modeling of system components, simulations results, introduced improvements and conclusions.
in chapter 2, technologies for islanded network operation is discussed in two sections. The first section presents an overview of distributed generation's definition, classification and technical and environmental benefits. Some of the most common types of distributed generation technologies along with their features and suitable application are discussed. In the second section different types of electrical energy storage (EES) technologies are in-

troduced. Classification, features and characteristics of the most common types of energy storage technologies in addition to their suitable application are presented. Also comparisons between the different technologies according to the most commonly used criteria are provided in that section.

The proposed control scheme implements solar PV generation plants for supplying an islanded network, hence, chapters 3 is addressed for PV technology. In this chapter, PV basic components and theory of operation are briefly described. PV panel modeling, characteristic curves, effect of temperature and solar radiation on PV curves along with maximum power point tracking (MPPT) are illustrated.

In chapter 4, a brief technical introduction about the use and the relation between DGs, BESS and islanded networks is presented. Layout of requirements and control of islanded networks is provided. This chapter focuses on the proposed control approach's description, design and implementation, then modelling of battery energy storage system (BESS) and PV generation plants in DIgSILENT environment. Simulation results are reported in this chapter where firstly, the modeled network is identified. Secondly, simulations are carried out to investigate system behavior under steady state conditions focusing on improvement in power quality as a result of utilizing DGs technologies. Thirdly, power, frequency and voltage dynamics are analyzed through simulated load perturbations. Finally, a one-day simulations are carried out to evaluate energy balance and the ability of the proposed control scheme in managing system components behavior.

In chapter 5, the proposed amendments of the developed control approach for minimizing the BESS size and efficiency improvement are discussed in two separate steps. Firstly, synchronous generators are introduced to supply the base load during night in order to minimize the size of the BESS, where the components of the generators are modelled in DIgSILENT environment and simulation results are printed and discussed. Secondly, a battery-supercapacitor hybrid ESS is implemented with simulation and results investigations.

Chapter 6 is addressed for the general conclusions and future works.

Chapter 2

Technologies for islanded network operation

2.1 Distributed Generation Technologies

2.1.1 Introduction

The idea behind distributed generation was not completely new. Early power systems were designed in the form that all costumers are supplied by a local generation plant at or near the point of use. The electric system was composed of individual systems being built and operated by different companies with multiple but isolated generation plants [10], [11]. As an example, local grids in the US, were operated in isolation and owned by 4000 individual electric utilities [12]. Later technologies, such as economics of large-scale generation plants and emergence of AC grids, allowing transportation of large bulk of electricity over long distances, lead to construction of massive electricity systems. The developed power systems, figure 2.1 [13], comprise of central generation power plants, large transmission systems to deliver power over long distances from generating plants to load centers, and the distribution system to supply different types of consumers. In the interconnected systems the failure of one power supply can be compensated by other power plants. Large-scale interconnected power systems were both reasonably secure and economic because of their economic and reliability associated advantages. Centralized generation plants typically utilize fossil or nuclear fuel for power generation and can be located anywhere from 10s to 100s of kilometers away from load centers.

Recently, due to new technical, economic and environmental factors arise in last decades the economic and reliability advantages of traditional power systems with centralized generation plants may no longer apply [14]. Deregulation and liberalization of energy market, petroleum fuel prices uncertainty and associated environmental constraints have attracted the attention of researchers and developers to implementation of distributed generation (DG) in distribution system planning. Distributed generation (DG) is a rela-

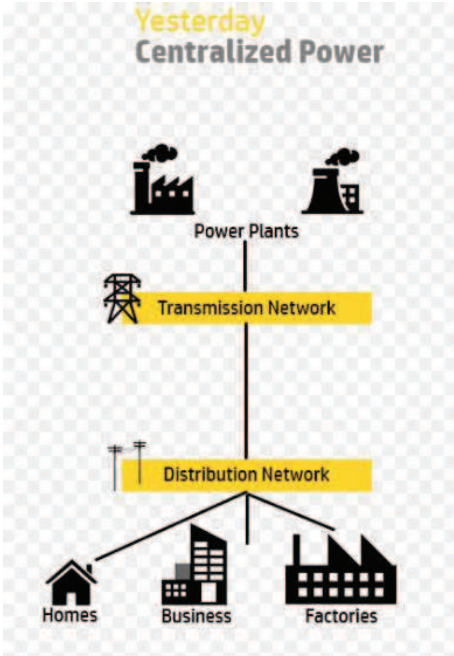

Figure 2.1: Traditional Electric Power System.

tively small power generation source sized from a few kW to $10sMW$, providing power from renewable energy or fossil energy and usually connected directly to the distribution network or connected to the network on the customer site of the meter, figure 2.2 [13].

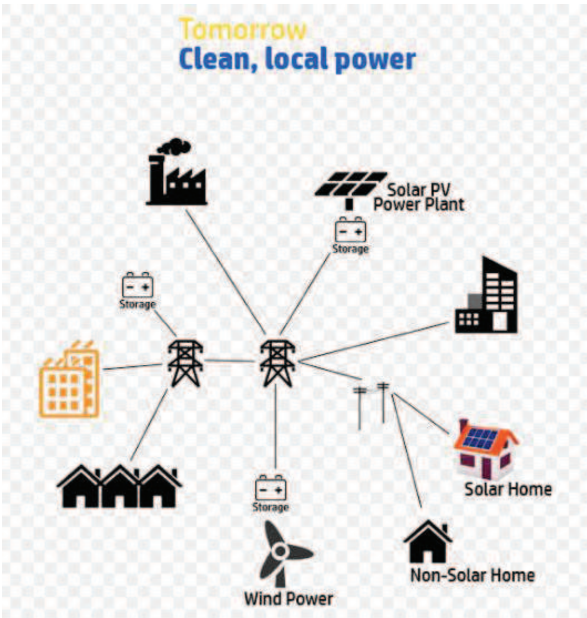

Figure 2.2: Integrated Electric Power System with Distributed Generation (DG).

2.1.2 Potential Benefits of DG Systems

The growth of DG and its integration into electric power system operation and planning was due to several technical and environmental potential benefits which are briefly discussed below.

2.1.2.1 Technical Benefits

- Efficiency improvement: DGs reduce waste in transmission of electricity from a power plant to a typical user which is about 4.2 to 8.9 percent due to transmission equipment aging, and growing congestion [15]. Simple cycle gas turbine Combined employs Heat and Power (CHP) technologies can increase the efficiency of the system by up to $70 - 80\%$ [16].

- Improving power quality: voltage variation may occur due to in proper switching operations, interruptions, and transients. DGs can help in improving power quality issues as voltage profile and reduced harmonics.

- Increasing reliability: Reliability problems refer to sustained interruptions. The Electric Power Research Institute reported that power outages and quality disturbances cost American businesses $119 billion per year. Industries such as chemicals, petroleum, and refineries, require high reliable power supply and they usually implement distributed generation technologies to ensure consistent power supplies [15].

- DGs can reduce congestion of power on transmission networks. Investments in transmission systems upgrading and expansion to meet the increased power demand can be minimized by building large number of localized DG units close to load centers [17].

- Generating power on site implementing the combined generation of heat and electricity (cogeneration technologies CHP) may result in energy conservation of 10% to 30%, compared to separate generation of heat and electricity utilizing fossil fuel [18].

- DGs location and size flexibilities can greatly effect energy prices [19].

- By supplying power to the grid, DGs can reduce the wholesale power price and help in "peak load shaving" [19], [20].

- DG can contribute in improving the security of the grid by reducing terrorist large-scale targets as nuclear power plants.

2.1.2.2 Environmental Benefits

Electricity generation plants are responsible for a significant part of greenhouse gas emission. IEO 2013 reports that world energy increases from $524 quadrillion Btu$ in 2010 to

$630 quadrillion Btu$ in 2020 and $820 quadrillion Btu$ in 2040 as illustrated in table 2.1 and figure 2.3 [21].

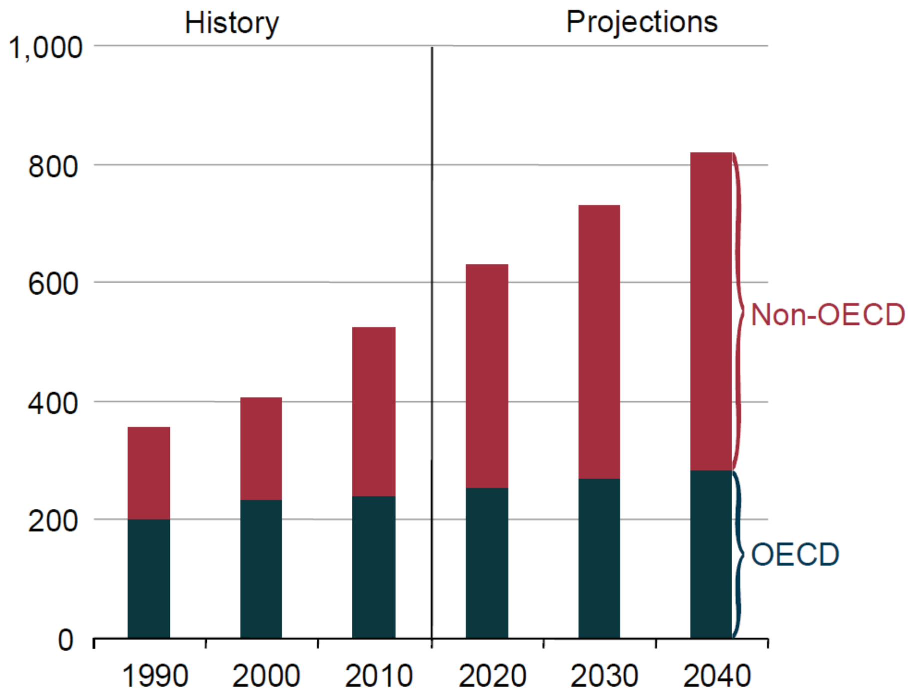

Figure 2.3: World total energy consumption, 1990-2040 (quadrillion Btu).

Note: Organization for Economic Cooperation and Development (OECD) member countries as of September 1, 2012, are the United States, Canada, Mexico, Austria, Belgium, Chile, Czech Republic, Denmark, Estonia, Finland, France, Germany, Greece, Hungary, Iceland, Ireland, Israel, Italy, Luxembourg, the Netherlands, Norway, Poland, Portugal, Slovakia, Slovenia, Spain, Sweden, Switzerland, Turkey, the United Kingdom, Japan, South Korea, Australia, and New Zealand. For statistical reporting purposes, Israel is included in OECD Europe.

Table 2.1: World energy consumption by country grouping, 2010-2040 (quadrillion Btu).

Region	**2010**	**2015**	**2020**	**2025**	**2030**	**2035**	**2040**	**Average annual percent change 2010-2040**
OECD	242	244	255	263	269	276	285	0.5
Americas	120	121	126	130	133	137	144	0.6
Europe	82	82	85	89	91	93	95	0.5
Asia	40	41	43	44	45	46	46	0.5
Non-OECD	282	328	375	418	460	501	535	2.2
Europe and Eurasia	47	50	53	57	61	65	67	1.2
Asia	159	194	230	262	290	317	337	2.5
Middle East	28	33	37	39	43	46	49	1.9
Africa	19	20	22	24	27	31	35	2.1
Central and South America	29	31	33	35	39	42	47	1.6
World	524	572	630	680	729	777	820	1.5

Environmental regulations have been adopted for minimizing CO2 emission. DGs utilizing renewable energy resources can be key factor for achieving this goal. Several policies are issued aiming to promote the development of distributed generation. In China the State Council has issued the strategy planning of energy development (2014–2020), it encourages development of renewable energy and other clean energy, minimizing utilization of coal, and promote energy structure optimization. The America proposed policies on promoting the application of distributed generation are listed in table 2.2 [22].

Table 2.2: Overall incentive policies of distributed generation in America.

Time Policies	Contents
1978 Bills of the utility regulations policies	1978 Bills of the utility regulations policies
2001IEEE-P1547/D08 “The standards draft about distributed generation interconnected with electric system”	The distributed generation systems are allowed to be connected to the grid and electricity could be sold to the grid. Part of distributed generation systems is as back-up when the grid power interruption happens.
2001 American long-term planning on developing distributed energy	By 2015,15% of nation wide existing buildings and 50% of new business and office buildings will use gas distributed energy. By 2020, the cleanest and most effective and reliable distributed energy production and delivery system will be established.
production and delivery system will be 2010 American Energy Outlook 2011(AEO2011)	From 2010 to 2020, America will increase 19.5$millionkW$ of distributed generation projects, while the proportion of distributed energy will be up to about 28%.

As illustrated in table 2.3 and table 2.4, for global environment and sustainable energy, contribution of government support, with power plants and power grid owners' active participations, in addition of positive response from consumers are required for development of distributed energy systems [22].

Table 2.3: Survey of international distributed energy policies and regulations (part 1).

Countries	Policies and regulations
The United States	• Issue regulatory bills, energy planning, a large number of investment and financing concessions and tax subsidy policies; • Propose the "CCHP" creativity and "CCHP program of 2020 years" focused on the development of natural gas distributed generation projects; • For grid connections, develop IEEE P1547/D08 "Draft on the standards of interconnection between distributed power and power system". • Therefore a guarantee mechanism of distributed energy development concluding technology, legal and economic levels has been established.
Germany	• Issue Renewable Energy Law, and it makes related regulations on power enterprises, grid enterprises, power user's behavior and pricing mechanism; • For tax subsidy policies, take different compensation proportions and subsidy decline system; • For the grid-connection, release the "Technology standards of medium-voltage distribution grid" (1–60 kV)and "Technology standards of low-voltage distribution grid" (1 kV and below), and specify thermoelectric enterprises' rights of grid connection.
Japan	• Release policies including "New energy plans", "Power career law", "New energy law" and "Energy saving law" to encourage the development of distributed energy; • Develop high depreciation and initial low tax loan policies; • Modify "Description of system grid technology elements" to solute the grid-connection security and technology problems; • Take easing policies, and establish green power trading market to advance market liberalization.

Table 2.4: Survey of international distributed energy policies and regulations (part 2).

Countries	Policies and regulations
Denmark	• Develop "Heating law" and "National gas supply law" to clarify the related legal terms and rules to encourage distributed power development; • For achieving effective government target, implement the Renewable Portfolios Standards (RPS); • For the grid-connection standards and pricing, issue the "Electricity Purchased law" and "Power supply law"; • Implement investment subsidies, tax offers, low cost financing and R&D fund policy.
Others The United Kingdom	• Make the distributed generation policies to encourage each family to have small power generation equipment. • Encourage the new built power stations to use interactive power supply; • Provide the tax exemptions and subsidies for the construction of distributed energy systems; • Propose new guidelines and new initiatives to stimulate the loads of combined heat and power.
Holland	• Enact the "Plan of environmental action" to clarify the energy-saving and emission-reduction effect of distributed energy; • Make the "Incentive plan of combined heat and power", and provide government's investment allowance. • Introduce the "Electricity Act" to force power supply departments to purchase distributed energy electricity with a minimum tax.

Despite the above mention benefits of DGs, high penetration of DGs can result in several technical challenges such as voltage fluctuations, reverse power flow [23]. DGs should be integrated to grid without any negative impacts in safety reliability and quality of supply.

2.1.3 Distributed Generation Classification and Technologies

Distributed Generation technologies can be classified based on one or more of the following categories.

- Type of primary energy source: Based on type of primary energy source, DGs can be split into two main groups which are renewable and non-renewable based DGs. Renewable energy sources are sources provide energy at a rate less than or equal to the rate at which the source is replenished [24]. Photovoltaic, wind turbines, and geothermal are some examples of renewable based DGs, whereas, internal combustion engines, micro turbines and fuel cells are examples of non-renewable based DGs.

- Output power characteristics: From the point of view of the output power, DGs can be grouped into dispatchable or non-dispatchable. The main difference between the two groups is the ability of the control of the output power based on the electric system requirments [25]. In dispatchable DGs, the output power can be evaluated by controlling the stored energy sources, whereas, in non-dispatchable DGs, the output power is a function of the availability of the primary energy sources which usually have unpredictable behaviors such as solar and wind.

- Type of connection: DGs can be either directly connected to the grid utilizing synchronous or asynchronous generators, or connected via power electronic converters. As examples of DGs with synchronous generators are IC engines, gas turbines and biomass while DGs with asynchronous generators are wind turbines. On the other hand, as examples for DGs connected through power electronic interface are photovoltaic fuel cells and wind turbines.

- Capacity of DG: DGs capacities can be divided into four groups namely micro, small, medium, and large ranging as shown in table 2.5. Module sizes of the most commonly used DGs are shown in table 2.6 [26].

- Applications: DGs can be applied in several ways for fulfilling load requirements [27]. Table 2.7 lists some applications and utilized DGs.

Table 2.5: Capacities of DGs.

Group	Power range
Micro distributed generation	$1W$–$5kW$
Small distributed generation	$5kW$–$5MW$
Medium distributed generation	$5MW$–$50MW$
Large distributed generation	$50MW$–$300MW$

Table 2.6: Distributed generation systems with modular sizes

No	DG Technology	Typical available power module size
1	Combined Cycle Gas Turbine	$35 - 400MW$
2	Internal Combustion Engines	$5kW - 10MW$
3	Combustion Turbine	$1 - 250MW$
4	Micro-Turbines	$35kW - 1MW$
5	Fuel Cells	$200kW - 2MW$
6	Battery Storage	$0.5 - 5MW$
7	Hydro power	$1 - 25MW$
8	Wind Turbine	$200W - 3MW$
9	Solar Photovoltaic power plants	$20W - 100kW$
10	Solar Thermal power plants based on central Receiver	$1 - 10MW$
11	Solar Thermal (Lutz System)	$10 - 80MW$
12	Biomass Gasification based power plants	$100kW - 20MW$
13	Geothermal	$5 - 100MW$
14	Ocean Energy	$0.1 - 1MW$

Table 2.7: Applications and utilized DGs.

Application	Description	DG Technologies
Standby	Loads such as hospitals and petrochemical industries require highly reliable supplies. DGs can be implemented to provide standby supply for these types of loads.	Traditional internal combustion engines (diesel engines)
Stand alone	distribution networks not easily connectable to grid, such as Islands and remote areas implement DGs as power providers.	Photovoltaic and Wind turbines in integration with battery energy storage systems.
Peak load shaving	Load curves have peak load periods with high price rate. DGs can be utilized to supply loads during these periods to reduce electricity cost for certain costumers.	Micro-turbines, and Traditional internal combustion engines (diesel engines).
Providing combined heat and power (CHP)	DGs with CHP technologies can provide heat and power with high efficiency to hospitals, large commercial areas, and industries.	Fuel cells.
Base load	DGs can be used to supply base load for grid support and improving system power quality.	Micro-turbines, Photovoltaic, and Wind turbines.

2.1.3.1 Internal Combustion Engine Generators (ICEs)

Internal combustion engine utilizes fuel to provide the mechanical power needed to drive the connected electrical generator. Suitable controls are associated with the engine and the electrical generator for operation in grid connected and islanded modes. Synchronous generators are usually utilized because of their ability of providing reactive power and consequently voltage regulation required for stand-alone operations. These DGs dominate the emergency or backup supplies because of the available wide size range from $1kW$ to more than $25MW$ [28], ability of fast starting, and good efficiency and reliability. A 55 kW engine generator is shown in figure 2.4 [29].
On the other hand, ICEs produce significant NOx and SOx emissions and noise pollution, and have high maintenance and fuel cost when compared to the other DG technologies [30].

Figure 2.4: A 55 kW engine generator.

2.1.3.2 Microturbines (MTs)

Microturbines are small capacity, lightweight and single staged gas turbines. They utilize different types of fuel such as natural gas, propane, and fuel oil. Micro-turbine simply comprises of the following components: compressor; combustion chamber, recuperator, small turbine, and generator. The size of individual units ranged between 25 and $500kW$ [31]. A $30kW$ oil fired MT with fuel tank is shown in figure 2.5 [32]. Individual units can be combined into systems of multiple units. MTs run at less temperature and pressure compared to traditional combustion turbines. They operate at high rotational speed ($100,000rpm$), and generate a high frequency AC power, hence, power electronic interfaces are required for connection to the grid. As a result of their low combustion temperature MTs provide less NOx emission. They also have lower noise levels compared with turbines of same sizes [33]. MTs have simple design and consequently less maintenance requirements [34]. Efficiency of a stand-alone turbine has a range of 25-40% which may be doubled with implementing CHP systems [35]. Main applications for MTs are off-grid combined heat and power (CHP) markets, standby, and peak load shaving [36].

Figure 2.5: 30 kW Oil Fired MT with Fuel tank and Filter assembly.

2.1.3.3 Fuel Cells (FCs)

A fuel cell is a device used to convert chemical energy of fuel through electrochemical process to electrical energy. A fuel cell is comprised simply of anode, cathode, and electrolyte as shown in the simple structure of figure 2.6 [37]. Unlike batteries that are energy storage devices and required recharging of their chemical energy, a fuel cell can be considered as a generation technology able to produce DC power as long as fuel is provided [35]. On another hand, it is quite different from other generating technologies which usually convert the fuel chemical energy to heat then to mechanical energy and finally to electricity, fuel cell produce electricity directly from chemical energy of fuel without combustion. Fuel cells can utilize different hydrogen rich fuels such as natural gas, biogas, methanol, ethanol, propane, and Kerosene. Characterized by the used type of the electrolyte and/or catalyst, there are different types of fuel cells being more applicable to certain distributed generation than the others. Solid oxide fuel cell (SOFC) can be applied for co-generation technology where high grade heat is required. While in other applications where heat is undesirable, low temperature fuel cells are more applicable. SOFCs have electrical efficiencies from 40-60%. The overall system efficiency can be increased to 85% by utilizing co-generation [38]. Different fuel cell technologies with their electrolytes, operating temperatures, electrical efficiencies, and energy outputs are listed in table 2.8. Absence of combustion in Fuel cell operations results in negligible harmful emissions, while, no involvement of rotating parts make FCs operate quietly and acceptable in residential areas [39]. The main challenge of FCs is the high investment cost, an entire system can have a high cost as \$4000$perkW$ [40].

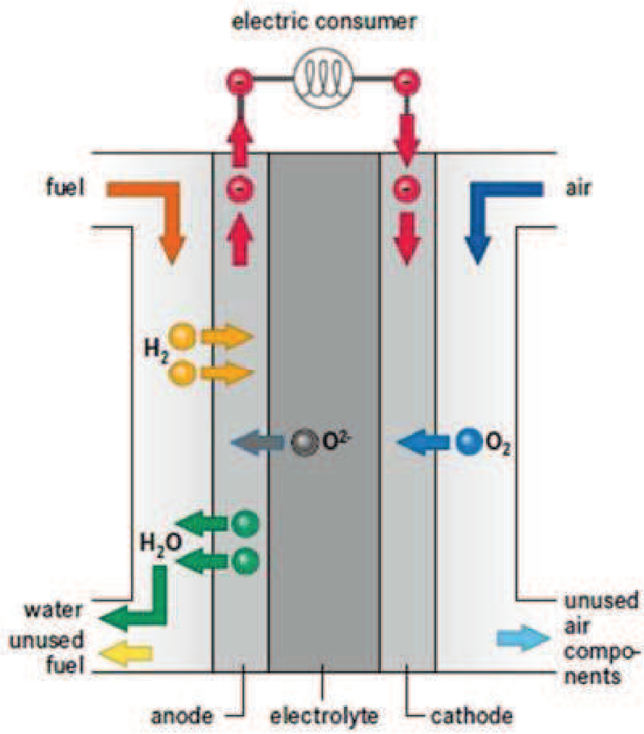

Figure 2.6: A simple structure of a fuel cell.

Table 2.8: Different fuel cell technologies and their characteristics.

Fuel Cell Tupe	**Elec-trolyte**	**Operating Tempera-ture**	**Electrical Efficiency**	**Energy Output**
AFC Alkaline Fuel Cell	Potassium hydroxide solution	Room tem-perature to 90°C	60 – 70%	$300W$ – $5kW$
PEMFC Proton Exchange Membrane Fuel Cell	Proton Echange Membrane	Room tem-perature to 80°C	40 – 60%	$1kW$
DMFC Dirct Methanol Fuel Cell	Proton Echange Membrane	Room tem-perature to 130°C	20 – 30%	$1kW$
PAFC Phosphoric Acid Fuel Cell	Phosphoric Acid	160 to 220°C	55%	$200kW$
MCFC Molten Carbonate Fuel Cell	Molten mixture of alkali metal carbonates	620 to 660°C	65%	$2-100MW$
SOFC Solid Oxide Fuel Cell	Oxide ion conducting ceramic	800 to 1000°C	60 – 65%	$100kW$

2.1.3.4 Photovoltaic (PV)

A photovoltaic (PV) cell utilizes semiconductor materials to convert sunlight from freely available solar irradiation into DC electricity. The most commonly types of semiconductor materials used for PV cells production are mono-crystalline, polycrystalline and amorphous silicon (Si) [41]. The PV cell is the fundamental device of the PV system. A group of PV cells can be connected together, in series (for increasing voltage) and in parallel (for increasing current), to form a PV panel or module. A PV array with a desirable voltage and current is formed by series and parallel connecting of PV modules. PV systems are considered as widely ranged capacity power sources capable of providing power for different applications from few micro watts to several megawatts. The output power of the PV system is strongly affected by weather conditions specially solar irradiation and ambient temperature resulting in unpredictable system behavior. Because of their fluctuation nature PV standalone systems are usually associated with Battery Energy Storage Systems (BESS), for storing energy in case of over production and using it whenever needed, to enhance system stability and provide load and generation power balance. PV systems are connected to the grid at desirable voltage and frequency through power electronic interfaces. Proper control of power electronic converters is required to enable the PV system to provide both active and reactive power to the network according to the implemented control strategy. A simple layout of a PV system is shown in figure 2.7 [42].

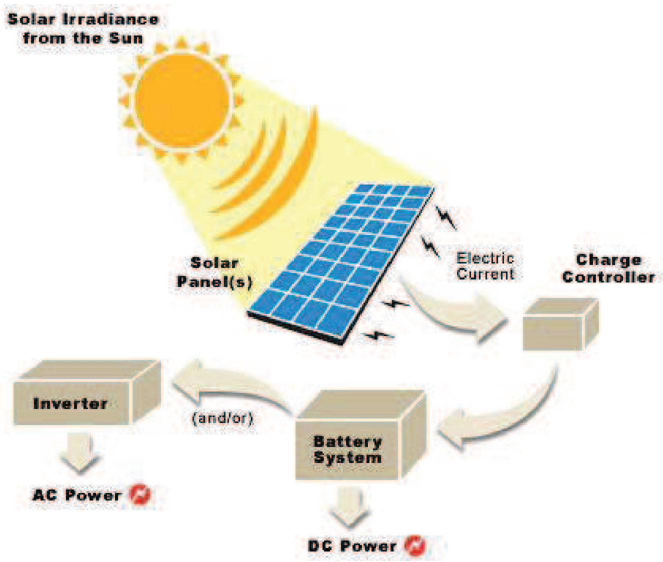

Figure 2.7: A simple layout of a PV system.

1. **Advantages of PVs:**

   - Low operating cost.
   - Unlimited availability of sunlight.

- Long life cycle.
- Negligible maintenance cost due to absence of moving parts.
- Minimum environmental harmful and silent operation.
- Short required time for design, installation and startup of a new plant.

2. **Disadvantages of PVs:**

- High capital and installation cost.
- Relatively low efficiency.
- Significant required installation area.
- Fluctuation output nature due to changes in weather conditions.

2.1.3.5 Wind Turbines (WT)

In last decades wind turbines technology has developed to sophisticated wind turbines implementing power electronics, aerodynamics, and mechanical drive train designs [43]. A wind turbine , as shown in figure 2.8 [44], comprises; the tower, the rotor and the nacelle. The nacelle houses the generator which converts the mechanical energy into electricity. Large wind turbine farms are more like central generation plants than DGs. However, small wind turbines can be utilized for DGs applications. Wind turbines provide clean energy at cost decreases with time, unlike, traditional oil fueled generation plants which provide energy with air polluting and cost increases with time. As the usual case with renewable energy sources based on nature forces, the main challenge of wind turbines is their outputs fluctuation nature affected by wind speed variations and hence cannot dispatch power on system demand.

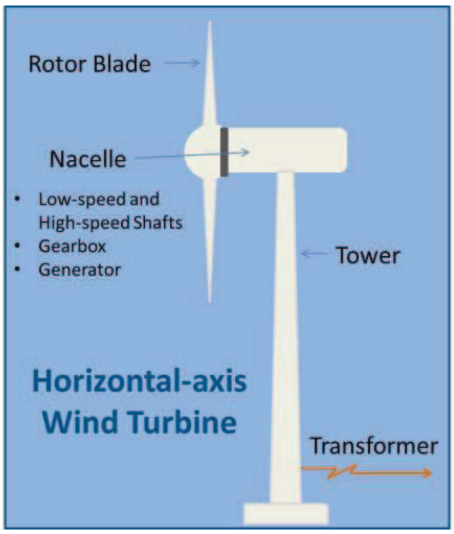

Figure 2.8: Basic parts of a wind turbine.

2.1.3.6 Small Hydropower (SHP)

For several decades hydropowers were generated in large scale benefiting from economic of scale and access to transmission networks. Liberalization of the electricity market in addition to other factors has encouraged independent power producers to develop small hydropower generators [45]. From capacity point of view, hydropowers with capacities less than 10MW are commonly termed as small hydropower generators (SHP), which can comprise two other groups namely micro and mini hydropower generators as shown in table 2.9 [46].

Table 2.9: Capacities of DGs.

Group	**Capacity**
Micro SHP	$< 100kW$
Mini SHP	$100kW$–$1MW$

2.1.3.7 Biomass

Biomass is an organic, carbon based material extracted from different types of waste such as agriculture, animal, and industry waste. Although, there are several technologies to produce electricity and/or heat from biomass, steam turbines are commonly implemented one, where the produced steam from the boiler as a result of the combustion of biomass used to turn a steam turbine which drive an associated generator. Biomass can be converted to fuel gas or biogas which usually utilized in combustion engines or CHP to generate electricity [47]. Power and CHP generation using biomass has steady increase in several European countries such as Germany, Denmark, and Finland. However, high cost and low conversion efficiency are considered main challenges of biomass technology.

As a brief conclusion table 2.10 shows a comparison between main selected DGs technologies and briefly illustrating merits and demerits of each technology [48].

Table 2.10: Comparison between main DG technologies.

No.	DG Technology	Merits	Demerits
1	Fuel Cell	• High efficiency. • Low noise. • Nearly zero emission • Fast load response.	• Pure hydrogen need. • High cost. • Low durability. • Fuel required processing.
2	Micro Turbine	• Low noise. • Low emission. • Light weight. • Small size.	• High cost. • Limited to low temperature. • Relatively low efficiency.
3	Wind Turbine	• Low production cost. • Low energy loss. • Environmental friendly. • Save land use. • No fuel demand.	• Affected by wind speed. • Variable power output. • Noise. • High investment cost. • Harm birds.
4	Solar PV	• Low maintenance. • Environmental friendly. • No fuel demand.	• High investment cost. • Affected by solar radiation.
5	CHP	• High efficiency. • Low emission. • Save energy loss. • Integration various fuels.	• Increased investment cost. • Need reasonable plan. • Decrease flexibility. • Complex technology need.
6	Gas turbine	• High reliability. • Low emission.	• High pressure gas need. • Low efficiency at low load.
7	Reciprocating engine	• Fast start- up. • Low investment.	• Relatively higher emission. • High maintenance cost.
8	Small hydro	• Free and renewable source of energy. • No impact on river eco-system. • Short installation time. • Environmental friendly.	• Power output depends on availability of water. • Affected by flood. • They can be suited where potential site exists. • Can't meet required load demand. • Continuous maintenance is required.
9	Biomass plant	• Uses renewable source. • Reduces dependency on fossil fuel. • Reduces greenhouse gas emissions.	• Expensive. • Causes pollution. • Limited source.

2.2 Electric Energy Storages (EES)

2.2.1 Introduction

The continuous global increased demand for energy along with increased pollution, running out of fossil fuels, and aging of electric transmission and distribution infrastructure have increased the concern of finding other alternatives than the existing traditional centralized generation technologies. Distributed generation (DG) technologies utilizing renewable energy sources (RES) have great potential in meeting these challenges. However, electricity generated from renewable sources (such as photovoltaic and wind turbines) are unpredictable in nature and cannot provide immediate response to demand requirements as the outputs from the traditional power sources. Thus, The increased penetration of renewable sources (particularly solar photovoltaic) into the power system networks means greater network load stability problems. Electric energy storage (EES) can be regarded as one of the most promising approaches to accommodate the variable nature of these new resources [79]. Energy Storage Systems allow storing of elecrical energy in a certain form reserving it in various mediums and convert it back to electrical energy when needed [1]. Although, there are many types of energy storage technologies available at present, each method of storage can have its ideal application environment and energy storage scale [80].

2.2.2 Types of Electric Energy Storage Systems

Electric energy storages can be classified in terms of different bases such as, type of application (permanent or portable), storage duration (short or long term), and type of production (maximum power needed) [81]. The most commonly used classification method is a one based on the form of stored energy. In this method, as illustrated in figure 2.9, energy storages comprise five categories namely mechanical, electrochemical, electrical, chemical, and thermal energy storages [82].

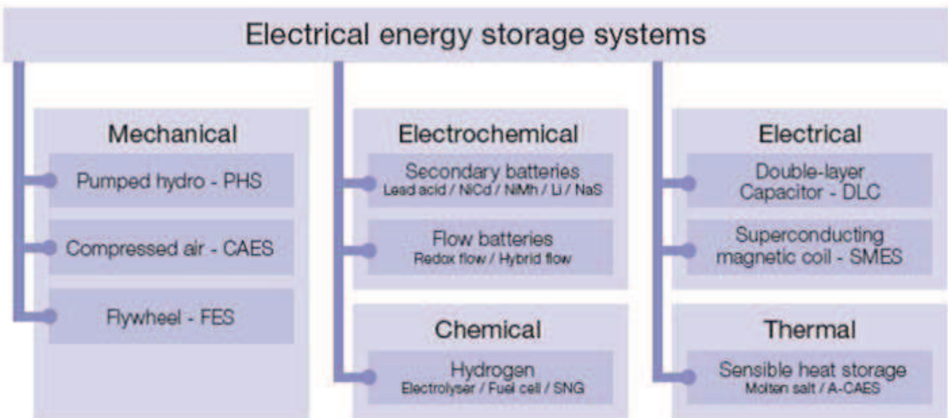

Figure 2.9: Classification of EES based on form of stored energy.

2.2.2.1 Mechanical Energy storage systems

- **Pumped Hydroelectric Storage (PHS):** The first Pumped Hydro Storage plants were used in Italy and Switzerland in the 1890s. Pumped hydroelectric storage is still the most dominant energy storage technology with about 98% share of total global installed electrical storage capacity [83]. As shown in figure 2.10 [84], a conventional pumped hydro storage system uses two water reservoirs at different elevations. During periods of high production and low electricity demand, water is pumped to the upper reservoir, storing the electricity in the form of potential energy (charging). When required, as during peak demand, the water can be released, flows back from the upper to the lower reservoir, powers turbine units which drive an electric generator to produce electricity (discharging). For upper and lower reservoirs alternatives, high dams can be used as pumped hydro storage plants, also flooded mine shafts or other cavities, and the open sea can be used for the lower reservoir. The amount of stored energy for PHS depends on the location, scale of the reservoirs and the height difference between them which can be from a few MWh to several GWh [83]. For the following advantages, PHS dominates electrical energy storages since tens of years, large power capacity (typically $100 - 1000MW$), high efficiency (ranged 65–85%) depending on design, very long lives on the order of 50 years, large storage capacity (1–24+h) [85]. However, the main drawbacks are large area and specific site's topographical conditions and high capital investment. PHS are mainly applicable for energy management, voltage and frequency regulation, spinning reserve, and non-spinning reserves.

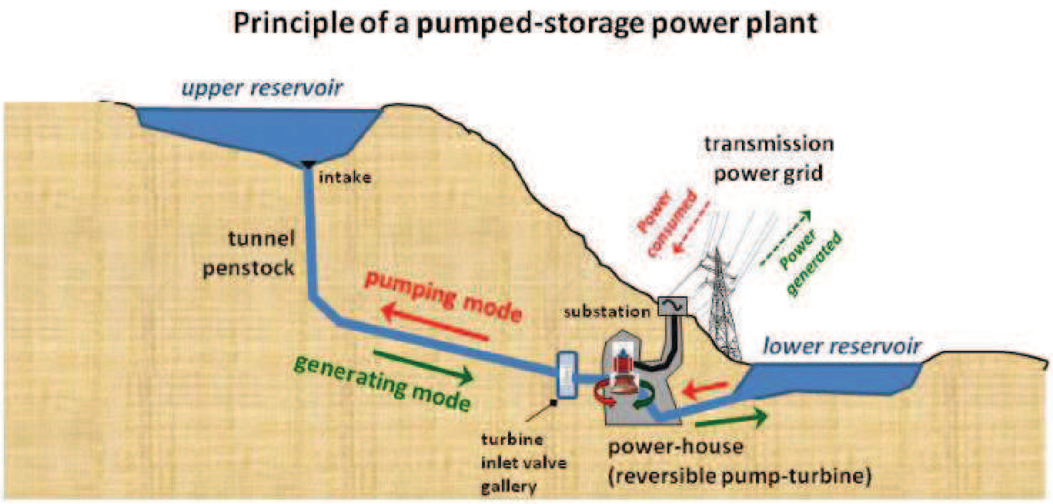

Figure 2.10: A pumped hydro storage plant layout.

- **Compressed Air Energy Storage (CAES):** Compressed air energy storage (CAES) in addition to PHS can be considered as the only existing storage technologies applicable for large-scale power and high energy storage [86]. As illustrated in figure 2.11 [87], CAES technology is based on using off-peak electricity to compress air and store it in underground caverns or above ground storage tanks. When load demand exceeds generated power, the stored compressed air is mixed with natural gas, burned, expanded and directed through a conventional turbine with generator to produce electricity.

CAES system has high power range of $50 - 300MW$ with storage efficiency range of $70 - 89\%$ [88]. CAES can be applied for wind variability mitigating and energy management [88].

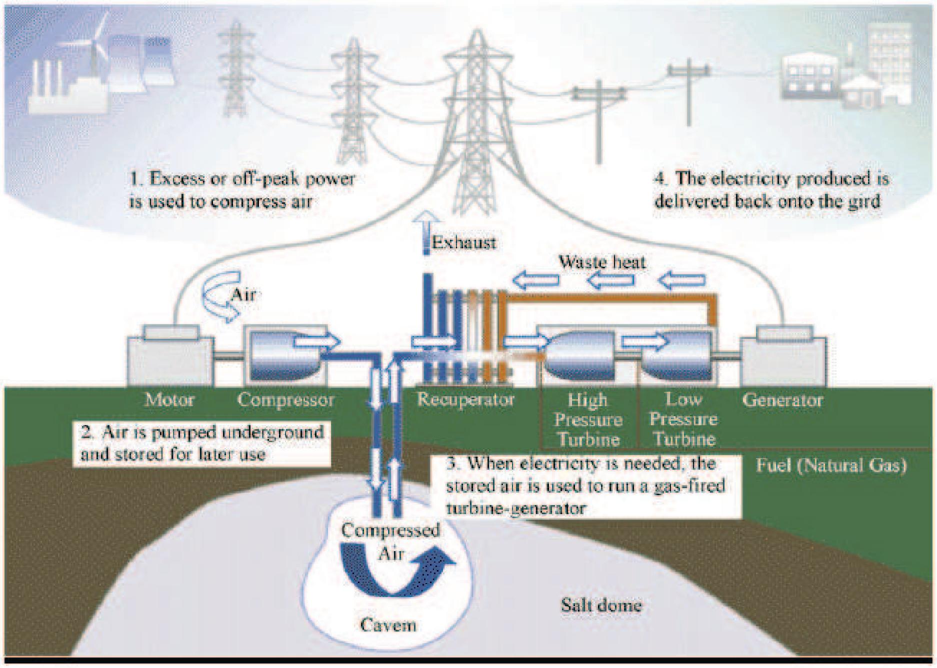

Figure 2.11: Schematic diagram of CAES.

- **Flywheel Energy Storage (FES):** FES technology is based on a flywheel which is a mass about an axis able to store energy in the form of kinetic energy. A simple structure of FES is shown in figure 2.12 [1] illustrating the main components which are; a flywheel, magnetic bearings, generator/motor unit, vacuum chamber and power conditioning. Magnetic bearings are used to reduce friction and system is placed in a vacuum chamber to reduce air resistance. The flywheel stores the energy by rotating in a constant speed, for charging, the flywheel is speeded up by a motor which can simultaneously acts as a generator for the discharging process. The stored energy of FES depends on the rotational velocity of the flywheel and its moment of enertia. Main advantages of FES are; high efficiency of $(90 - 95\%)$, long cycling life of $(100,000 - 1000,000)$, and long life of $(15 - 20$ years) [85]. FES can be considered as a high power short duration devices so they are mostly suitable for uninterruptible power supplies and power conditioning.

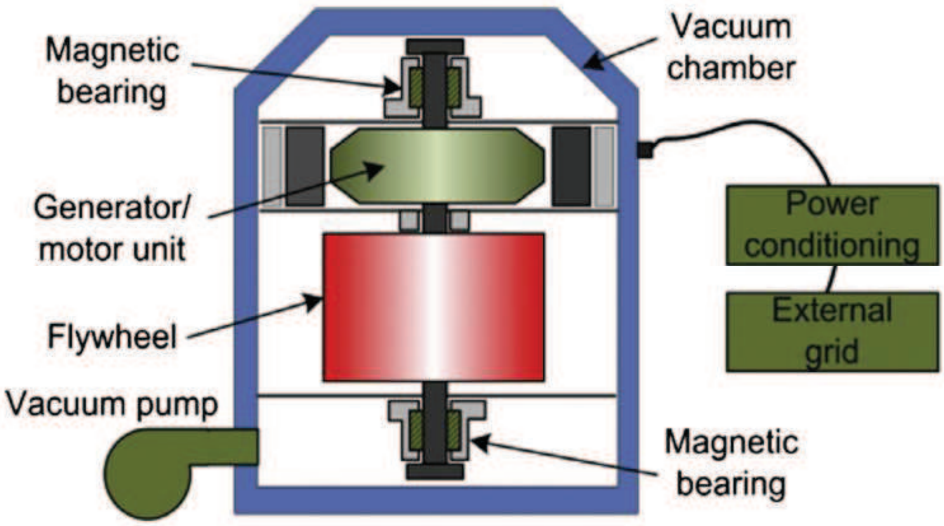

Figure 2.12: A simple structure of FES.

2.2.2.2 Electrochemical Energy storage systems

1. **Secondary Batteries Energy storage systems:** Battery energy storage (BES) is the most commonly used electrochemical technology. Batteries store energy in chemical form and produce electricity through electrochemical reactions. A battery storage may comprise a number of cells connected in series and/or in parallel to obtain the desired voltage and current. A cell consists mainly of two electrodes namely anode and cathode plunged into an electrolyte. To charge the battery a power supply is connected to the two electrodes, electrons flow from cathode to anode and reverse reactions take place during discharging as illustrated in figure 2.13 [89]. BES can be classified into two categories; secondary batteries (such as; Lead acid, Li-ion, NaS, etc.) and flow batteries such as VRB which are briefly described below.

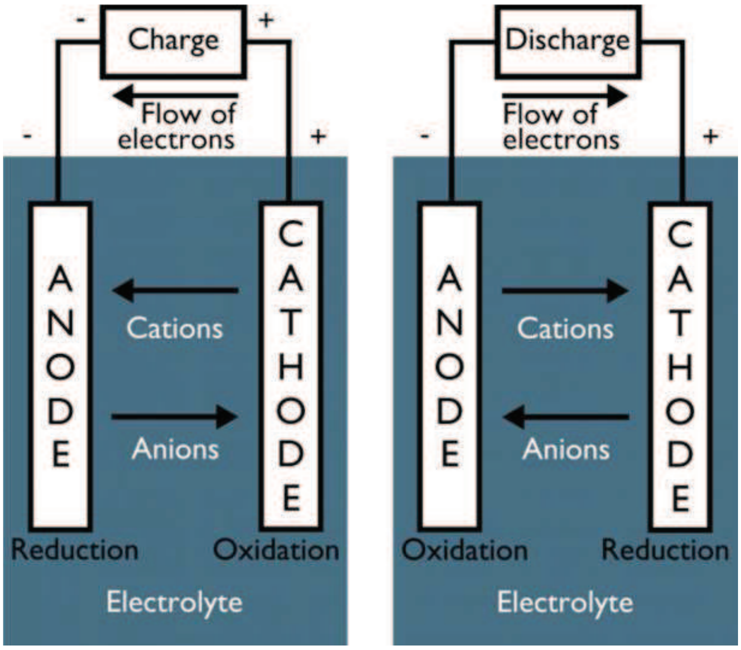

Figure 2.13: Rechargeable battery diagram.

- **Lead acid Batteries:** Lead acid batteries are the oldest and most widely used battery technology. They usually involve a number of cells spongy pure lead anodes and lead acid cathodes. Lead acid batteries reliable, relatively cheap ($\$300 - 600/kWh$) and have high efficiency ranged (70–90%) [79]. However lead acid batteries have short cycle life ($100 - 1000$cycles), low energy density ($30 - 50Wh/kg$), considerable maintenance cost and lower capacity at low temperatures [88], [90]. Lead acid batteries can be used for both stationary and mobile applications. They may be a typical choice for power quality, uninterruptable power supply and in stand-alone systems to mitigate fluctuations of PV outputs [91], [92].
- **Lithium- ion (Li-ion) Batteries:** Lithium- ion Batteries were commercially produced by Sony in 1991. The cathode is metal oxide, such as LiCoO2 and LiNiO2 and the anode is made of layer structured graphitic carbon, while the electrolyte is made up of aqueous organic liquid with lithium salts, such as LiClO4 [93]. Lithium ion batteries are considered a typical choice for mobile and portable electronic systems due to their high energy density of $200Wh/kg$, high efficiencies of over 95% and life cycle of 3000 cycles. However, the lifetime of lithium-ion batteries can be affected by temperature and deep of discharge (DoD). The main drawbacks of lithium-ion batteries are their high cost and requirement of safety and protection circuits.
- **Sodium sulfur (NaS) Batteries:** A sodium sulfur battery, as shown in figure 2.14 [94], has molten sulfur as a positive electrode and molten sodium as a negative electrode and uses beta alumina as a solid electrolyte. To en-

sure the electrodes liquid states, the reaction for charging and discharging may require a temperature of 300-350°C and an extra heating system may be required [95], [96]. Sodium sulfur batteries are highly efficient (75 – 90%), have high power densities of $(150 - 240W/kg)$, with almost no self-discharge and can be cycled 2500 times. These in addition to their pulse power capability of 600% of their continuous rating (up to 30s) make them one of the typical choices for power quality and peak shaving applications [79], [97]. The batteries are sealed and made from almost recyclable inexpensive and non-toxic material which make them environmentally acceptable [85], [93]. However, the NaS batteries main drawbacks are the initial capital cost and the operating temperature requirements [90].

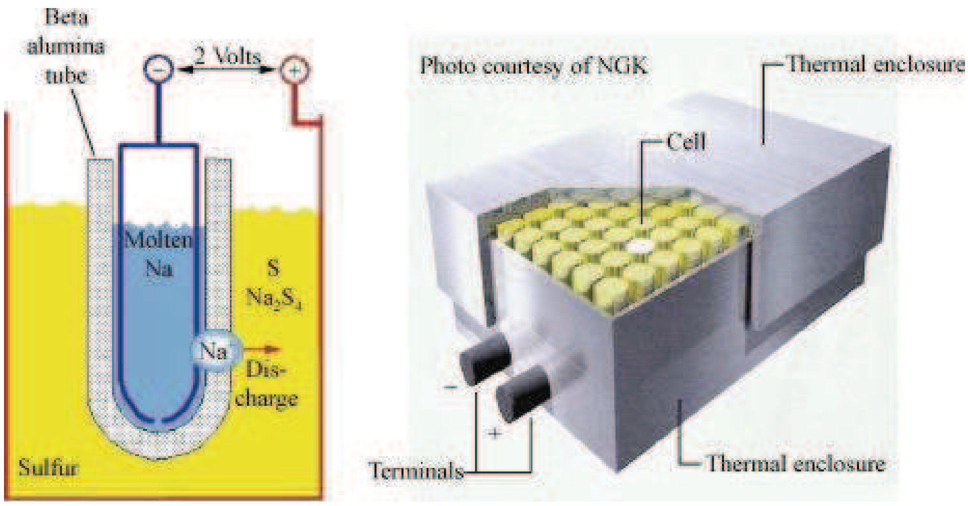

Figure 2.14: Sodium sulfur (NaS) Battery.

- **Nickel-cadmium (NiCd) batteries:** In Nickel cadmium batteries, the positive electrode and the negative electrode are made of nickel hydroxide and cadmium hydroxide respectively and separated by alkaline electrolyte. NiCd batteries have relatively high energy density $(50 - 75Wh/kg)$, they are reliable with very low maintenance requirements. NiCd batteries are favored for UPS and generator starting. Because of the toxicity of cadmium, environmental issues are raised related to disposal of these batteries in Europe making them used only for stationary applications [92]. NiCd batteries suffer from what called "memory effect" where the battery's capacity decreased dramatically if the battery has been recharged before fully discharged, which make them unsuitable to be integrated with unpredictable outputs of solar PV and wind turbine generation plants [79].

2. **Flow Batteries Energy storage systems:**

- **Vanadium redox batteries (VRB):** Vanadium redox batteries (VRB) are one of the most common type of flow batteries. A VRB as shown in figure

2.15 [98] comprises three main components: electrolytes, electrodes and membranes. The electrodes are made of highly porous carbon felt. The Electrolytes are contained in external tanks, and are pumped to electrochemical cell in which there are two electrolyte flow components separated by ion selective membranes. The reaction in the electrochemical cell converts the chemical energy to electricity and vise versa. In VRBs, the power is independent of the storage capacity. The power is determined by the size and design of the electrochemical cell while the storage capacity depends on the quantity and concentration of the electrolyte [99], [100]. Upgrading of the system can be carried out at relatively low cost by increasing the electrolytes volume and/or adding new cell stacks for more energy and/or power respectively [85]. Efficiencies of VRBs are relatively high up to 85% with high life cycle of $(10,000 - 16,000)$ cycles [101]. VRBs may provide power at high rate of discharge for range of $(4 - 10h)$ [102]. They have negligible self-discharge as a result of keeping the electrolytes in external separate tanks [93]. Because of their relatively low energy density, VRBs are more suitable for stationary applications. VRBs may be used for a wide range of applications such as; load leveling, power quality, UPS, power security and mitigating the intermittent output nature of renewable energy sources such as solar PV and wind turbines [79], [1], [85].

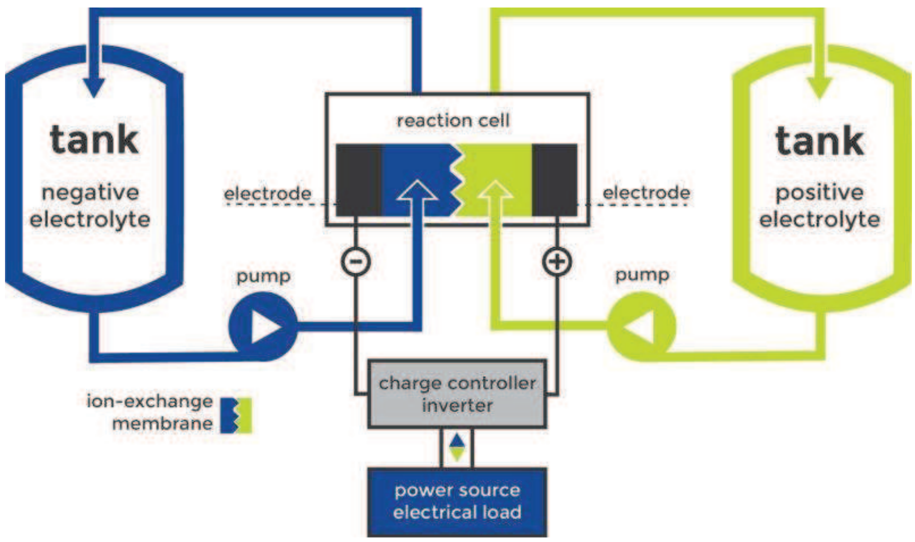

Figure 2.15: Structure of vanadium redox batteries.

Main characteristics of electrochemical energy storage technologies are summarized in table 2.11.

Table 2.11: Summarized technical characteristics of electrochemical energy storage technologies.

Technology	**Maturity**	**Cost ($/kW)**	**Cost($/kWh)**	**Efficiency**	**Cycle Limited**	**Response Time**
Lead Acid Batteries	Demo to Mature	950 - 5,800	350 - 3,800	75-90%	2,200 ->100,000	Milliseconds
Lithium-ion Batteries	Demo to Mature	1,085 - 4,100	900 - 6,200	87-94%	4,500 ->100,000	Milliseconds
Sodium Sulfur	Demo to Deploy	3,100 - 4,000	445 - 555	75%	4,500	Milliseconds
Flow Batteries (Vanadium Redox)	Develop to Demo	3,000 - 3,700	620 - 830	65-75%	>10,000	Milliseconds
Flow Batteries (Zinc Bromide)	Demo to Deploy	1,450 - 2,420	290 - 1,350	60-65%	>10,000	Milliseconds

2.2.2.3 Chemical Energy storage systems

- **Hydrogen Energy Storage:** A typical hydrogen energy storage process is based on the use of off-peak electricity to produce hydrogen, store hydrogen for later use, and use stored hydrogen to produce electricity when needed. To achieve these, the hydrogen storage system, as shown in figure 2.16 [103], comprises three components; an electrolyzer, a storage tank and a fuel cell. The electrolyzer utilizes the off-peak electricity to produce hydrogen by splitting water into hydrogen and oxygen. The produced hydrogen can be stored in a high pressure tank to be used when required. The fuel cell comprises two electrodes separated by an electrolyte and uses electrochemical conversion to generate electricity. Electricity is produced when hydrogen and oxygen from air react (hydrogen acts as the reactant while oxygen acts as the oxidant) in presence of electrolyte, water is produced with heat released [92]. There are several groups of fuel cells according to the used fuel and electrolyte. Table 2.12 lists the most common types of fuel cells with their fuel types and applications [104].

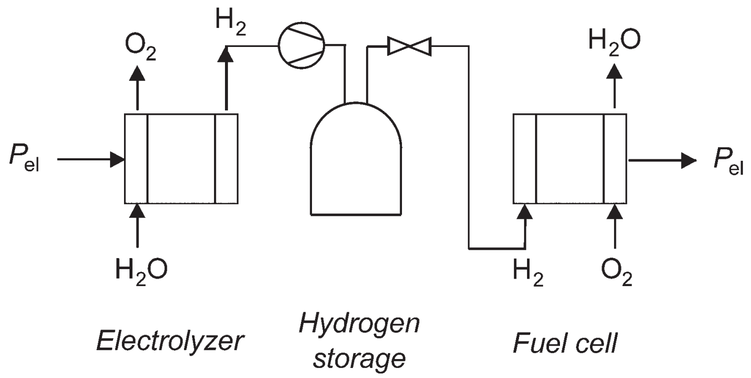

Figure 2.16: Schematic of a hydrogen fuel cell storage.

Table 2.12: Main fuel cells types and their applications.

Fuel cell Type	Applications
Alkaline Fuel Cell (AFC)	Military, space applications
Phosphoric Acid Fuel Cell (PAFC)	Distributed generation
Solid Oxide Fuel Cell (SOFC)	Utility EES, distributed generation
Molten Carbonate Fuel Cell (MCFC)	Electric utility EES, distributed generation
Proton Exchange Membrane Fuel Cell (PEMFC)	Backup power, small distributed generation
Direct Methanol Fuel Cell (DMFC)	Transportation, portable devices

Hydrogen fuel cell storages offer wide range of scales ($1kW - 100'skW$), high energy density 600-1200 Wh/kg). However, they still expensive ($\$6 - 20/kWh$) and have low round-trip efficiency (20–50%) [1], [105].

2.2.2.4 Electrical Energy storages

- **Supercapacitors:** Capacitors and supercapacitors have the ability of faster charge and discharge and much greater number of cycles than conventional batteries. Conventional capacitors made up of two electrodes separated by solid non-conducting material. The energy is stored by depositing the electrons between the electrodes and a potential is created between the separated electrodes. In the supercapacitors, unlike the conventional capacitors, the electrodes are usually made up of highly porous carbon materials with large specific area separated by electrolyte solution. As a result of the very large surface area of the carbon electrodes (up to $2000m^2/gm$ and the very small distance between the plates (<1nm), the supercapacitors energy storage capabilities are much greater than that of the conventional capacitors [79], [106]. Supercapacitors have a very high power density of $10,000W/kg$, high cycle efficiency of $(84 - 97\%)$, very long life cycle of 100,000 cycles, quick recharge, deep charge/discharge capability, and wide range of operating temperature ($-40 to 70$°C) [79], [80], [107] [108]. However the main drawback of supercapacitors are their capital cost which can be up to $\$20,000/kWh$ and their daily discharge rate of $(5 - 40\%)$ [85]. Due to their high power density along with their fast discharge, supercapacitors are typical for providing a short term peak power boost, and a short duration back up peak power for UPS. Generally, supercapacitors can be suitable for small scale power quality applications ($< 250kW$). Supercapacitor can integrated with battery systems for mitigating RES intermittent nature.

- **Superconducting Magnetic Energy Storage (SMES):** SMES systems are based on storing energy in the form of magnetic field in a superconducting coil. A typical SMES system, as shown in figure 2.17 [109] consists of the following components:

  - Superconducting coil.
  - Power conditioning system.
  - Cryogenically cooled refrigerator.

  Once a direct current flow in the circular superconducting coil which can be made of materials with very low resistance such as vanadium or mercury at very low temperature, energy can be stored with almost no losses [110]. Niobium–Titanium with a superconducting critical temperature of 9.2 K is one of the most commonly used superconducting which usually immersed in a coolant liquid helium at 4.2 K for maintaining superconductor properties [91]. The stored energy can be released to a load through the power conditioning system which uses a converter module. SMES has high efficiency around 95%, and fast response time [111]. Unlike other storage systems, SMES has an ability to discharge almost the total stored energy. Moreover, it has long lifetime. The main drawbacks are its high capital cost, high self-discharge and environmental issues related to its strong magnetic field [1], [112].

Due to the mention features, SMES can be considered as a good choice for UPS and for improving power quality. Because of its low energy density along with the high energy requirements of the refrigeration system and as indicated by a research, SMES is not devoted for renewable energies integration [85].

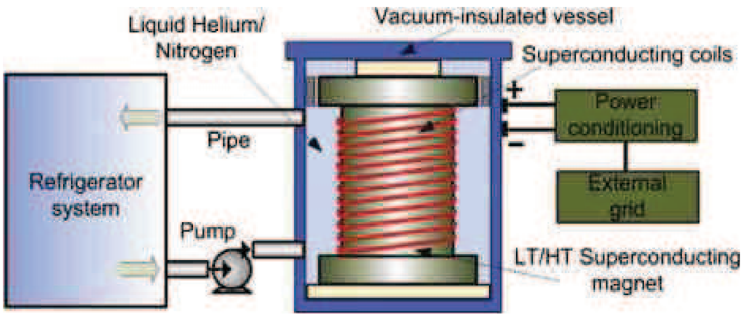

Figure 2.17: A simple structure of SMES.

2.2.2.5 Thermal Energy storages (TES)

TES is based on utilizing specific materials by keeping them at high/low temperature, the recovered heat/cold can be used through heat engine cycles to produce electricity. The charge phase can be provided by heating of an electrical resistance or cryogenic/refrigeration procedures [79]. TES can be categorized into two groups, high and low temperature TES. High temperature TES systems are composing of three types (latent-fusion heat TES, sensible heat TES, and concrete storage), whereas low temperature TES systems comprise (aquiferous low-temperature TES (AL-TES) and cryogenic energy storage (CES)) [81]. Although TES technology is still under development, it may have relatively high energy density ($80-250Wh/kg$), very low daily self-discharge of ($0.05-1\%$) and relatively low capital cost [1]. TESs are mostly suitable for peak shaving applications, however, they cannot be considered yet to be devoted for renewable energies integration.

2.2.3 Comparison of the different storage technologies

Different electrical energy storage technologies have been briefly described in the previous sections. Each EES technology has its own features and capability to meet different demand requirements. In order to be able to compare various types of EES, a list of criteria is needed to be specified. The most commonly used criteria are; power rating and discharge time, storage duration (self-discharge), capital cost, cycle efficiency, energy and power density, life time and cycle life and environment impact. Figures (2.18 - 2.20) illustrate some comparisons of different features of EESs.
Before illustration of the comparisons of EES technologies, technical characteristics of various EESs are summarized in tables 2.13.

Table 2.13: Technical characteristics of electrical energy storage technologies [79], [1], [97].

	Power rating (MW)	**Daily Self discharge**	**Capital power cost** ($\$/kW$)	**Capital energy cost** ($\$/kWh$)	**Cycle Efficiency (%)**	**Energy density** (Wh/kg)	**Power density** (W/kg)	**Lifetime (Years)**	**Lifetime (cycles)**	**Environmental impact**
PHS	100–5000	Very small	600–2000	5–100	75–85	0.5–1.5	0.5–1.5	40–60	>13,000	Large
CAES	5–300	Small	400–800	2–50	70	30–60		20–40	>13,000	Moderate
FES	0.25		350	5000	93–95	10–30	400–1500	∼15	20,000	Benign
Lead-acid Battery	0–20	0.1–0.3%	300	400	70–90	30–50	75–300	5–15	2000	Moderate
Li-ion Battery	0.1	0.1–0.3%	4000	2500	85–90	75–200	150–315	5–15	4500	Moderate
NaS Battery	0.05–8	∼20%	3000	500	80–90	150–240	150–230	10–15	4500	Moderate
Ni–Cd battery	0–40	0.2–0.6%	1500	1500	85–90	50–75	150–300	10–20	3000	Moderate
VRB	0.03-3	Small	600–1500	150–1000	75–85	10–30	166	5–10	12,000+	Moderate
Hydrogen Fuel cell	0–50	Almost zero	1500–3000	15	20–50	800–10,000	500+	5–15	1000+	Small
Supercapacitor	0-0.3	20–40%	100–300	2000	90–95	2.5–15	500–5000	20+	100,000+	Small
SMES	0.1–10	10–15%	300	10,000	95–98	0.5–5	500–2000	20+	100,000+	Moderate
TES	0–60	0.05–1%	200–300	30–60	30–60	80–200	10–30	5–15	13,000+	Small

Cycle efficiency is defined as the ratio of the system electricity output to electricity input. From table 2.13, the cycle efficiency of EES technologies can be categorized into three groups named low, high and very high efficiencies. EES with low efficiencies ($\sim< 60\%$) are FCs, TES, and CES. PHS, CAES, batteries and flow batteries have high efficiencies (60-90%). Technologies have very high efficiencies ($> 90\%$) such as SMES, flywheel, supercapacitors and Li-ion batteries.
The overall investment cost is significantly affected by Lifetime and cycling times of an EES technology. It can be seen form table 2.13 that electrical energy stored systems such as SMES and supercapacitors have very high cycle lives higher than $20,000$. Mechanical energy storage systems, such as PHS, CAES and flywheels, also have high cycle lives ($\sim 10,000$). Whereas, batteries, flow batteries, and fuel cells have lower cycle lives due to chemical deterioration with the operating time.

Figure 2.18 [92] plots the rated power against the energy content of different EES along with the nominal discharge time at rated power which ranged from seconds to months. From fig.4.10 discharge time can be categorized into three parts short (seconds to minutes), medium (minutes to hours) and long (days to months) discharge times. For short discharge time, the more suitable EES are supercapacitors, SMES, and FES, while battery technologies (LA, Li-ion, and NaS) are dominant for medium discharge time. PHS, CAES and RFB are in between of medium and long discharge time whereas H2 and SNG are more devoted for long discharge time applications.

A comparison of the power density (per unit volume not weight) against the energy

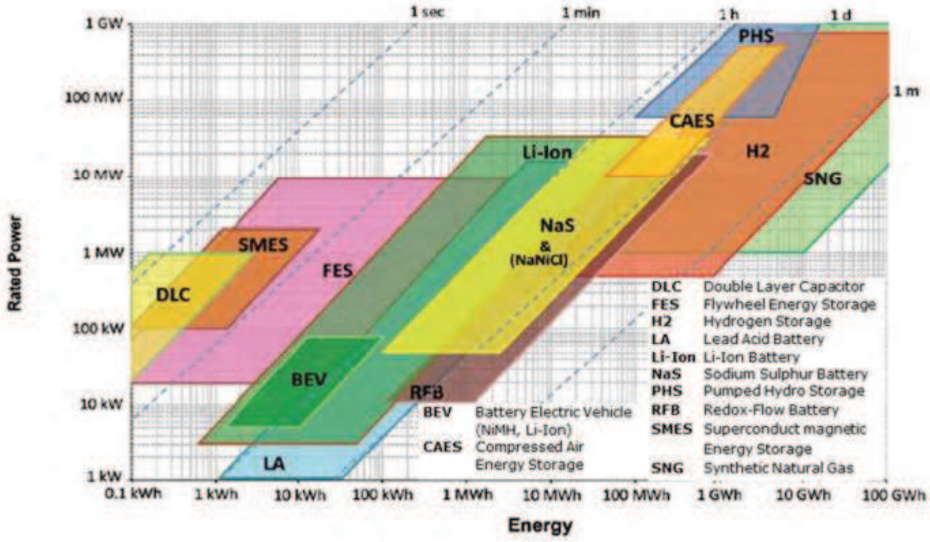

Figure 2.18: Comparison of rated power, energy content and discharge time of different EES technologies.

density of various EES techniques are shown in figure 2.19 [1]. The power and energy densities of an EES are inversely proportional to its volume. So that large volume EES technologies with low energy densities and suitable for stationary applications, such as

PHS and CAES, can be located at the left bottom corner, whereas, compact EES technologies can be found at the right top corner which are suitable for mobile applications. Supercapacitors have high power densities but their energy densities are low making them suitable for peak applications with short duratios.

Energy storage technologies can be used to mitigate several challenges facing electrical

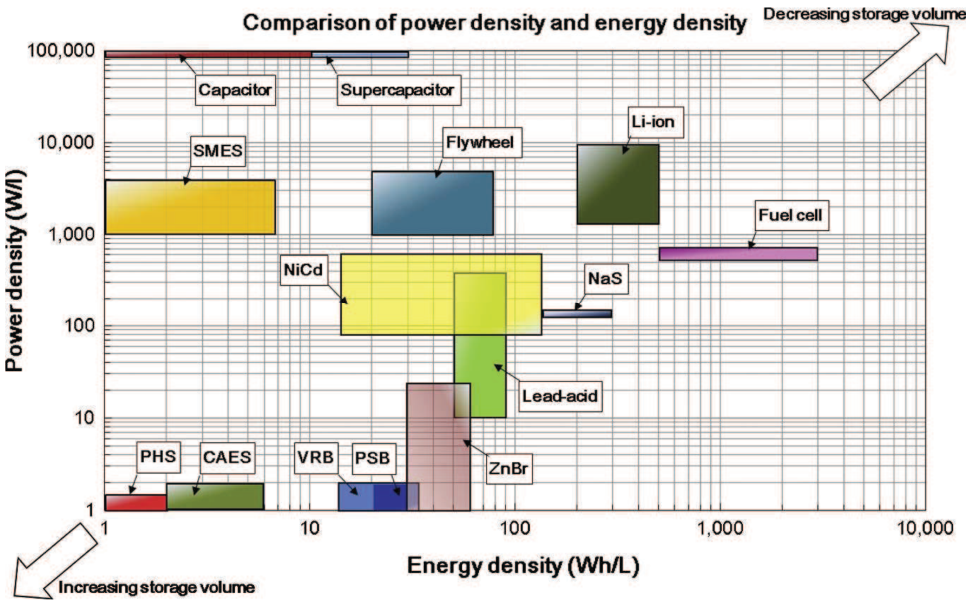

Figure 2.19: Comparison of energy density and power density.

systems. They can provide backup power during supply shortages and power interruptions, cover the load requirement during peak demand and can also be utilized to mitigate the intermitted nature of renewable energy sources such as solar PV and wind turbines. An overview and comparison of different EES technologies sorted by their power rating and discharge times along with the most suitable applications are shown in figure 2.20 [112].

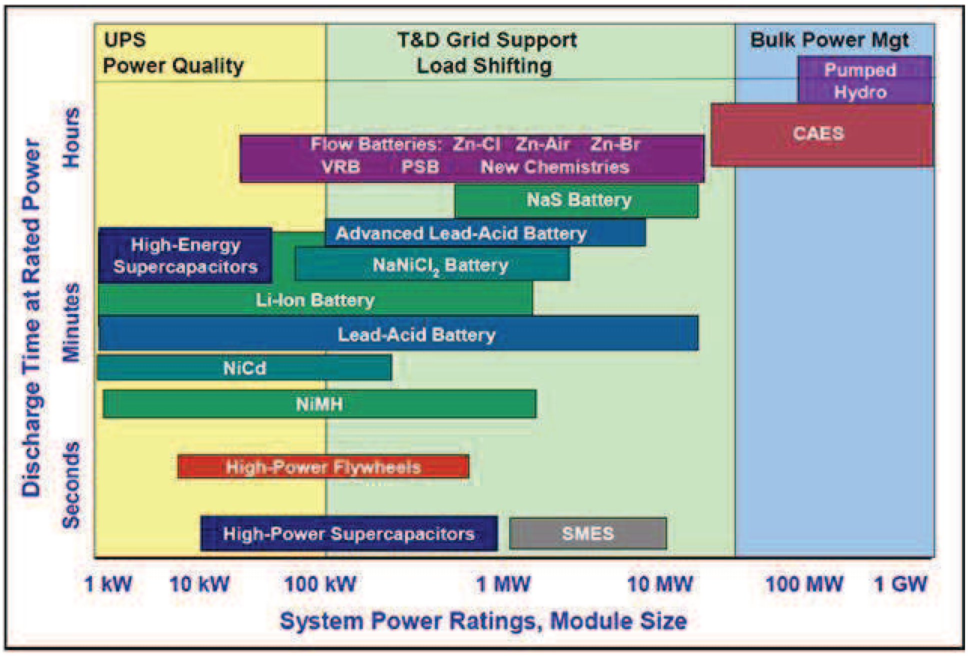

Figure 2.20: Comparison of power rating, time discharge and suitable applications.

Chapter 3

Photovoltaic Systems (PV)

3.1 Introduction

The significant concern about the dramatic growth of global energy demand with depletion of fossil fuel, in addition to environmental pollution constraints, have forced researchers to study and investigate alternative non-depleted energy resources with negligible greenhouse gas emission. Renewable energy resources such as wind, solar, hydropower, and biomass can be considered as a key factor for tackling these challenges [49]. Utilizing one type or another of renewable technologies is constrained by the resource availability, advantages and disadvantages of each technology. Solar photovoltaic (PV) systems convert solar irradiation directly to electricity with a solar panel. Photovoltaic (PV) can be considered as one of the most promising renewable technologies because of several advantages such as; unlimited availability of sunlight, negligible maintenance cost due to absence of moving parts, minimum environmental harmful and silent operation, short required time for design, installation and startup of a new plant, and long life cycle. A few years ago, solar energy had negligible contribution into the electricity market due to high cost and unpredictable output behavior. However, rapid decrease in PV panel prices, in recent years, has led to significant growth in PV industry. This can be illustrated in figures 3.1 and 3.2 where the global solar PV cumulative installed capacity at the end of 2005 was only $5,364MW$. This amount has rapidly increased to $102,156MW$ at the end of 2012 and further increased to $178,391MW$ at the end of 2014 [50], [51].

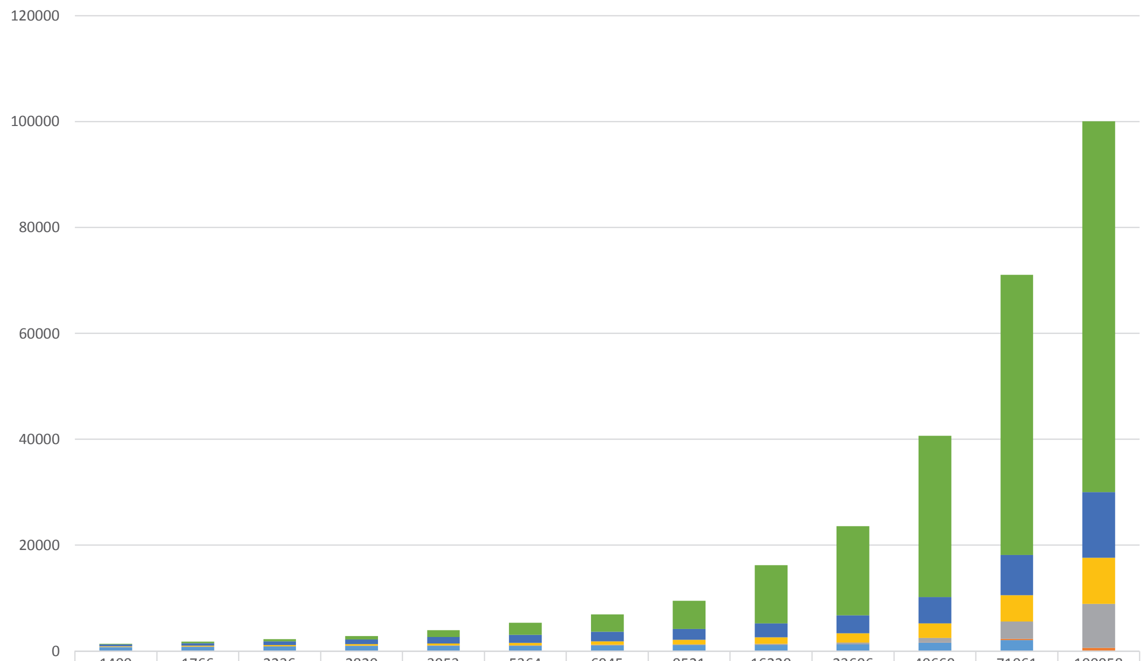

	1400	1766	2236	2820	3953	5364	6945	9521	16229	23606	40669	71061	100058
	2000	2001	2002	2003	2004	2005	2006	2007	2008	2009	2010	2011	2012
Europe	129	262	396	598	1305	2289	3281	5310	11020	16850	30472	52884	70043
APAC	355	495	686	916	1198	1500	1825	2096	2631	3373	4956	7628	12397
Americas	146	178	225	290	394	501	650	863	1209	1752	2780	4959	8717
China	19	24	42	52	62	70	80	100	140	300	800	3300	8300
MEA	0	0	0	0	1	1	1	2	3	25	71	192	601
ROW	751	807	887	964	993	1003	1108	1150	1226	1306	1590	2098	0

Figure 3.1: Global solar PV cumulative installed capacity 2000-2012.

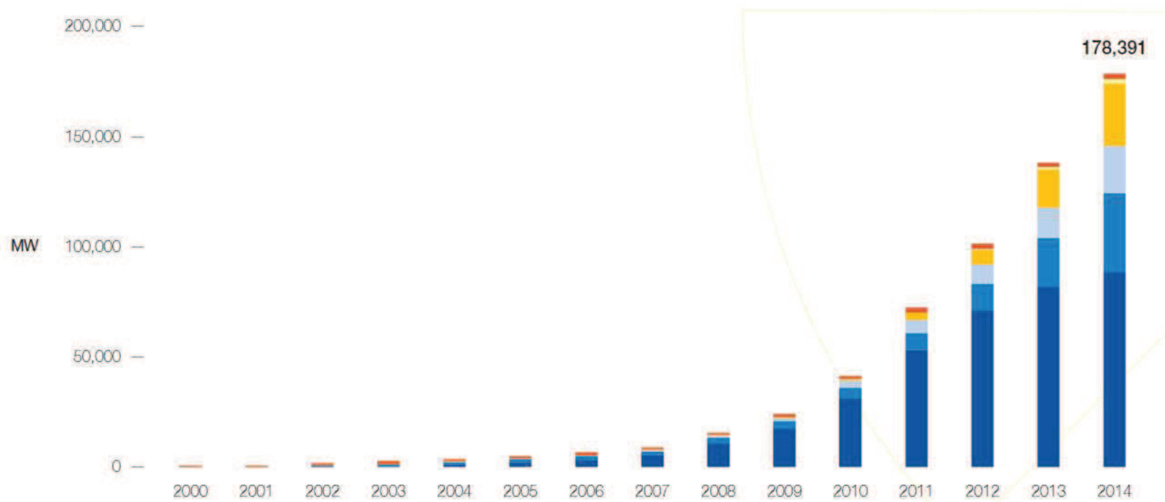

Figure 3.2: Global solar PV cumulative installed capacity 2000-2014.

In the last two years, solar PV power have experienced an extraordinary growth, thanks to the tremendous continued cost reductions in solar technology which has declined, at the end of 2014, by 75% in less than a decade. Consequently, PV solar power became a considerable cost competitive technology in electricity market. The global grid-connected solar (PV) systems, (grid connected are generally lower than installed capacities), have a remarkable growth to 229GW in 2015 increased 25% to about 50.1GW in a single year, compared to that in 2014 of 40.2GW figure 3.3 [52]. For the second year, China was the

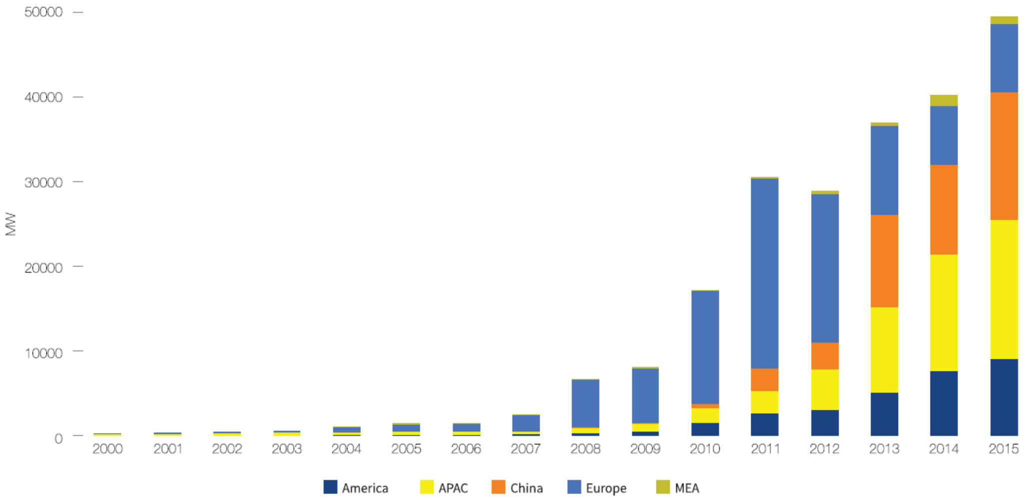

Figure 3.3: Global solar PV annual grid-connected capacity 2000-2015

largest global solar market increasing by 43% to 15.1GW in 2015 from 10.6GW in 2014. In the second place was Japan adding 10GW and 9.7GW of solar power to the grid in 2015 and 2014 respectively. The USA was in the third place. It has added 7.3GW of new grid connected solar power in 2015 increasing 12% over 6.5GW in 2014. With a total installed capacity of 43GW by the end of 2015, China was the largest solar market instead of Germany.

In 2015 Europe solar market has also a strong annual growth of 8.1GW increased by 15% over the 7GW in 2014. Figure 3.4 illustrates the annual global solar market sharing from 2010 to 2015. Europe's share has a decreasing tendency, where the solar PV power which have been added by each of China and Japan were more than that added by the entire European Continent. Despite its share decreasing, Europe has kept its title as the largest solar continent with a total solar PV grid-connected capacity of 96.9GW at the end of 2015 figure 3.5 [52]. The four driving countries are Germany, Italy, The UK, and France, with a remarkable increase in the UK contribution in 2014 and 2015.

As a conclusion, it is clear that solar PV technology can be considered as an important contributor to the global energy market. In Europe solar PV provides about 4% of power consumption while in Italy, as the leading country of solar contribution in electricity demand, solar covers nearly 8% of the electricity consumption figure 3.6 [52].

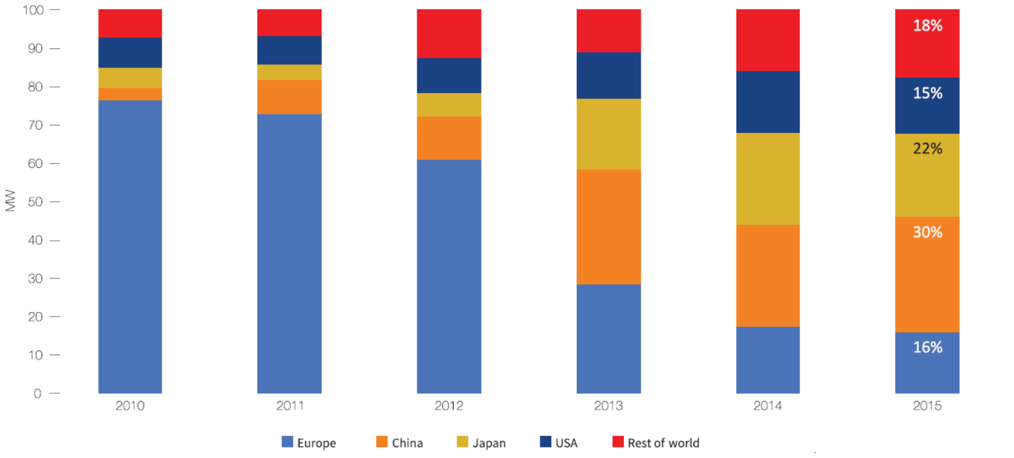

Figure 3.4: Annual European solar PV grid-connection shares compared to other regions 2010-2015.

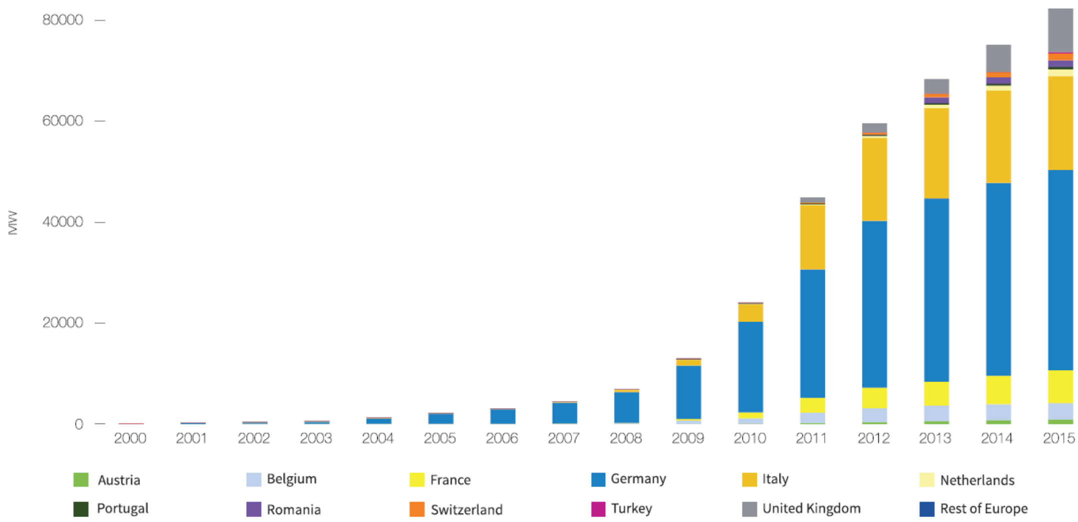

Figure 3.5: European total solar PV grid-connected capacity 2000-2015.

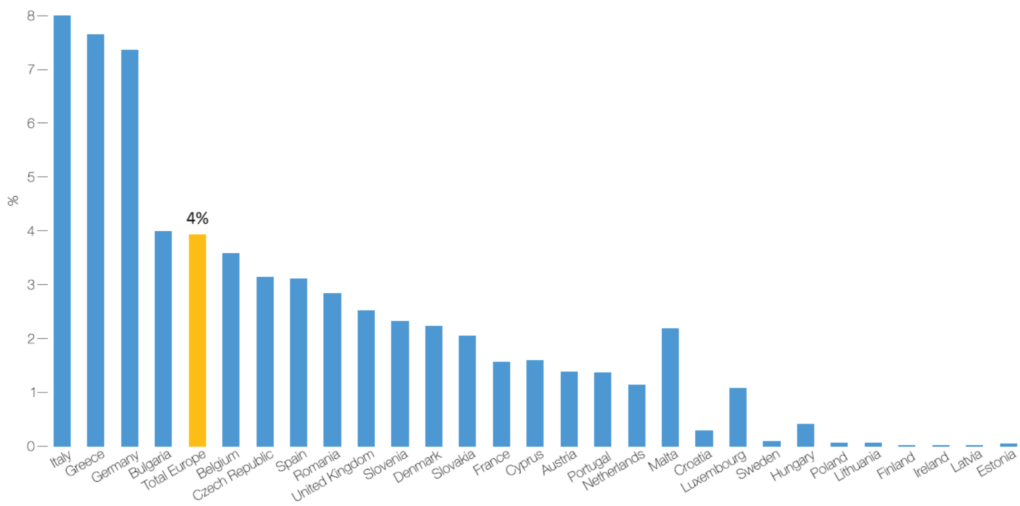

Figure 3.6: Share of solar electricity demand covered by solar PV in European countries in 2015.

3.2 Photovoltaic Cell

Photovoltaic (PV) cells use the photoelectric effect to directly convert the sunlight into dc electricity [53]. The PV cell is the fundamental device of the PV systems. A set of PV cell are connected in series to form a PV module [54], [55]. Numbers of PV modules can be connected in series and parallel to get a PV array with the desirable voltage and current respectively [56]. Although different semiconductor materials are used for developing solar PV cells. Major cell types are made from silicon. The most commercially known solar cells are mono crystalline, polycrystalline and amorphous silicon (Si) [41]. The photoelectric effect phenomena used by PV cells may be simply described as exposure of PV cells to light (form sun radiation) breaks electron bonds in the semiconductor, resulting in creation of hole-electron pairs. The free electrons can be driven through an external circuit to feed a load. Efficiencies of PV cells are generally still below 20% [57]. Photovoltaic panel information in manufacturer's datasheet are usually provided with reference to Standard Test Conditions (STC) which stands for cell temperature of 25°C, irradiance of $1000 W/m^2$ and an average solar spectrum at Air Mass (AM) of 1.5.

3.3 PV panel modeling

3.3.1 Electrical models

In order to analyze the output characteristics of a PV panel, several equivalent circuit models can be considered.

- The simplest model, as shown in figure 3.7, comprises a current source for providing the photovoltaic current I_{ph}, and a diode representing the p-n junction of the cell. This model commonly known as the ideal diode model.
  The output current of the PV panel, I_{pv}, for this model is given by 3.1.

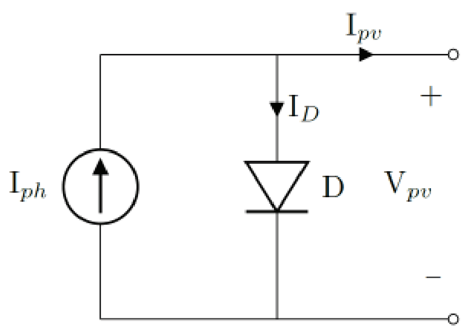

Figure 3.7: PV module equivalent circuit (ideal diode model).

$$I_{pv} = I_{ph} - I_{sat}[exp(\frac{V_{pv}}{N_s A V_T} - 1)] \tag{3.1}$$

$$V_T = \frac{kT}{q} \tag{3.2}$$

Where:
I_{pv}: The PV module terminal current (A).
I_{ph}: The photovoltaic current (A).
I_{sat}: The diode saturation current (A).
V_{pv}: The PV module terminal voltage (V).
V_T: The diode thermal voltage (V).
A: The diode ideality factor (1 $\leq$ A $\leq$ 2).
N_s: The number of cells connected in series.
k: Boltzmann's constant (1.3806503 E (-23) J/K).
T: Temperature (K).
q: Charge of electron (1.60217646 E (-19) C).

- Single diode model: It comprises five parameters and four parameters single diode models as shown in figures 3.8 and 3.9 respectively. This model considers the resisters that account for power losses, where figure 3.8 includes both the series and parallel resistances (R_s) and (R_p) respectively, while the model in figure 3.9, for simplifying the model, neglects Rp which is generally large and is considered for the leakage current losses. Single diode model is simple, more accurate than the ideal diode model and can be considered as the most commonly used for PV systems [58]. The terminals output current (I_{pv}) for equivalent circuit of figures 3.8 is described by equations 3.3.

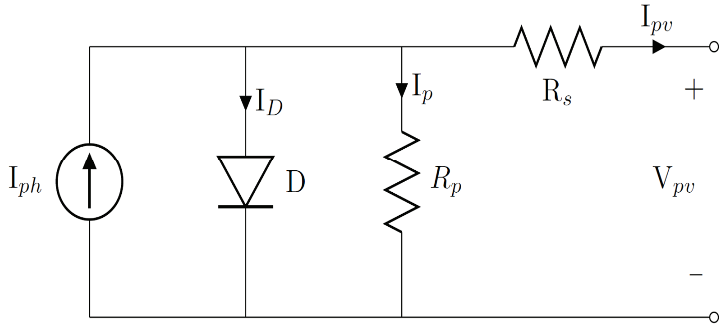

Figure 3.8: Single diode five parameters model.

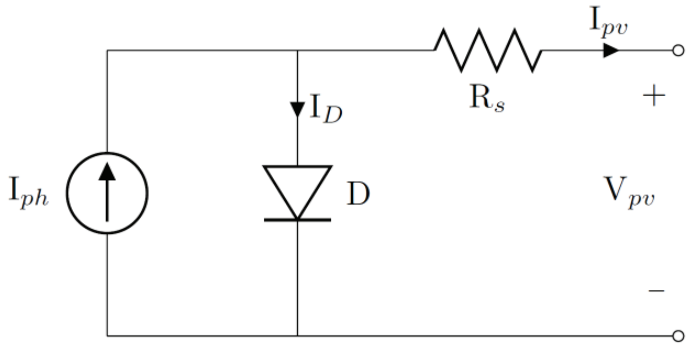

Figure 3.9: Single diode four parameters model.

$$I_{pv} = I_{ph} - I_{sat}[exp(\frac{V_{pv} + I_{pv}R_s}{N_s A V_T} - 1)] - [\frac{V_{pv} + I_{pv}R_s}{R_s}] \tag{3.3}$$

Where:

R_s: The equivalent series resistance (Ω).

R_p: The equivalent parallel resistance (Ω).

- Double-diode model: The two diode model, shown in figure 3.10, is more accurate than the single diode model but with increased complexity. They both have almost the same accuracy at STC while differ at low irradiance [59]. The mathematical equation for the two diode model is given by 3.4.

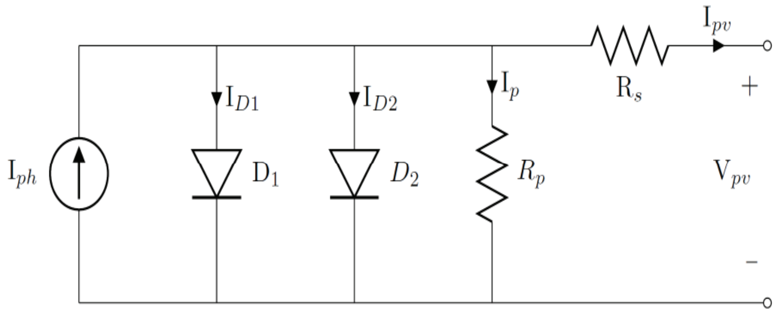

Figure 3.10: Double diode model.

$$I_{pv} = I_{ph} - I_{sat1}[exp(\frac{V_{pv} + I_{pv}R_s}{N_s A_1 V_{T1}} - 1)] - I_{sat2}[exp(\frac{V_{pv} + I_{pv}R_s}{N_s A_2 V_{T2}} - 1)] - [\frac{V_{pv} + I_{pv}R_s}{R_s}] \tag{3.4}$$

Despite the better accuracy of the double diode modes than that of the single diode model issued by some authors, the single diode model was preferred by many researchers in simulating PV systems with many interconnected models for its compromising between simplicity and accuracy [41], [60].

3.3.2 Characteristic curves

A typical current voltage (I-V) and power voltage (P-V) characteristics for a single diode model at STC are shown in figures 3.11 [61] and 3.12 [62] respectively.

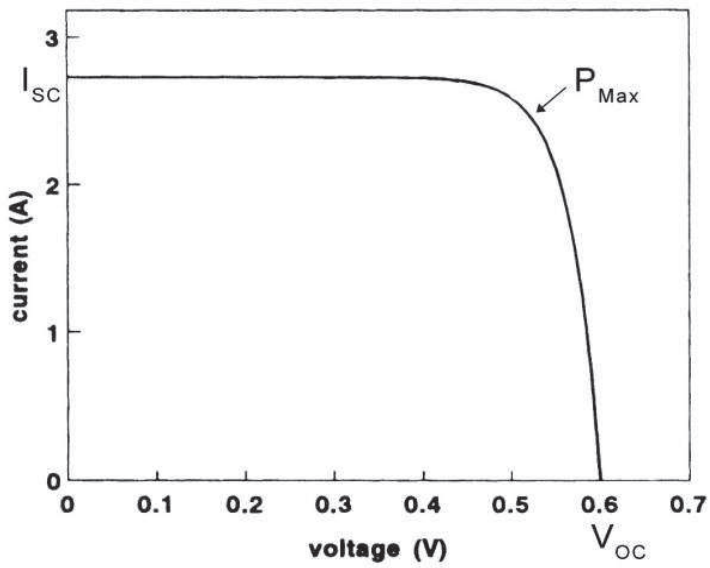

Figure 3.11: I-V characteristics.

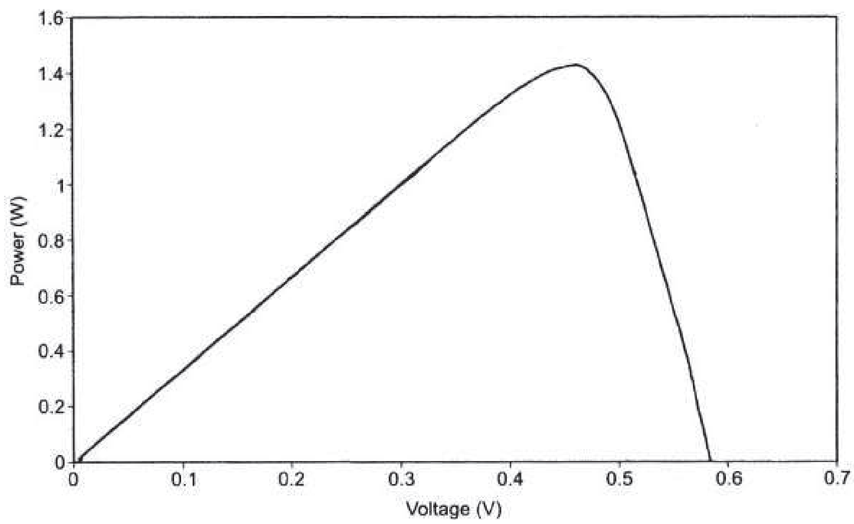

Figure 3.12: P-V characteristics.

The PV panel model typical variables which commercially provided in the manufacturer datasheet are listed in table 3.1.

Table 3.1: Typical variables of PV panel model.

Variable Name (Unit)	Variable description
P_{mpp} (W)	Maximum power.
V_{mpp} (V)	Maximum power voltage.
I_{mpp} (A)	Maximum power current.
V_{oc} (V)	Open circuit voltage
I_{sc} (W)	Short circuit current.
K_i (A/°C)	Short circuit current temperature coefficient.
K_v (V/°C)	Open circuit voltage temperature coefficient.
K_t $(°Cm^2/W)$	Cell temperature proportionality factor
N_c	Number of cells in module.
R_s (Ohm)	Series resistance.
R_p (Ohm)	Parallel resistance.
a	Diode Ideality factor.
$Q(1.6 * 10^{-19}\text{C})$	Electron charge.
k $(1.38 * 10^{-23}\text{J/K})$	Boltzmann's constant.
V_T (V)	Thermal voltage.
I_0 (A)	Diode reverse saturation current.
I_{pv} (A)	Module current.
V_{pv} (V)	Module voltage.

The fundamental parameters characterize the solar panel, as shown in figures 3.11 and 3.12, are briefly described as following:

- Short circuit current (I_{sc}): It is usually considered as the maximum current that can be provided by the cell. It is provided at short circuit condition i.e. $V = 0$.
- Open circuit voltage (V_{oc}): It is the maximum voltage across the diode (p-n junction) at open circuit condition i.e. $I = 0$.
- Maximum power point (P_{mpp}): It is the point corresponds to I_{max} and V_{max} with a maximum power can be provided to the load.
- Fill factor (FF): It is the ratio of the product of the voltage and current at the maximum power point to that of V_{oc} and I_{sc}. as given by equation 3.5.

$$FF = \frac{V_{mpp} I_{mpp}}{V_{oc} I_{sc}} \tag{3.5}$$

- Efficiency (η): It is the ratio of the output power to the input. It can be expressed in several forms as given in equation 3.6.

$$\eta = \frac{V_{mpp} I_{mpp}}{P_{in}} = \frac{V_{oc} I_{sc} FF}{P_{in}} \tag{3.6}$$

$$P_{in} = G_a A \tag{3.7}$$

Where:
P_{in} , G_a and A respectively represent the incident light power, the ambient irradiation, and the cell area.

3.3.3 Effect of temperature and solar radiation on PV characteristic curves

The temperature and irradiance have significant effects on basic electrical outputs, such as current and voltage, of the PV device.
The output voltage significantly decreases with increased temperature, while the temperature variation has a minor effect on the output current. As a result, high temperature reduces the PV device's output power and efficiency [63]. The effects of temperature on (I-V) and (P-V) characteristics of a PV device are demonstrated in figures 3.13 [64] and 3.14 [65]. The relationship of change in temperature with short circuit current and open circuit voltage are presented in equations 3.8 and 3.9 respectively [66], [67].

$$I_{sc}(T) = I_{sc}(T_{STC})(1 + K_i(T - T_{STC})) \tag{3.8}$$

$$V_{oc}(T) = V_{oc}(T_{STC}) + (K_v(T - T_{STC})) \tag{3.9}$$

Where:
K_i : Temperature coefficients of I_{sc}.
K_v : Temperature coefficients of V_{oc}.
T : Temperature (°K)

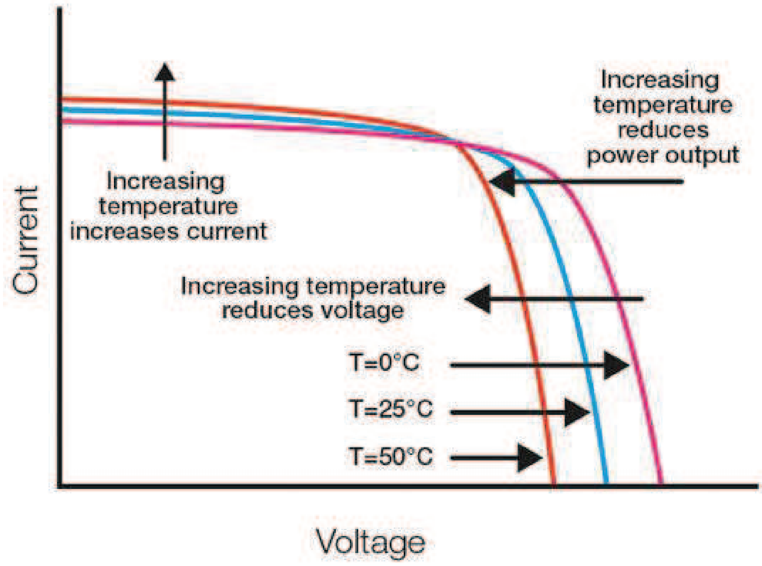

Figure 3.13: Temperature effect on the I-V characteristics of a PV device.

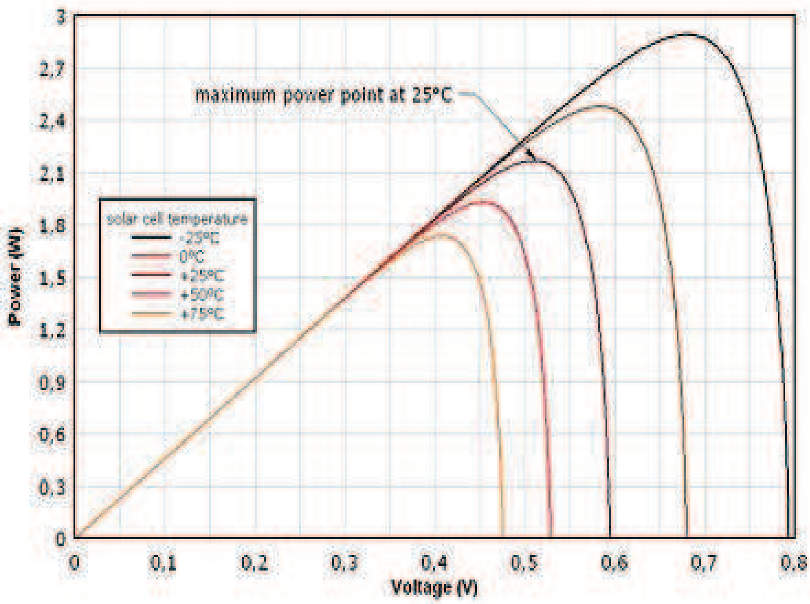

Figure 3.14: Temperature effect on the P-V characteristics of a PV device.

The irradiance has a significant effect on the short circuit current with a high directly proportional relationship, whereas the open circuit voltage is slightly affected by irradiance. Hence, the net result is an increase in output power and efficiency of the PV device as a consequent to irradiance increase. Figures 3.15 [68] and 3.16 [69] respectively demonstrate the effects of irradiance on (I-V) and (P-V) characteristics of a PV device, while equations 3.10 and 3.11 present the short circuit current and open circuit voltage as functions of irradiance changes.

$$I_{sc}(G) = \frac{G}{1000} I_{sc}(G_{STC}) \tag{3.10}$$

$$V_{oc}(G) = V_{oc}(G_{STC}) + N_s V_T \log(\frac{G}{1000}) \tag{3.11}$$

Where:

N_s : The number of cells connected in series forming the PV module.

V_T : The thermal voltage constant which is approximately $25.85mV$.

G : irradiance (W/m^2).

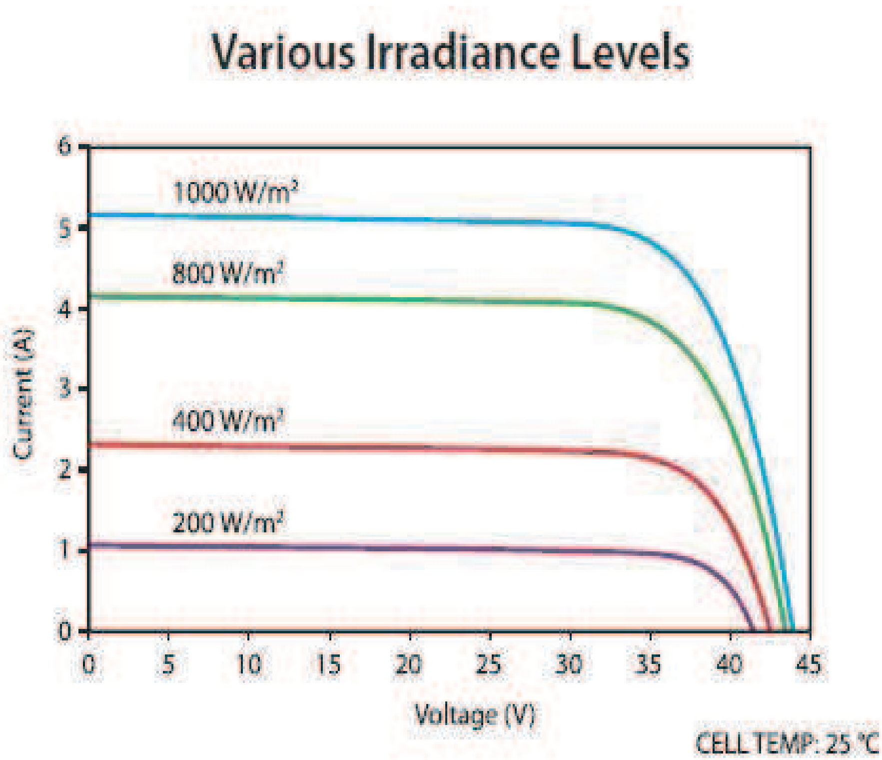

Figure 3.15: Irradiance effect on the I-V characteristics of a PV device.

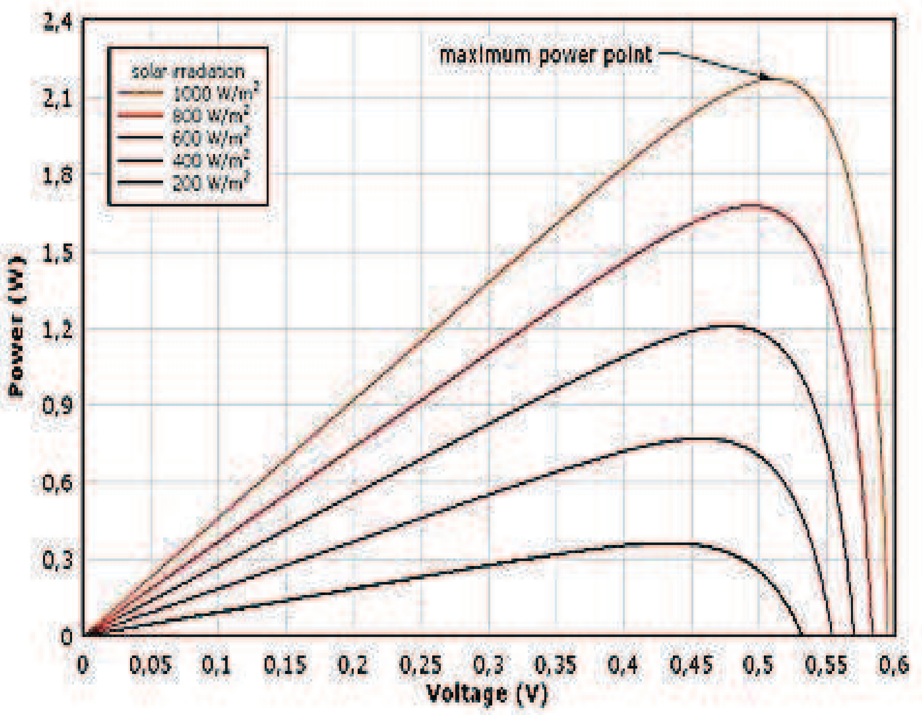

Figure 3.16: Irradiance effect on the P-V characteristics of a PV device.

3.3.4 Maximum power point tracking (MPPT)

As has been mentioned in the previous section, the PV system outputs are significantly affected by environmental conditions specially temperature and solar irradiation. In order to extract the maximum power available from the PV panel, it needs to operate at the Maximum Power Point (MPP). The PV characteristics, in figures 3.11 and 3.12 illustrate that there is always a voltage level at which a maximum power can be extracted. PV panels are usually connected through power electronic converters associated with suitable controllers to be operated at a given reference voltage. A controller with MPPT algorithm can be implemented to insure that the converter operates at the optimal reference voltage. Several MPPT methods have been proposed and implemented for different applications [70]. Selection of the most suitable MPPT technique is driven by different factors such as complexity, convergence speed, and cost.

- Perturb and Observe (P&O) method in addition to Incremental Conductance (I C) method are considered by many researchers as the most widely used MPPT techniques [71]- [72]. Perturbation and Observation (P&O) method's algorithm is based on a perturbation of the reference voltage by small increment and observe the change in output power. Increased output power ($dP/dV > 0$), as illustrated in figure 3.17 [73], indicates that the operating point is to left hand side of MPP and the voltage perturbation is continued in the same direction, whereas, decrease in output power ($dP/dV < 0$) means that the operating point is to right hand side of

MPP and the reference voltage signal should be perturbed in the opposite direction in the next step. The maximum output power can be extracted at MPP at which $dP/dV = 0$.

A flowchart of the perturb and observe MPPT algorithm is shown in figure 3.18 [74]. Perturb and Observe (P&O) method is blamed of not providing MPP accurate tracking under fast changes in atmospheric conditions.

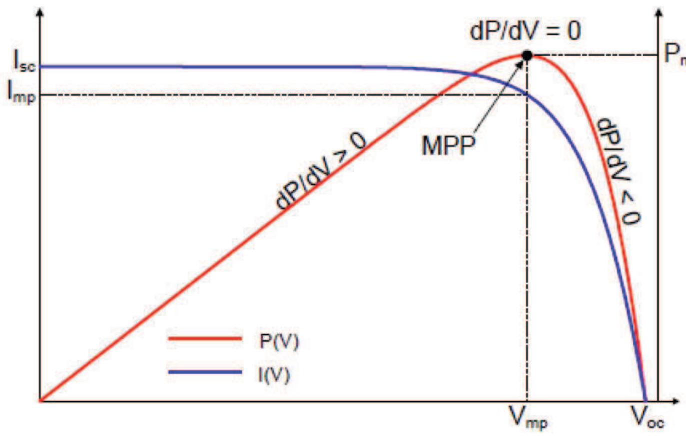

Figure 3.17: Perturbation and Observation (P&O) method.

Figure 3.18: A flowchart of the perturb and observe MPPT algorithm.

- Incremental conductance (IC) method provides better tracking even under fast changes in atmospheric conditions. For the maximum power point, the derivative of the output power with respect to the output voltage is equal to zero.

$$\frac{dP}{dV} = \frac{d(VI)}{dV} = I + V\frac{dI}{dV} = \frac{I}{V} + \frac{dI}{dV} = 0 \tag{3.12}$$

(I/V) represents instantaneous conductance while (dI/dV) represents incremental conductance. Incremental conductance (IC) method's algorithm is based on comparing the incremental panel conductance with instantaneous conductance for tracking the Maximum Power Point (MPP) [75]. As illustrated in figure 3.19 [74], for $((dI/dV + I/V) > 0)$ the operating point is to right side of MPP and the voltage need to be increased in the next step, whereas $((dI/dV + I/V) < 0)$ indicates that the operating point is to right side of MPP.

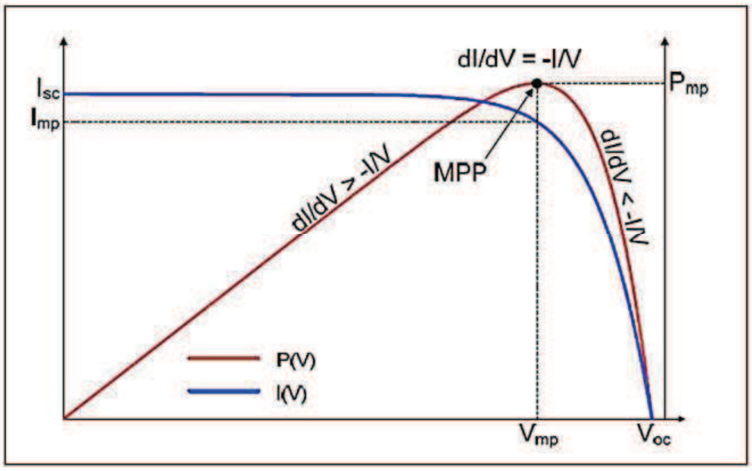

Figure 3.19: Incremental conductance (IC) method.

3.4 Types of PV systems

As illustrated in figure 3.20 [76], PV systems comprise two main types stand alone and grid connected systems.

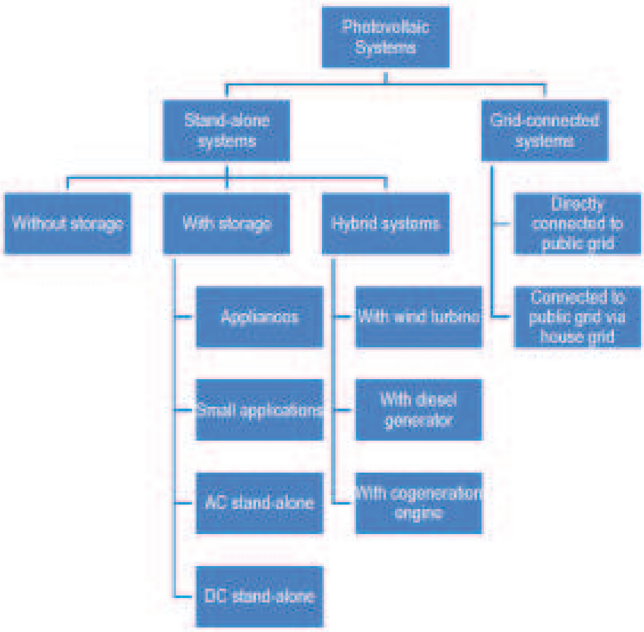

Figure 3.20: Types of PV systems.

3.4.1 Stand-alone systems

Whenever a distribution network is not easily connectable to the grid (remote areas or islands), stand-alone systems make use of renewable energy are interested. Since the PV has a discontinuous and unpredictable output, a battery energy storage system is required to preserve system stability and energy balance of load and generation as shown in figure 3.21 [77].

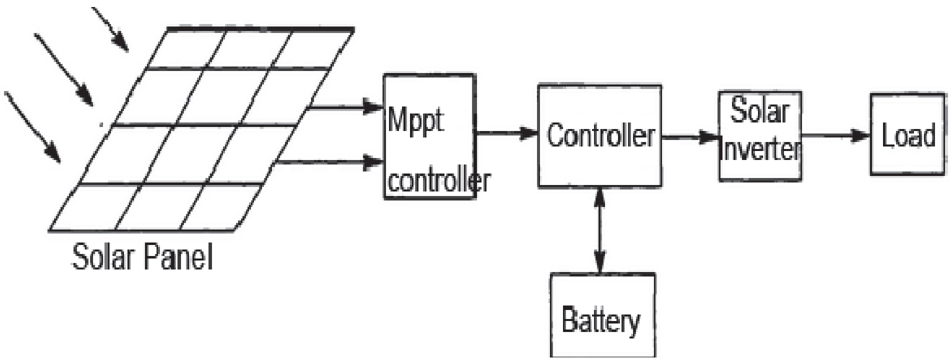

Figure 3.21: PV stand-alone system with a battery storage.

3.4.2 Grid connected systems

In grid connected type the PV system operates in parallel with the electricity grid and may exchange electricity to and from the grid. The PV system frequency and voltage must be synchronized with those imposed by the grid. An example of a grid connected PV system is shown in figure 3.22 [78].

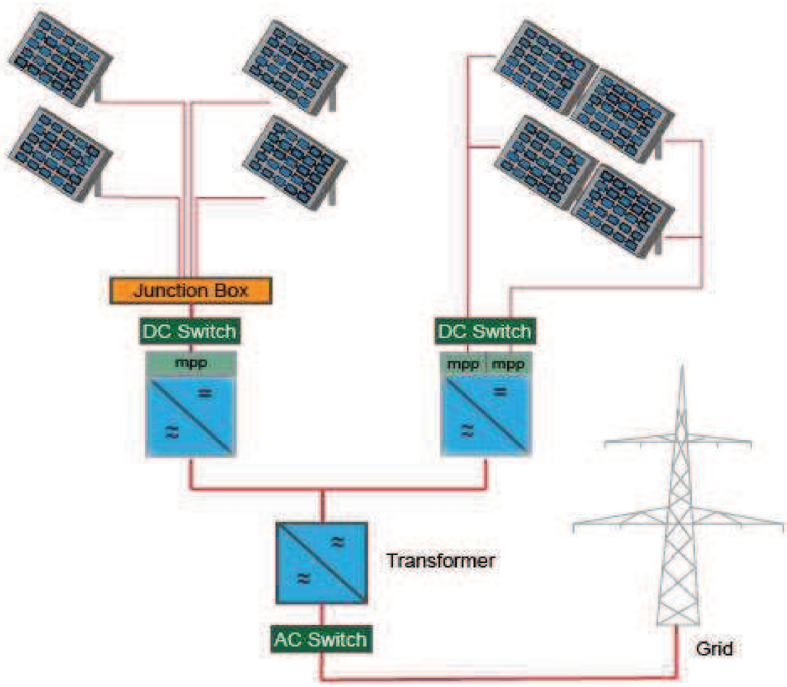

Figure 3.22: PV grid connected system.

Chapter 4

Islanded Distribution Networks supplied by Distributed Generation

4.1 Introduction

The traditional electric power systems use centralized large-scale generating plants and usually located far from load centers. The generating plants are typically utilizing combustion or nuclear technologies. These centralizing systems require long distances transmission networks. In addition to technical and economic issues, traditional systems have environmental disadvantages as; greenhouse gas emission, nuclear waste production. The continuous rise of power demand necessitates a dramatically grown in electricity generation. The annual electricity production for 2012 reached about 22,200 TWh, 70% of which were utilizing fossil fuel [1].

Modern Electric Power Systems move toward decentralization through the deployment and use of Distributed Generation (DG) technologies. The continuous rise of power demand with increasingly tense of traditional energy supply issues as; depletion of fossil fuels, transmission distance, greenhouse gas emission, production of nuclear waste, inefficiencies, power loss and security related issues have promoted a rise number of researches in Distributed Generation technologies [113], [114]. Distributed Generation systems utilize relatively small-scale power generators connected to the Medium Voltage (MV) and the Low Voltage (LV) distribution networks close to the end users, often provide power from renewable energy or fossil energy. MV islanded systems, for economic and political interests, are predicted to attract more attention for management and control of distribution network in future smart grids [115]. Concerning DGs' utilize renewable energy, solar generation plants (PV) seem to be the most promising, in particular in case of small installations: easy installations, prime source wide availability, scalable size plants, almost negligible operational costs, low emission, advance in technology and rapid drop in prices [116], [117]. PV generator plants are attractive options in terms of environmental sustainability and fuel consumption reduction. They have the fastest growing renewable category in the US with a 60% growth rate [118]. However, PV outputs are based more directly on nature and as such they may exhibit large fluctuations and low power quality. This poses a great challenge in maintaining generation /load balance and system's stability and reliability. Energy Storage Systems may be considered as a good alternative approach for tackling these challenges. A common use of energy storage systems is for peak load shaving by absorbing energy during surplus generation and injecting energy back during peak demand. They can be also used as reserve power plants in cases of lack generation or rapid demand perturbation [118].

Referring to grid connected DG plants, Distribution System Operators (DSOs) are called to adopt new planning and management strategies to enhance the DG potentials and to face the DG disadvantages at the same time. Stand-alone systems utilize renewables combined with local energy storage devices can reduce the long-term cost of small-scale power supply system. In islanded operation, the Battery Energy Storage Systems (BESS) bridges the gap between generation and demand, storing energy when excess is produced and releasing when the generation is reduced or absent [1].

In terms of islanded network regulation strategy, DGs and BESS have to be coordinated aiming to maximize the primary sources usage, to reduce losses and to preserve quality of supply, which primarily means frequency and voltage magnitude [119]. For more than one DG supply the islanded system, the total load should be shared between the DG units basing on their rated capacity to avoid over loading of single sources [120]. Several control strategies implementing Energy Storage Systems to deal with DGs intermittency and system stability enhancement have been proposed [121], [122], [123]. A control scheme based on state of charge to reduce the effect of PV fluctuations on system reopens is proposed in [121].

PV plants are usually connected to the grid through power electronic converters and controlled to provide maximum active power with unity generation power factor. A BESS is also interfaced to grid through a converter, operates as a slack node, monitors the network operating conditions, regulates both the voltage and frequency at its connection to preserve energy balance and system stability. For stand-alone systems implementing PV generation plants, storages using Valve Regulated Lead Acid (VRLA) battery are the most commonly used technology, because of cost and availability point of view [124].

4.2 Islanded Network

Whenever a Distribution Network not easily connectable with the main grid (i.e. remote areas and islands), Islanded systems are interested. Stand-alone systems making use of renewable energy sources becomes viable for supplying local networks with weak connection to main grid to preserve end-user power quality in case of temporary blackout. Generally, a stand-alone system, figure 4.1, may operate in grid connected or in islanded mode.

In grid connected mode, the AC bus voltage and frequency are regulated by the main

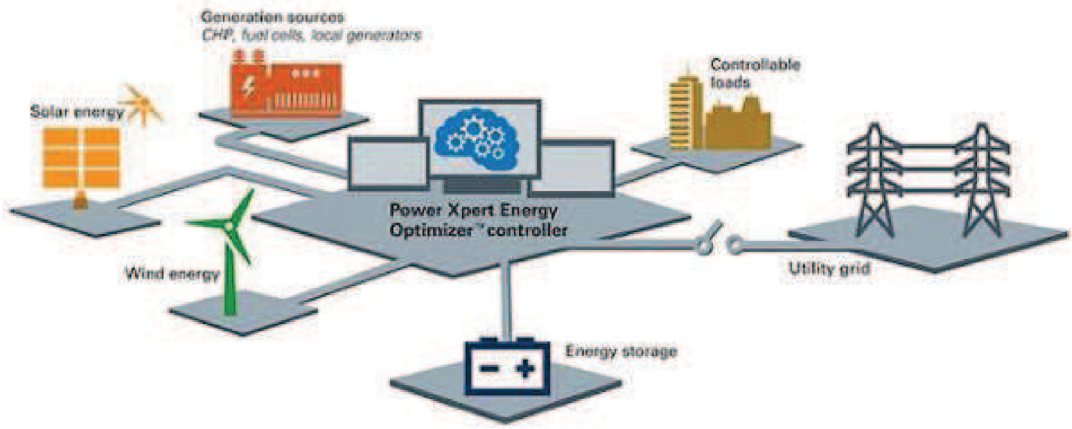

Figure 4.1: Layout of an islanded system

network while all the DGs are called to work as grid following units to exchange power with main grid. However, in islanded mode, DGs must be equipped with the proper controllers to maintain the system voltage and frequency and to regulate their power to preserve generation/Load balance [125].

Control configuration can be classified into centralized or decentralized algorithms. In centralized approach, the central controller receives measurement signals from system's elements, process the data, and sends back commands. The centralized control is considered more flexible for balancing the power between generation and consumption [126]. However, centralized control requires communication systems which become more complicated with increased number of widely spread DGs [127]. Decentralized control, using bus-signaling method (BSM) or frequency bus signaling method (FBS) are proposed in [128] and [129] respectively, to overcome limitation due to communication systems.

Considering that most of DGs are inverters interfaced, the main two kinds of inverters control are:

- PQ Control: the inverter provides a given active and reactive power depending on its reference points. This control is usually achieved by utilizing a current controlled voltage source [130].

- Voltage Source Inverter (VSI) control: the inverter provides demand requirements while preserving defined values for voltage and frequency. Load fluctuations directly impact on the real and the reactive power outputs of the inverter. The VSI approach adopts the concept of frequency and voltage control used in a synchronous machine supplying an islanded system.

For Islanded Systems implementing renewable energy sources DGs integrated energy storage systems (ESS), master/ slave control strategies are commonly considered which comprise:

- Single Master Operation (SMO): in this approach, a VSI (master) is used as voltage and frequency reference whereas all the other inverters (slaves) operate in PQ mode.
- Multi Master Operation (MMO): in which several inverters operate as a VSI with specified droop characteristics [131].

When master-slave control strategy is used to manage PVs integrated battery energy storage systems (BESS) in islanded systems, PV units are usually controlled to provide their maximum available active power (using MPPT control) with no reactive power contribution. Consequently, all reactive power requirement is provided by BESS which negatively affects the BESS ability of active power regulation [132]. Several researches have been carried out to investigate reactive power contribution of DGs [133], [134], [135].

4.3 Developed Control Approach

A SMO master/slave control strategy, implementing BESS and PV to supply an islanded network has been devoloped in detail. The BESS (master) operates as a slack node, while PVs (slaves) are controlled as PQ generators. BESS modulates the voltage and frequency at its point of common coupling (PCC) in order to indirectly control the PVs reference signals. According to BESS operative curve, illustrated in figure 4.2, depending on BESS active power exchanged with the islanded network and batteries SOC, BESS modulates the frequency at its PCC i.e. $\Delta f = f(P_{BESS})$. If the BESS active power overpasses the stability dead-band, a frequency deviation is imposed to control the PVs active power behaviour.

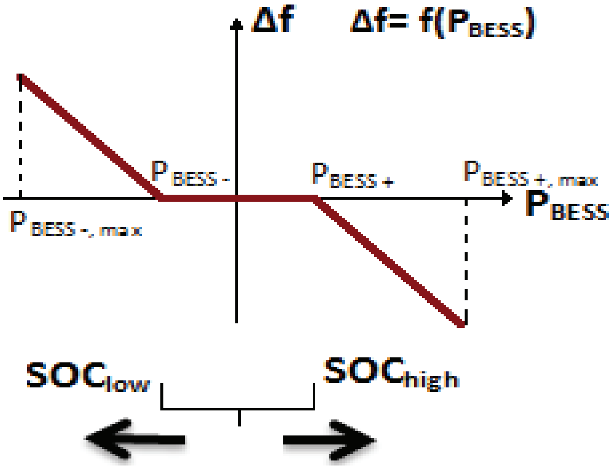

Figure 4.2: BESS operative curve.

On the other hand, figure 4.3 shows the PV operative curve where the active power provided by the PV is a function of frequency deviation ($P_{PV} = f(\Delta f)$). If the stability dead-band is violated by the frequency imposed by the BESS, the PV regulates its active power accordingly.

In this way the BESS is able to rapidly absorb or inject active power up to its rated value in case of rapid overall load fluctuations and modulates PVs references in order to minimize its active power exchanges with the islanded system. Following the same manner PVs regulate their reactive power depending on the voltage modulated by the BESS.

However, for improving the BESS capacity of active power regulation to maintain generation and consumption balance, considering the total output power rating of the converter is fixed, the voltage at PCC of the BESS is modulated aiming to reduce to zero the BESS reactive power exchange with the rest of the islanded system at steady state. In this way, the BESS inverter capability curve is not reduced by reactive generation and the power electronic converter losses are minimized. The developed control strategy uses

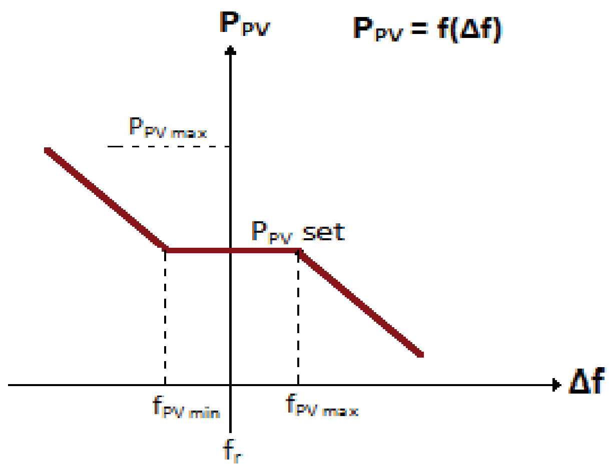

Figure 4.3: PV operative curve.

frequency and voltages to coordinate the BESS power exchanges with the PVs outputs which means, no explicit communication channels are required for the optimal operation of the islanded system.

4.4 Implementation of Proposed Control Strategy in PowerFactory (DIgSILENT) Environment.

PowerFactory (DIgSILENT) is an advanced simulation software package for studying and analyzing of electrical power systems. The software provides a list of simulation functionalities as; Load flow analysis, Short circuit analysis, Harmonics analysis, Reliability analysis, Optimal power flow, among others [136]. The software works within a fully integrated graphical, editing and results windowing environment. Editing windows are designated for system components, from which multiple windows can be opened to show different aspects as shown in figure 4.4 . PowerFactory package incorporates a global library and user library with respective access and modification rights. Global library contains a comprehensive model library, powerful built-in functions and equipment types. The user may define additional control models and calculation functionality (user defined models). This can be done by using DIgSILENT Simulation Language (DSL). DSL allows the creation of any kind of static or dynamic multi-input/multi-output model.

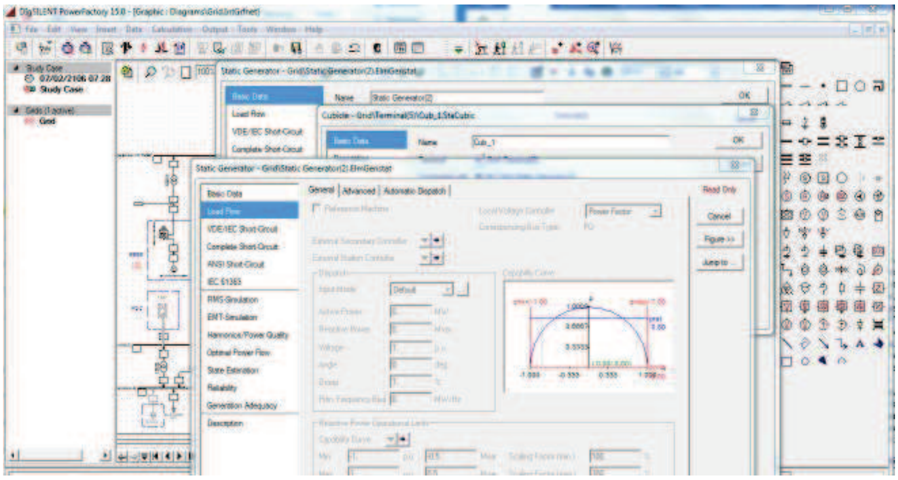

Figure 4.4: Digsilent windows

4.4.1 Model of power electronic converter for DG in DIgSILENT

In recent years the level of DG units in distribution systems has dramatically increased due to several reasons as; environmental concerns, fuel cost uncertainties, liberalization of electricity markets and advances in DG technologies. This growth has benefits, on one hand, as loss reduction, power quality and reliability improvement, and provision of ancillary services. On the other hand, the rising penetration level of distributed generation units has a considerable impact on the control and operation of the power system network. Many renewable energy distributed generation units as PVs and wind turbines

utilize power electronic converters for connection to the network. In order to study the respond of DGs and the grid to steady state and transient conditions, simulation models are required for both the grid network and the inverters of the DGs.
Figure 4.5 [137] shows a single line representation for a DG unit connected to the grid through a power electronic converter. The DC source represents the DG primary source connected to the DC side of the PWM. The AC side of the PWM is connected to the point of common coupling PCC through a LCL filter.

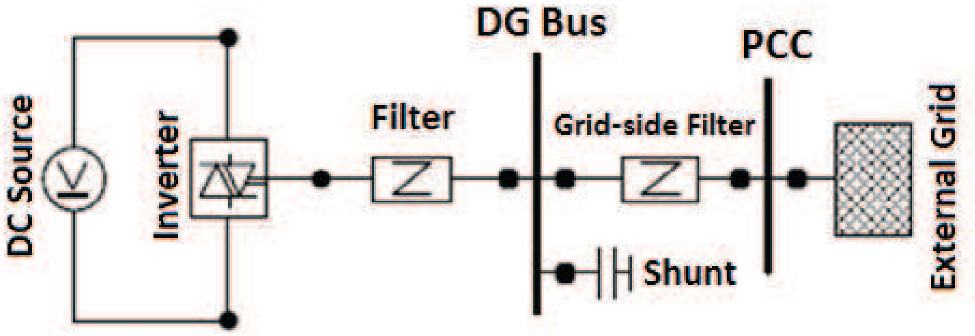

Figure 4.5: Single line representation for a DG unit connected to the grid through a power electronic converter.

The control scheme for a DG utilizing a power electronic converter interface, as proposed in [137], is presented in figure 4.6. Power control and current control algorithms are implemented in this control scheme.
The frame control for modeling of power electronic converter in PowerFactory, as pre-

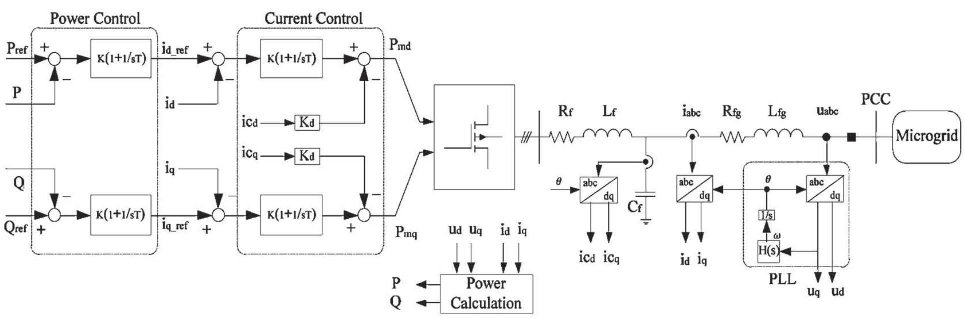

Figure 4.6: Control scheme for a DG utilizing a power electronic converter interface.

sented in figure 4.7, comprises PLL system, ab2dq transformation block, power control (PQ) model, current control model, inverter model, measuring devices and signals flow.

1. **PLL bock:** PLL bock is utilized for synchronization to the grid by providing the synchronous frame reference angle to the (ab2dq) transformation block;

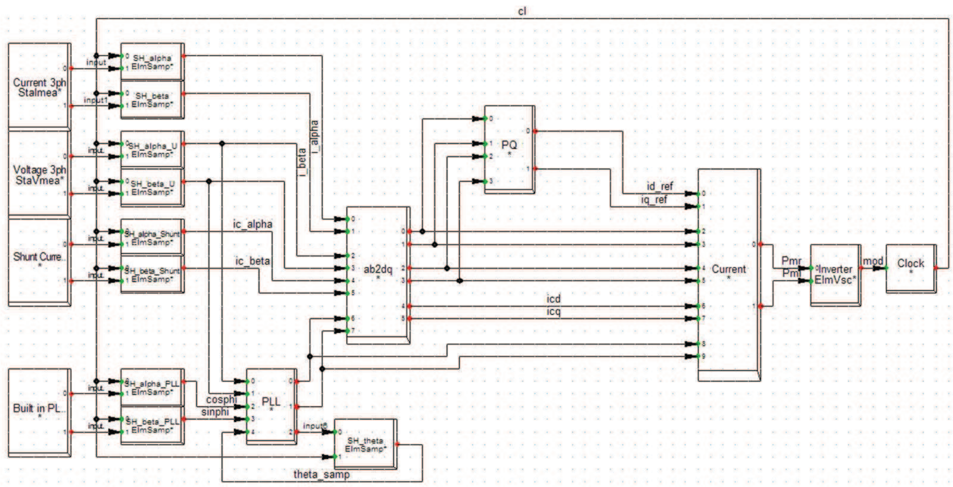

Figure 4.7: Control frame of the DG converter controller implemented in PowerFactory.

2. **ab2dq Transformation block:** The measured abc quantities need to be transformed into a synchronous rotating dq reference frame, to be used for the power and current controllers which operate on dc converter variables. ab2dq Transformation block utilizes 4.1 for abc to dq transformation.

$$\mathbf{I_{dq0}} \quad = \begin{bmatrix} \cos\theta & \cos\theta - \dfrac{2\pi}{2} & \cos\theta + \dfrac{2\pi}{2} \\ -\sin\theta & -\sin\theta - \dfrac{2\pi}{2} & -\sin\theta + \dfrac{2\pi}{2} \\ \dfrac{\sqrt{2}}{2} & \dfrac{\sqrt{2}}{2} & \dfrac{\sqrt{2}}{2} \end{bmatrix} \begin{bmatrix} I_a \\ I_b \\ I_c \end{bmatrix} \tag{4.1}$$

Where: $Idq0$: is the current elements in d, q and 0 axis.

3. **Power control model:** The inputs to this model, as illustrated in figure 4.8, are (u_d, i_d, u_q, i_q) provided by the ab2dq model, and two signal for active and reactive power references which may be provided by a remote controller or given as desired set points;

   The model utilizes the equations defined in 4.2 and 4.3 to calculate the measured active and reactive powers.

$$P = u_d i_d + u_q i_q \tag{4.2}$$

$$Q = u_q i_d - u_d i_q \tag{4.3}$$

Where:
u_d, u_q: are measured voltages at PCC in dq frame.

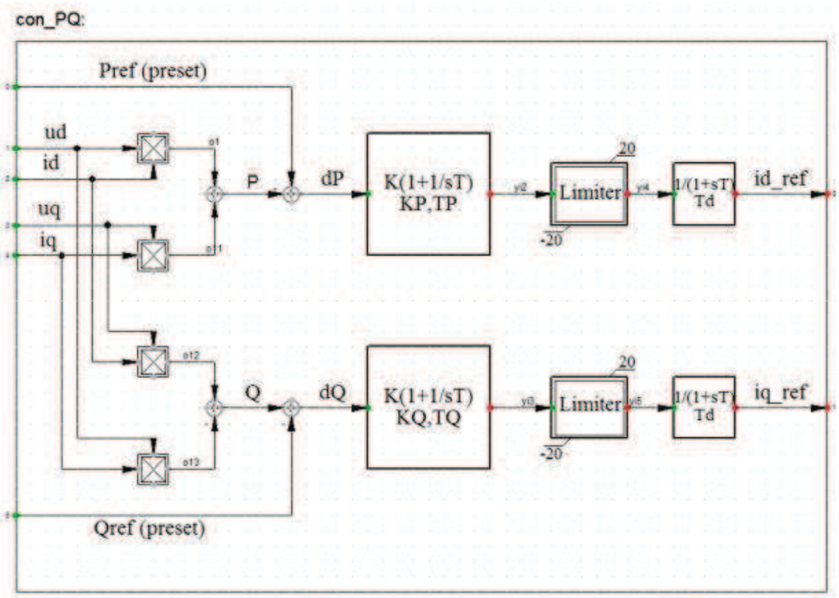

Figure 4.8: Power control model.

i_d, i_q: are measured currents at PCC in dq frame.

The calculated active and reactive powers are compared against their reference values. The differences dP and dQ are regulated by a PI controller to provide dq frame current references ($i_{d_{ref}}$ and $i_{q_{ref}}$) to the current control model.

4. **Current control model:** In the current control model shown in figure 4.9 , the dq frame measured currents (i_d and i_q) are respectively compared against the reference dq frame currents ($i_{d_{ref}}$ and $i_{q_{ref}}$), provided by the power control model. The current errors are processed by standard close loop current regulator with proportional gain (K_p) and integral time constant (τ_i) as defined in 4.4 and 4.5 respectively [137];

$$K_p \approx \frac{\omega_c(L_f + L_{fg})}{V_{DC}} \tag{4.4}$$

$$\tau_i = \frac{10}{\omega_c} \tag{4.5}$$

Where:
ω_c: is the crossover frequency.
L_f and L_{fg}: are the LCL filter inductances on the inverter side and grid side respectively.
The LCL filter's shunt capacitor currents in dq frame (i_{c_d} and i_{c_q}), with a damping gain

of K_d, are added as additional feedback after the PI regulators. The resultant dq frame voltages are converted back into stationary frame $\alpha\beta$ and are fed to the converter model.

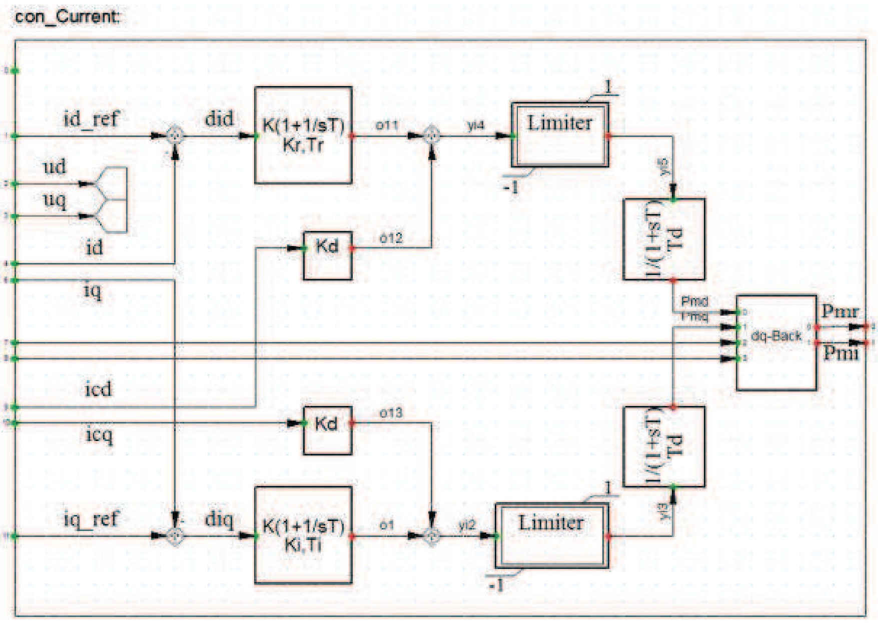

Figure 4.9: Current control model.

4.4.2 Modelling of Battery Energy Storage System BESS

Battery Energy Storage System (BESS) was modelled in DIgSILENT by a DC voltage source and a PWM converter as shown in figure 4.10.

The Battery element is based on the model of a DC voltage source element (ElmDcu). The equivalent circuit of the model, as shown in figure 4.11, consists of an ideal DC voltage source and an output impedance [138].

The internal voltage is kept constant and only the internal resistance R_i is considered while the internal inductance L_i is neglected according to [138].

$$U_i = U_{nom} U_{set} \tag{4.6}$$

$$U_{DC} = U_i - I_{DC} R_i \tag{4.7}$$

Where:

U_i: is the internal voltage in [kV].

U_{nom}:is the nominal voltage of the battery in [kV].

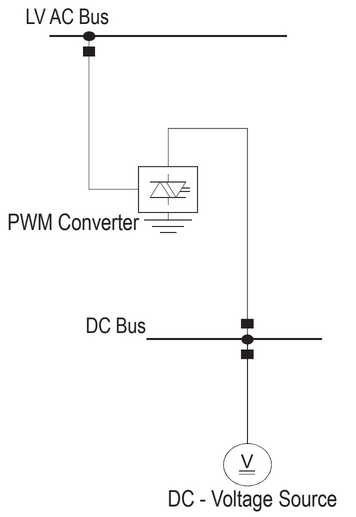

Figure 4.10: BESS modelling in Digsilent using DC voltage source and PWM converter

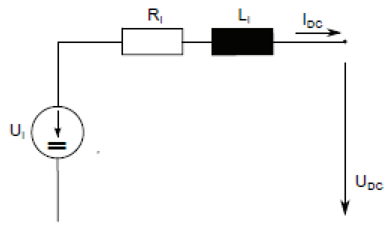

Figure 4.11: DIgSILENT Battery Model

U_{set} :is the voltage setpoint in [p:u:].
U_{DC}:is the DC voltage in [kV].
I_{DC}:is the DC current in [kA].
R_i:is the internal resistance in [Ohm].

In the proposed control strategy, the BESS acts as a master with power electronic converter operating in VSI mode to control the voltage and frequency at its Point of Common Coupling (PCC) with quick dynamic performances and to modulate the references of the slaves (PV generation units) which operate in PQ mode. Figure 4.12 shows the control scheme for the BESS. Frequency calculation block works according to BESS operative curve illustrated in figure 4.2. If the BESS active power overpasses the stability dead-band, and according to the State of Charge (SoC) of batteries, a frequency deviation is imposed to regulate the PVs set points. SoC is evaluated starting from the initial condition and integrating the battery current. Specifically, the BESS forces the PVs to inject more active power in case the BESS has to face a generation deficit and to reduce injection at load reduction or generation surplus.

The voltage at the BESS PCC is modulated aiming to reduce to zero the storage system

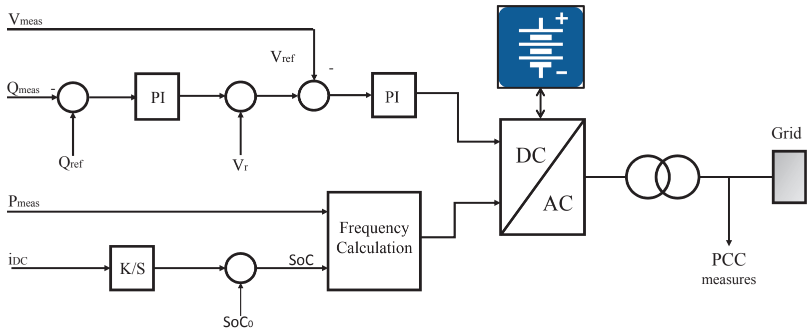

Figure 4.12: Modeling of the BESS VSI unit (master device).

reactive exchange with the rest of the islanded system. In this way, the BESS inverter capability curve is not reduced by reactive generation and the power electronic converter losses are minimized.

For describing the BESS modelling in more details, figure 4.13 shows the BESS frame or composite model which comprises the main BESS controller or common model, PWM converter model, measuring devices and flow signals.

The BESS main controller provides the control signals to the PWM converter in order to

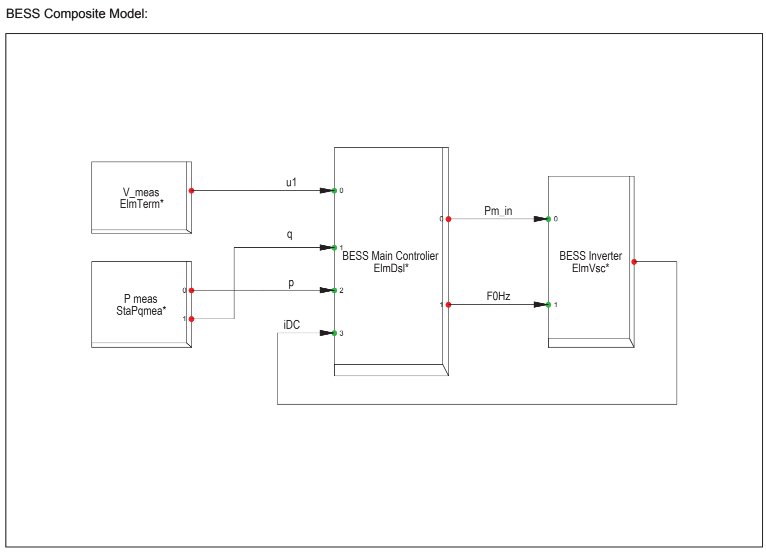

Figure 4.13: BESS frame or composite model.

modulate the frequency and voltage at PCC of the BESS. As illustrated in figure 4.14 the lower part of the BESS main controller, starting with input current i_{DC} and implementing the below equations with given model parameters, I_{Cell} is calculated in the first block, the integrator in the second bock calculates cell capacity in Ah, and the SoC is evaluated in

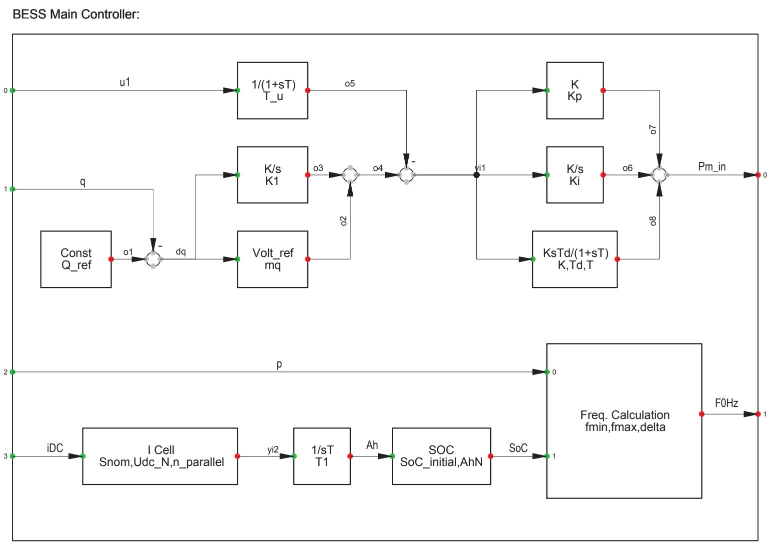

Figure 4.14: BESS main controller.

the third block.

$$I_{cell} = \frac{I_{DC}}{J} \tag{4.8}$$

$$C_{cell,Ah} = \int \frac{I_{DC}}{3600} \tag{4.9}$$

$$SoC = SoC_0 - \frac{C_{cell,Ah}}{C_{BESS,Ah}} \tag{4.10}$$

Where:
I_{cell}: is cell current (A).
I_{DC}: is the current flowing to BESS inverter (A).
J : is the number of arrays connected in parallel.
$C_{cell,Ah}$: is the cell capacity (Ah).
SoC: is the batteries State of charge.
SoC_0:is the initial value of the State of charge.
$C_{BESS,Ah}$: is the BESS total capacity (Ah).
Finally, the fourth block (Frequency Calculation), by using the measured BESS active power and the SoC as inputs and implementing BESS operative curve shown in figure 4.3, evaluates the frequency imposed by the BESS.
On the other hand, the upper part of the BESS main controller, with two inputs (measured BESS reactive power and measured voltage at PCC of BESS), works to provide the modulated voltage at PCC of BESS. The measured BESS reactive power is compared by

Q_{ref}, which is given as a parameter with 0 value aiming to equalize BESS reactive power to zero at steady state condition. The difference signal dq is passed through a droop and an integrator. Summation of the two outputs is considered as a reference signal to be compared against the measured voltage. The error signal is processed by the PID controller to provide the control signal for the modulated voltage. In PowerFactory set values such as gain, time constants, limit values, nominal values for the blocks in the model are defined as Model Parameters. Model parameters evaluate the performance of the model. Parameters of BESS main controller model implemented in the developed control scheme are given in Table 4.1

Table 4.1: Parameters of BESS main controller model.

Parameter	**Description**	**Value**
T_{mis_u}	Filter time constant, voltage meas. path (s)	0.01
T_2	Controller time constant, u_ref path (s)	0.5
mq	Q-V droop slope (pu/pu)	0.03
K_p	Propotional gain Pm_in cotroller (pu)	0.16
K_i	Integrator gain Pm_in cotroller (pu)	250
f_{min}	Minimum frequency (Hz)	49
f_{max}	Maximum frequency (Hz)	51
$delta$	Stability dead band (pu)	0.1
K	PID controller gain (pu)	0.005
T_d	Diff. time constant of PID controller (s)	0.048
T	Integ. time constant of PID controller (s)	0.012
S_{nom}	Nominal Power (VA)	1000000
V_{dc_N}	Battery volatage (V)	720
$n_{parallel}$	Number of parallel rows	34
T_1	Integrator time constant, DC current path (s)	3600
$SoS_{initial}$	Initial valur of battery state of charge (pu)	0.5
AhN	Cell capacity (Ah)	40
$Q_{refBESS}$	BESS reactive power reference value (pu)	0
K_1	Integrator gain, u_ref path (pu)	0.05

4.4.3 Modelling of PV Generation Plants

According to the developed control strategy the following considerations must be pointed out;

1. PV generators work as slaves DG units with PQ control.;
2. In grid connected mode, PVs provide their maximum available active power.;
3. In islanded mode, PVs active power outputs are regulated considering both the primary source availability and the frequency deviation imposed by the BESS ($P_{pv} = f(\Delta f)$);
4. PVs reactive power outputs are evaluated according to the voltage reference signal modulated by the BESS, at their PCC. The voltage steady-state condition is reached at zero BESS reactive power, i.e. the reactive power is fully supplied by PVs.;

Figure 4.15 shows the control frame for PV plants developed in DIgSILENT Power Factory environment. The PV generation model considers the solar radiation availability and the ambient temperature to define the voltage and current parameters on the Direct Current (DC) side of the PV inverter. The following models; solar radiation, temperature, photovoltaic, active power reduction, and static generator are included in the powerfactory built in template control frame as described in appendix (A.1.2). The other three models; active power control, reactive power control, and PV main controller shall be described in this section:

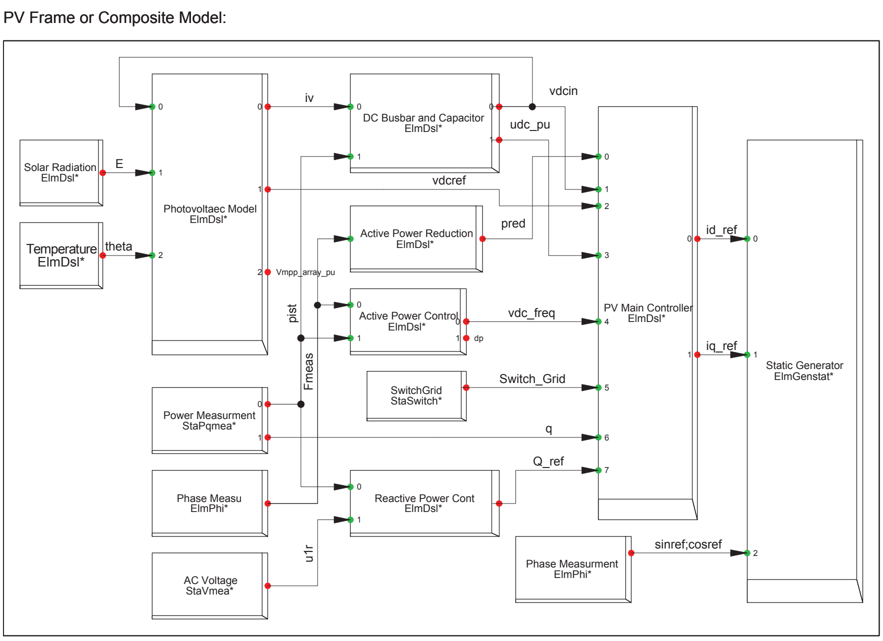

Figure 4.15: PV Frame or Composite model.

- **Active power control model:** As illustrated in figure 4.16, the model has two inputs, measured frequency F_{meas} and measured PV active power P_{in}. The measured frequency is compared with frequency reference, filtered, and used as an input to an integral controller. Block Pset_2 has the signal provided by the integrator and the measured frequency signal as two inputs along with P_0, f_{pv_min}, f_{pv_max} and p-f droop slope (m_p) as parameters. This block provides P_{ref} as defined in 4.11.

$$P_{ref} = P_0 + m_p(f_r - f) + K_i \int f_r - f)dt \tag{4.11}$$

Where:
P_0: is initial PV active power (MW).
m_p: is p-f droop slope.
f_r : is the rated frequency(Hz).
f : is the measured frequency (Hz).
f_{pv_min} and f_{pv_max}: are limits of the dead-band (Hz).
The signal P_{ref} is compared against the measured PV active power (P_{in}), the resultant signal dp is used as an input to a PI controller to provide the reference signal $vdcref$ for the PV main controller to regulate the PV active power according to the frequency imposed by the master (BESS).
As demonstrated by eq 4.11 the PV can provide primary control $[m_p(f_r - f)\ ]$ and secondary control $[K_i \int f_r - f)dt]$. PV contribution in primary or secondary control can be modified by adjusting models parameters. Model parameters are listed in

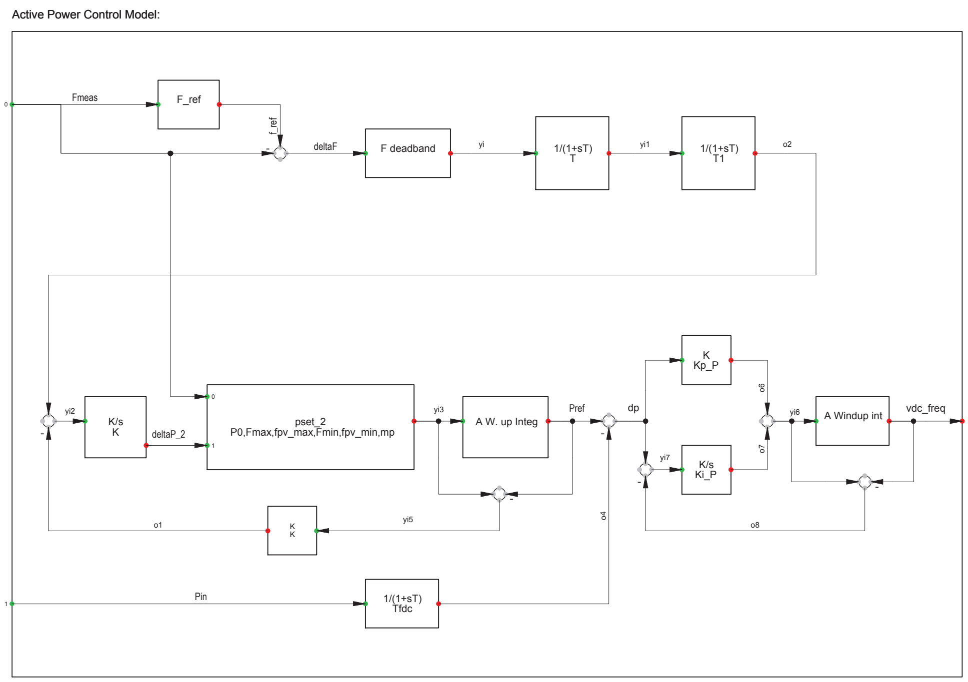

Figure 4.16: Active power control model.

table 4.2.

Table 4.2: Parameters of active power control model.

Parameter	Description	Value
T_{fdc}	Filter time constant, act. power meas. path (s)	0.005
K_{p_p}	Proportional gain of PI parallel controller (pu)	0.2
K_{i_p}	Integrator gain of PI parallel controller (pu)	50
T_1	Filter2 time constant (s)	0
K	Integrator gain (pu)	0.3
T	Filter1 time constant (s)	0
P_0	Active power initial setpoint (pu)	0.3
F_{max}	Maximum frequency (Hz)	51
f_{pv_max}	PV stability dead band upper limit (Hz)	50.2
F_{min}	Minimum frequency (Hz)	49
f_{pv_min}	PV stability dead band lower limit (Hz)	49.8
mp	p-f droop slope (pu/pu)	0.2

- **Rective power control model:** This model as illustrated in figure 4.17, has two input signals; the measured voltage at PCC of the PV (u_{r1}) and the measured active power of the PV (P). The measured voltage is compared with the reference voltage, and the resultant signal used as an input to an integral controller. The output of the integrator, along with measured active power P, and voltage error du are implemented in block Q_{ref} with use of model parameters; mq , Q_{min}, and Q_{max}, to evaluate PV reactive power reference Q_{ref} for the PV main controller according to the voltage modulated by the master (BESS) as defined in 4.12.

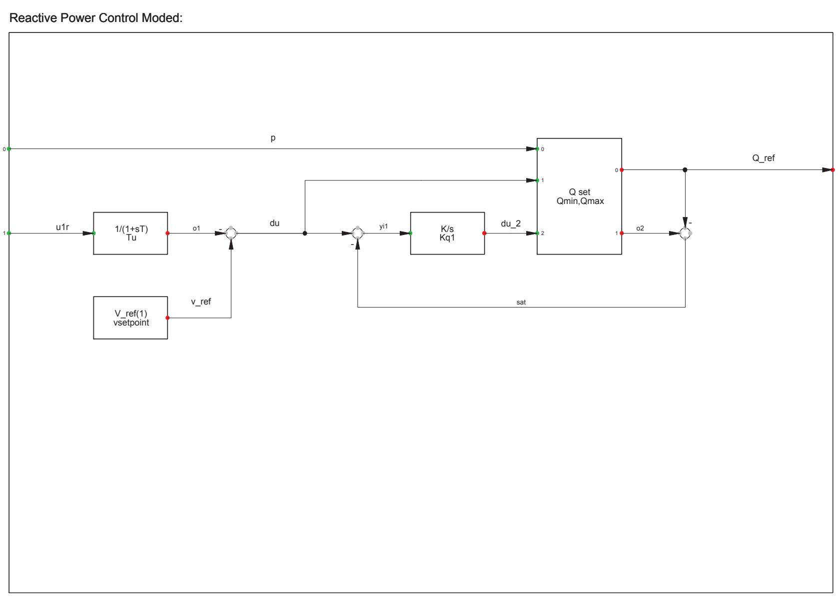

Figure 4.17: Reactive power control model.

$$Q_{ref} = m_q(v_r - v) + K_i \int v_r - v)dt \tag{4.12}$$

Where:

m_q: is q-v droop slope.

v_r : is the rated voltage (V).

v : is the measured voltage (V).

Q_{min}, and Q_{max}: are reactive power limits (p.u.).

Model parameters are listed in table 4.3.

Table 4.3: Parameters of reactive power control model.

Parameter	Description	Value
T_u	Filter time constant (s)	0.1
$V_{setpoint}$	Volage set point (V)	1
K_{q1}	Integrator gaim (pu)	200
Q_{min}	Reactive power maximum limit (pu)	0
Q_{max}	Reactive power minimum limit (pu)	1

- **PV main controller model:** The PQ control scheme is implemented to regulate the active and reactive power outputs of the PV generators. Making use of Park's transformation, AC quantities are converted to DC quantities in *dq*- frame. The phase locked loop (PLL) synchronizes the reference frame with the voltage vector resulting in a constant direct axis component voltage V_d and a zero quadrature voltage component V_q. Hence the active and reactive power outputs of the PV can be regulated by controlling the dirct and quadrature axis components of current, i_d and i_q respectively as defined in 4.13 and 4.14 [139].

$$P_{pv} = v_d i_d \tag{4.13}$$

$$Q_{pv} = -v_d i_q \tag{4.14}$$

Therefore, power set points can be used for evaluating the reference currents, i_{dref} and i_{qref}, to respectively regulate the active and reactive power outputs of the PV as defined in 4.15 and 4.16.

$$i_{dref} = \frac{P_{ref}}{v_d} \tag{4.15}$$

$$i_{qref} = -\frac{Q_{ref}}{v_d} \tag{4.16}$$

The PV main controller model, as shown in figure 4.18 has two reference signals for the active power regulation;

1. $vdcref$ from the photovoltaic model for providing the maximum active power available by the primary source.;
2. P_{freq} from the active power control model for regulating the active power according to the frequency deviation imposed by the BESS.;

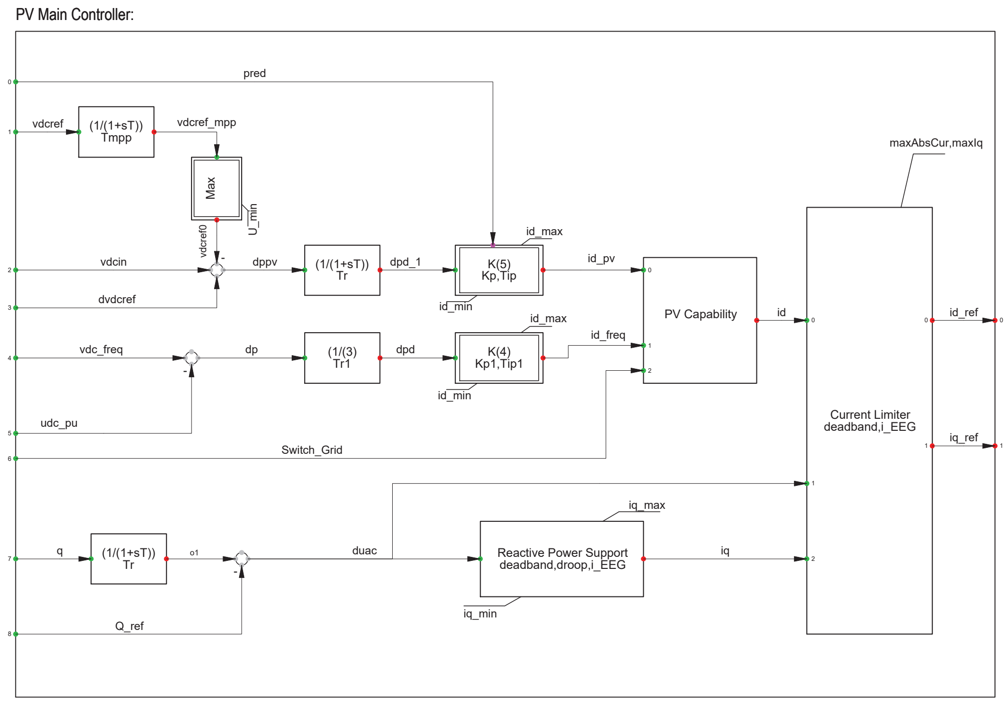

Figure 4.18: PV main controller model.

These two signals are compared with dc voltage signal from dc busbar and capacitor model, the errors are eliminated by PI controller to evaluate the two currents i_{dpv} and i_{dfreq}, within the limit parameters i_{dmin} and i_{dmax}, which are passed to PV capability block. In PV capability block, depending on the grid status switch (0 grid isolated OR 1 grid connected), in islanded mode the PV active power is regulated by frequency deviation reference signal P_{freq} within the limits of the maximum availability by the primary source reference signal $vdcref$. In grid connected mode only $vdcref$ reference signal is used to provide the maximum available active power with implementation of P_{red} signal provided by active power reduction model to decrease PV active power output in over frequency transient according to a p-f characteristic shown in figure 4.19 [131]. The output of the PV capability block is passed through the current limiter to provide the d-axis component of the reference current i_{dref} which regulate the active power output of the static generator. On the other hand, reactive power regulation can be achieved by controlling i_{qref} as in 4.16. The reference signal Q_{ref} is provided by the reactive power control model, as have been described previously in this section. Q_{ref} is compared against the measured reactive

power of the PV, the error is injected to the reactive power support block. The reactive power support block using Q-V characteristic with a deadband and droop control, as shown in figure 4.20 [131], provides the current i_q within limit parameters i_{qmin} and i_{qmax} for the current limiter to evaluate the q-axis component of the reference current i_{qref} which regulates the reactive power output of the static generator. The deadband and droop are defined as model parameters and can be changed according to the implemented standard recommendations.
Model parameters are listed in table 4.4.

Table 4.4: Parameters of PV main controller model

Parameter	**Description**	**Value**
T_{r1}	Measurment delay (s)	0.001
T_{mpp}	Time delay MPP tracking (s)	5
$deadband$	Dead band for AC voltage support (pu)	0.1
$droop$	Static for AC voltage support	2
i_EEG	0 = *acc.* TC2007; 1 = *acc.* SDLWindV	1
T_r	Measurment delay (s)	0.001
K_p	Propotional gain, id_pv PI controller (pu)	0.005
T_{ip}	Integrator time constant id_pv PI controller (s)	0.03
K_{p1}	Propotional gain, id_freq PI controller (pu)	5
T_{ip1}	Integrator time constant id_freq PI controller (s)	0.03
U_{min}	Minimum allowed DC voltage (V)	333
i_{q_min}	Min. reactive current limit (pu)	1
i_{d_min}	Min. active current limit (pu)	0
i_{q_max}	Max. reactive current limit (pu)	1
$maxAbsCur$	Max. allowed absolute current (pu)	1
$maxI_q$	Max. abs reactive current in normal operation (pu)	1
i_{d_max}	Max. active current limit (pu)	1

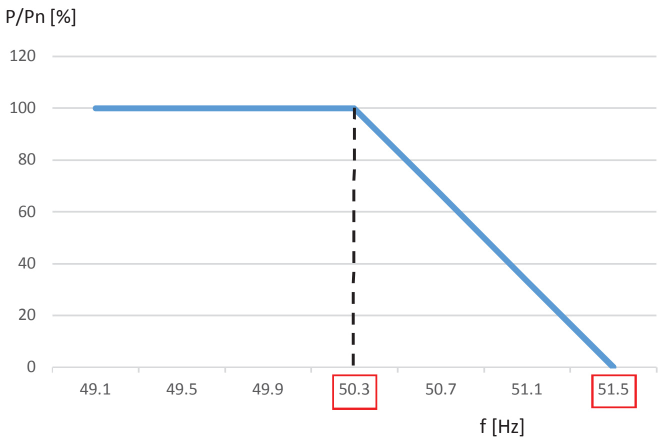

Figure 4.19: p-f characteristic as stated by Italian CIE standard 0-16.

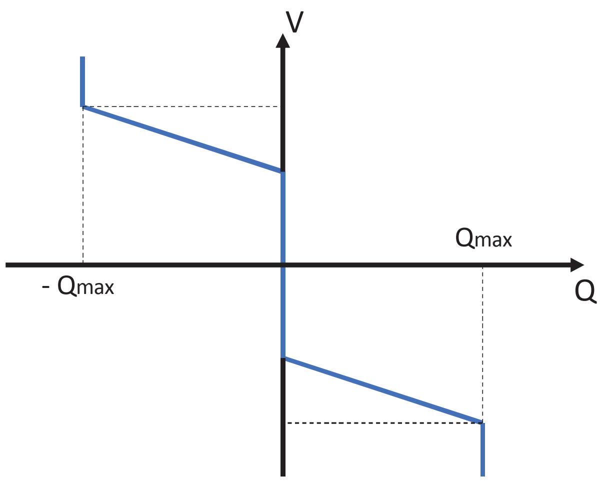

Figure 4.20: Q-V characteristic with a deadband and droop control as stated by Italian CIE standard 0-16.

4.5 Simulation and Results

4.5.1 Identification of the case study

A MV distribution network for a remote typical Libyan oasis town (Al-Kufra) is assumed as a case study. Al-Kufra is located in the southern east of Libya in an area with an annual Direct Solar Irradiance of more than $2800kWh/m^2$ [5]. Despite of this large energy resource the area experiences permanent outages which last for days in certain occasions. Al-Kufra area network is fed through a long, 800 km, radial transmission line from the north with a local gas power plant at sub-transmission system as shown in figure 4.21. The network, as shown in figure 4.22, comprises 7 distribution substations ranged from 2MVA to 13MVA and supplied individually from a sub transmission system [140]. The mentioned distribution networks are considered as weakly connected to the grid because of the long transmission line crossing the desert, lack of maintenance and security issues. A MV (11kV) distribution network is modeled for the case study. The modelled network, as reported in figure 4.23, comprises:

- Two main step down transformers 66/11kV, 7.5MVA each;
- Twenty two bus bars;
- Twenty equivalent loads with overall peak load of 2.365 MVA;
- Twenty two Connection overhead lines;
- Six step-up or step down transformers;

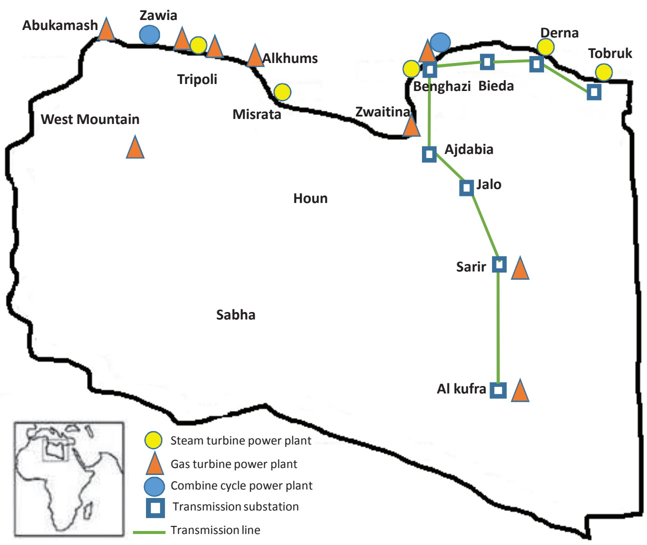

Figure 4.21: Generation power plants and Transmission line from Benghazi to Al Kufra.

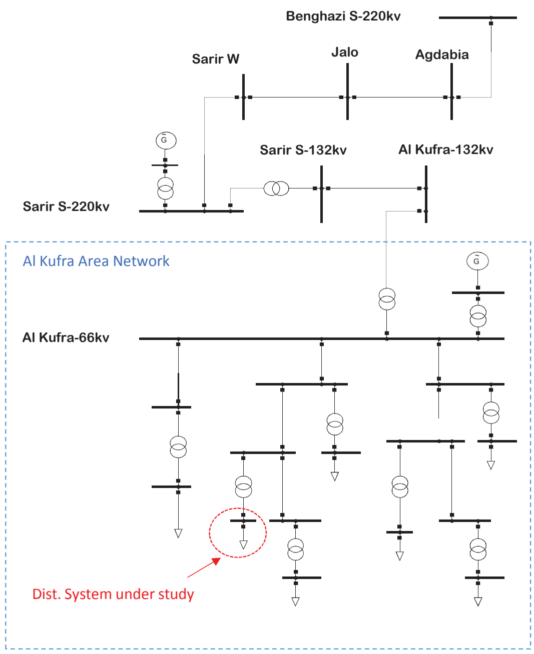

Figure 4.22: Al Kufra network and feeding transmission line.

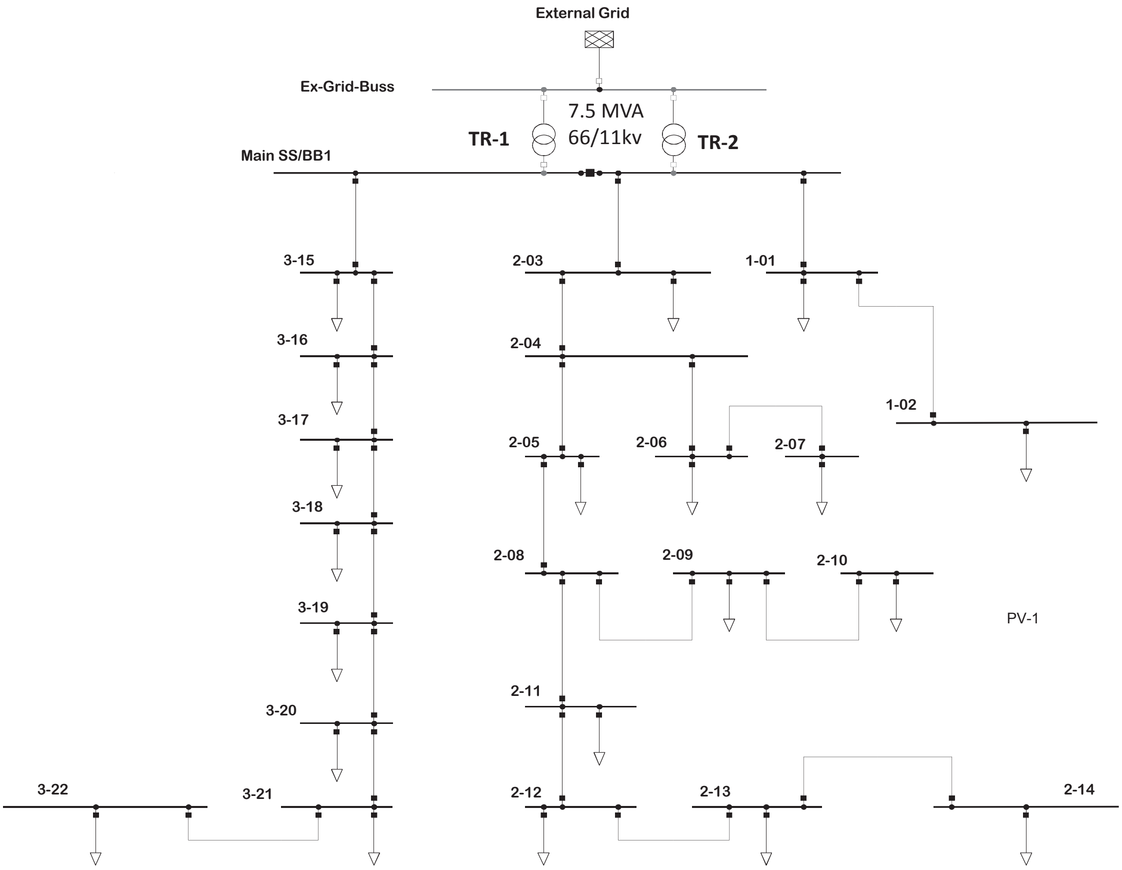

Figure 4.23: Case study single line representation.

4.5.2 steady-state conditions and network power quality levels

Distributed Generators (DG) have the following advantages, among others, voltage profile improvement, power losses reduction , decrease in transmission and distribution lines loading, and an improvement of distribution system efficiency and security of supply [141]. Simulation in DIgSILENT Power Factory environment was carried out considering different scenarios in steady state conditions to investigate the benefits of implementing distributed generation (DG) technologies using solar energy resources PV and battery storage system to improve system power quality level.

4.5.2.1 Voltage profile;

- **Grid-connected mode:**
  Load flow study is carried out to investigate the passive network voltage profile, it appears that in normal operation the voltage levels of the different nodes are somewhat uneven. Figure 4.24 shows the system voltage profile Grid-connected

mode, without any DG. In particular, buses $(2-14)$, $(2-13)$ and $(2-12)$ at feeder no. 2 have the lowest and unacceptable voltages.

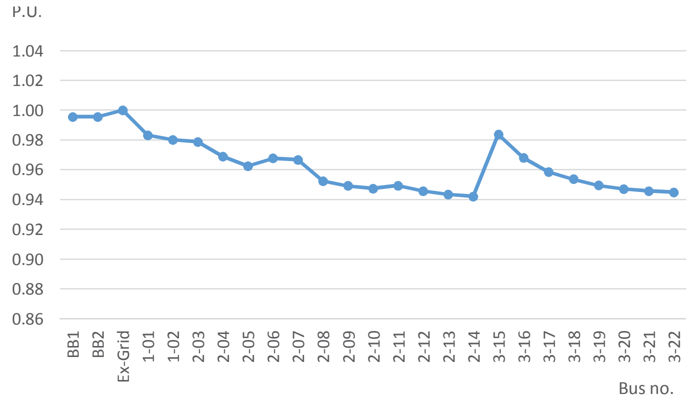

Figure 4.24: System voltage profile Grid connected without any DG.

At first, distributed generation could be used to improve the voltage profile at the more depressed nodes. To this aim a load sensitivity analysis has been implemented to find the sensitivity ratio [(dv/dp)/(dv/dq)] for feeder no.2 at nodes $(2-14), (2-13), (2-12)$. Bus $(2-14)$ is found to be the most effective as shown in figure 4.25 and thus chosen as a good location for the first DG.

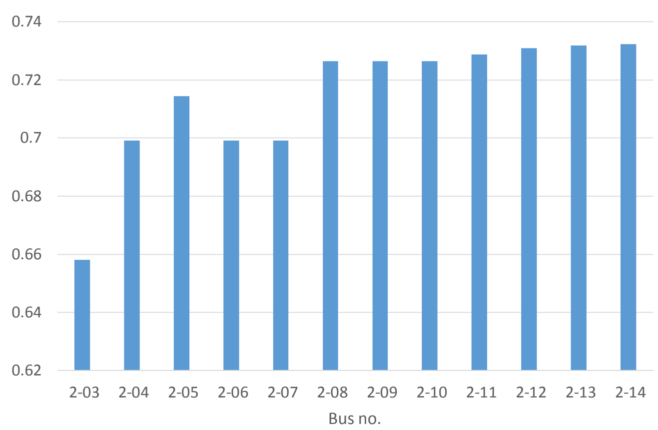

Figure 4.25: Sensitivity ratio at bus (2-14).

Figure 4.26 shows voltage profile for system in grid connected mode with one DG at bus $(2-14)$, some node voltages are still unacceptable.

Running load flow analysis and using sensitivity ratio, with the above described procedure, a second DG was located at bus $(3-22)$ and a third DG was located at bus $(1-02)$ as illustrated in the single line diagram of the case study shown in figure 4.27.

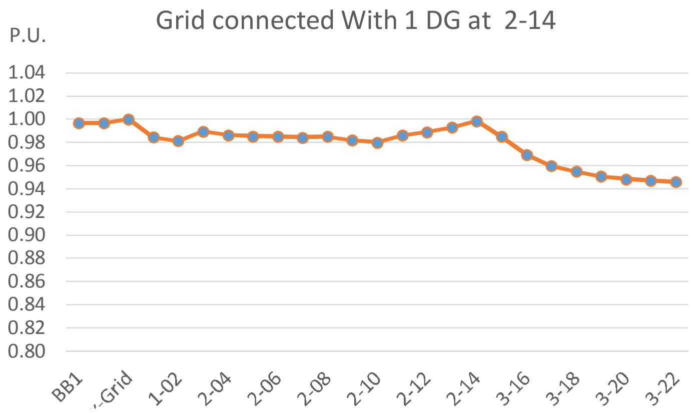

Figure 4.26: System voltage profile Grid connected with one DG at bus (2-14).

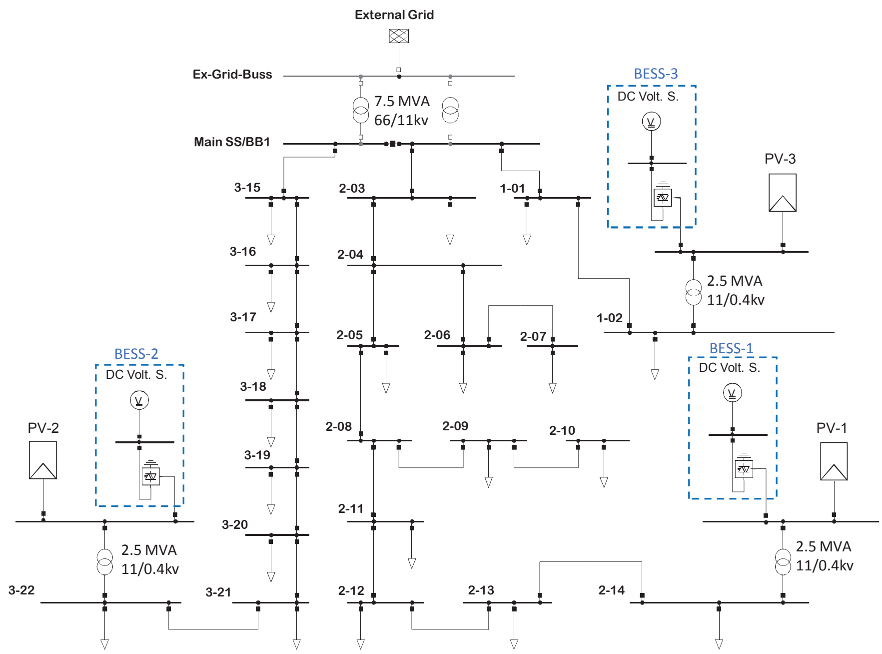

Figure 4.27: Single line diagram of the case study with proposed BESS and distributed PV generation units at selected locations

- **Islanded mode :**

  In a second step we can think of using the DG as a backup system during the frequent and prolonged blackouts. In this case system voltage profile, in islanded mode with three DGs at bus' $1-02$, $2-14$, $3-22$ is presented in figure 4.28.

  Figure 4.29 demonstrates the improvement in voltage profile by implementing DG technologies both in grid connecting and islanded mode.

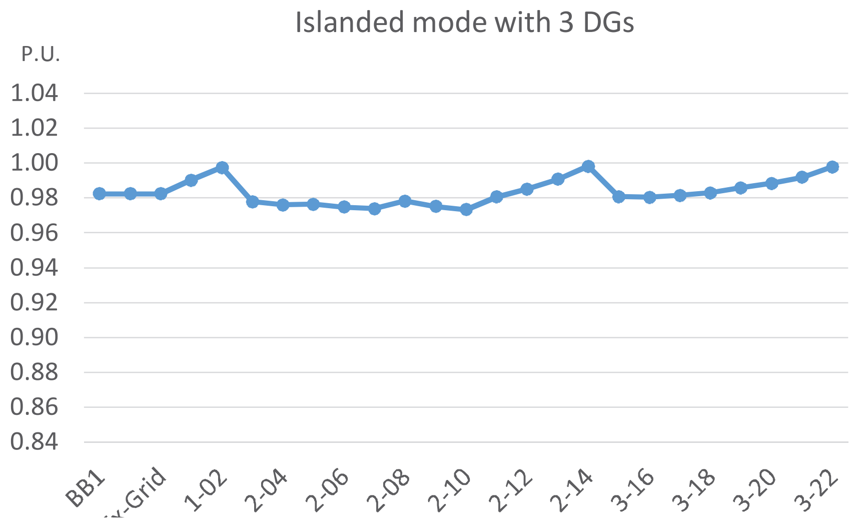

Figure 4.28: System voltage profile in islanded mode with 3 DG's.

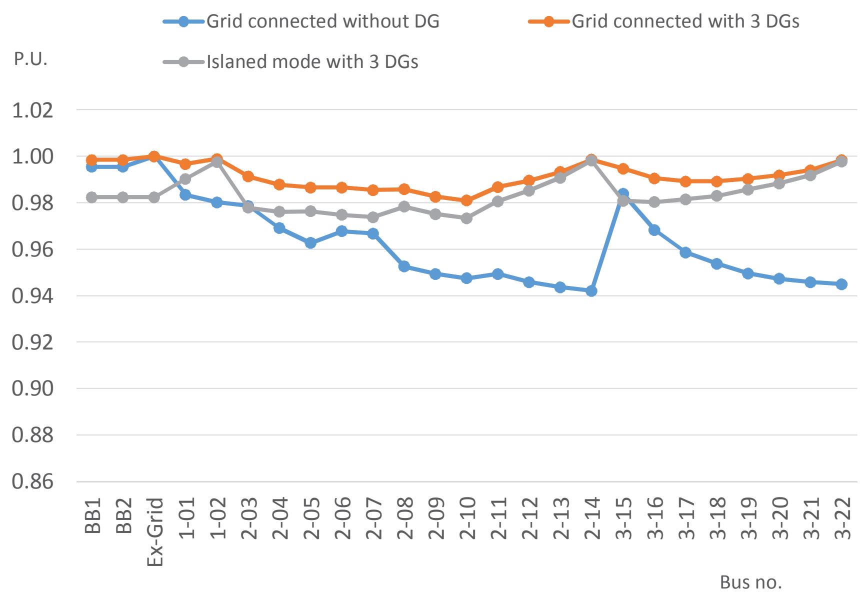

Figure 4.29: Voltage profile with and without DGs in grid connected and islanded modes.

4.5.2.2 Lines loading and power losses

Distributed generation units are usually installed close to the end user, as a result of that lines' loading and consequently power losses are expected to be reduced. Figures 4.30 and 4.31 illustrate respectively the benefits of reduction in lines loading and losses due to the use of DGs.

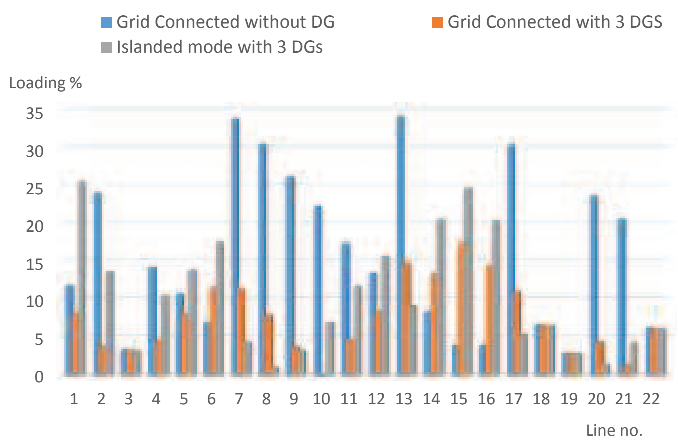

Figure 4.30: Lines Loading with and without DGs in grid connected and islanded modes.

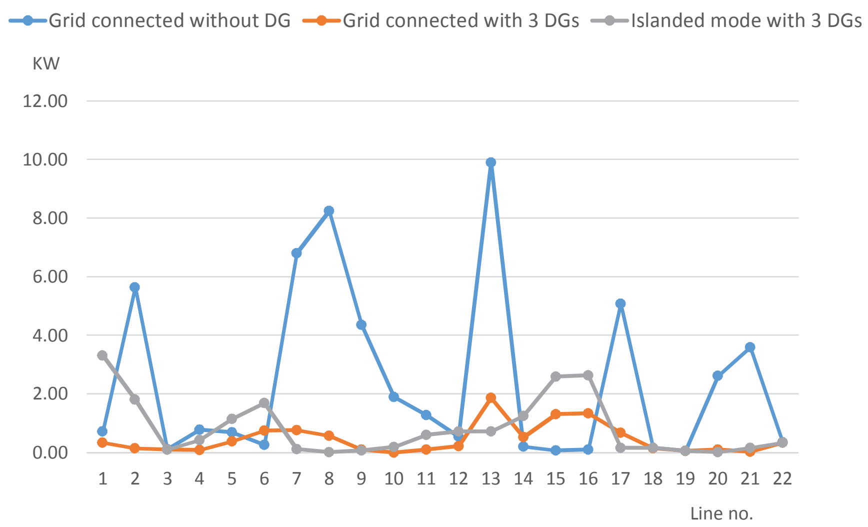

Figure 4.31: power losses with and without DGs in grid connected and islanded modes.

4.5.3 Power, frequency and voltage dynamics.

In section 5.3, a (SMO) master/slave control strategy implementing Battery Energy Storage System (BESS) and PV generation plants was developed for electrification of modeled remote distribution network in islanded mode. A MV (11kV) distribution network is modeled for the case study with proposed BESS and PV generation units at selected locations to supply the load in islanded mode. The modelled network, as reported in figure 4.32, comprises:

- A Battery energy storage system BESS;
- Three PV generation plants (PV1, PV2, and PV3) with capacities of 2, 2, and 1 MVA respectively composed by 2 or 4 equal units (0.5 MVA/unit);
- Twenty equivalent loads with overall peak load of 2.365 MVA;
- Six step-up or step down transformers;
- Twenty two interconnection overhead lines;

The scope of the developed control approach is to coordinate the role of both the solar generation and the energy storage system in facing active and reactive power requirements of the connected loads in islanded mode.

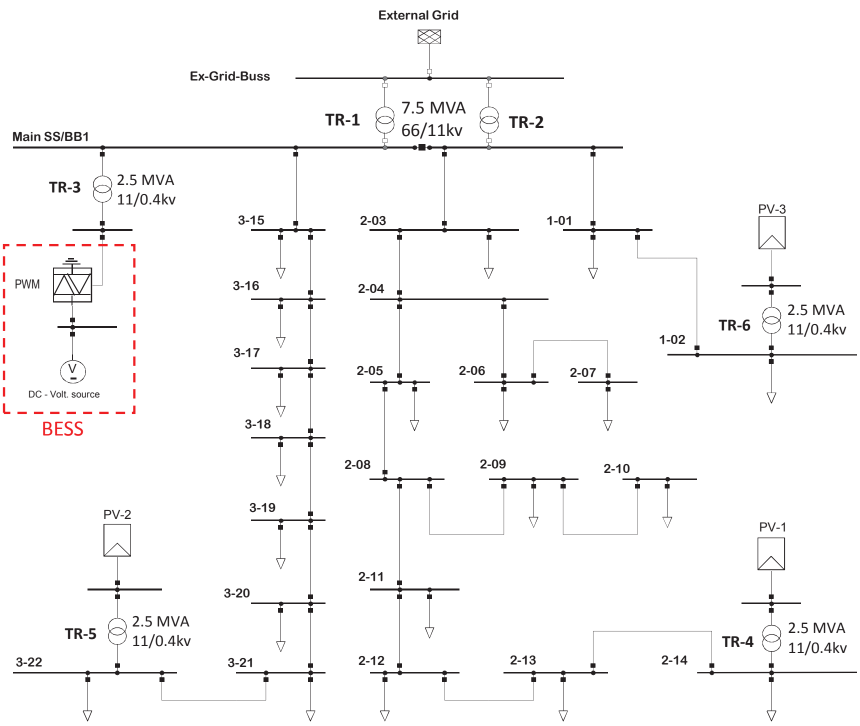

Figure 4.32: Case study for the developed control strategy.

In order to validate the developed models and to investigate the ability of the control scheme in evaluating the contributions of BESS and DGs in islanded network supply, simulations have been carried out making use of DIgSILENT PowerFactory® software. Different operating conditions have been considered to test the accuracy of the control strategy and to measure the system response time to load perturbations.
Starting from a steady-state condition, where the BESS is operating in its stability dead-band with reduced power exchange with the islanded network, the following load perturbation events have been considered.

1. At $t = 4s$, the overall load is step increased from $1.257MW$ to $1.434MW$ by switching on a couple of loads;
2. At $t = 8s$, the overall load is further step increased to $2.076MW$.
3. At $t = 14s$, some end-users are switched off to reduce the overall load to $1.502MW$.

4.5.3.1 Frequency control and active power regulation.

In islanded operation mode, the trend of the active power provided by the PV's, that injected or absorbed by the BESS and the total active power consumed by the load are reported in figure 4.33. The deviation in frequency, due to above mentioned load perturbations and system response according to the developed control scheme, as measured at the PCC of BESS is illustrated in figure 4.34.

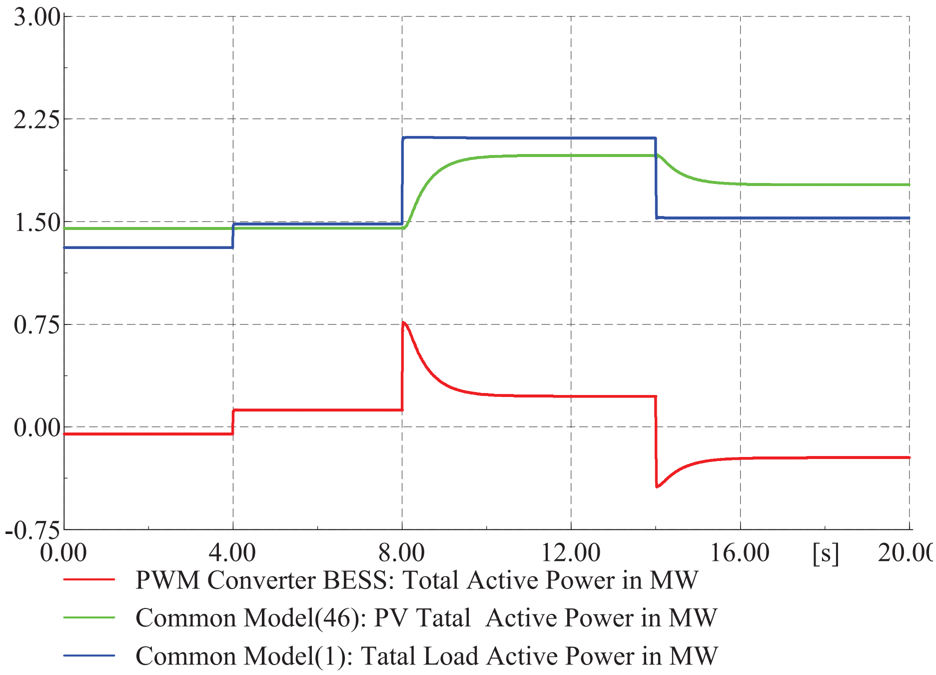

Figure 4.33: Active power trends in islanded mode.

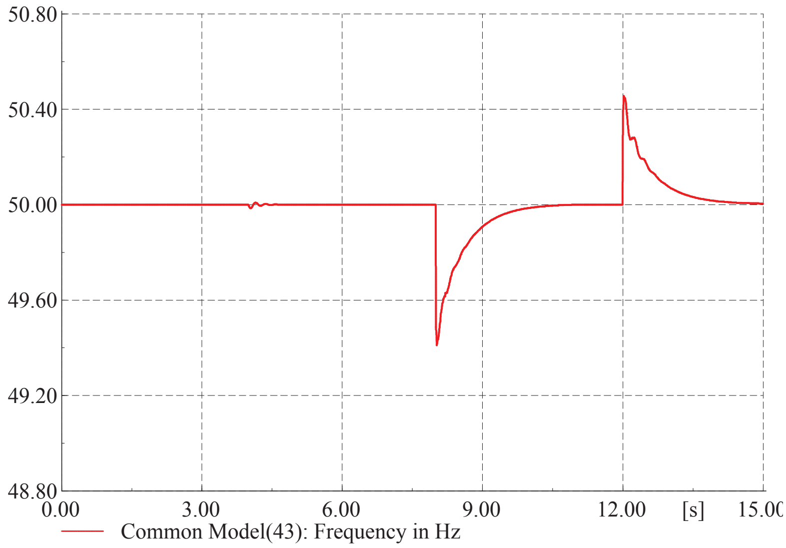

Figure 4.34: Frequency deviation.

From the active power trends and frequency deviation shown in figures 4.33 and 4.34 respectively, it can be observed that due to the first load perturbation the BESS active power exchange with islanded network is increased, but the increase does not overpass the BESS stability dead-band, consequently, no frequency deviation is imposed by the BESS and no active power contribution is required from the PVs. However, the active power provided by the BESS, as a respond to the second load perturbation, overpasses its stability dead-band causing the BESS as a master imposes frequency deviation (under frequency) at its PCC to force the PVs to regulate their active power outputs. As a result of the under frequency deviation, PVs increase their active powers injection, within the primary sources capabilities, to bring the frequency back to its rated value. Conversely, in the third load perturbation, when the BESS active power exchange with the network is decreased and overpassed the stability dead-band, the BESS imposes an over frequency deviation to instruct the PVs to reduce their active power injected to the network aiming to reduce the frequency back to its rated value.

The magnitude of the frequency deviation imposed by BESS depends on BESS active power exchange with the islanded network and SoC of batteries. Whereas, from the PV plants point of view, the frequency alteration as measured at their PCC, forces the plants to maximize their active power outputs, if the primary sources are further available.

As defined by equation 4.11 in section 6.5.2 the PV can provide primary control $[m_p(f_r - f)$] and secondary control $[K_i \int f_r - f)dt]$. PV contribution in primary or secondary control can be modified by adjusting models parameters.

For the PV active power trend presented in figure 4.33, the PVs were set to provide only secondary control. The PV active power trend with primary and secondary control for the same load perturbations is reported in figure 4.35 where we can see a rapid respond due to the primary control and a slower tracking by the secondary control.

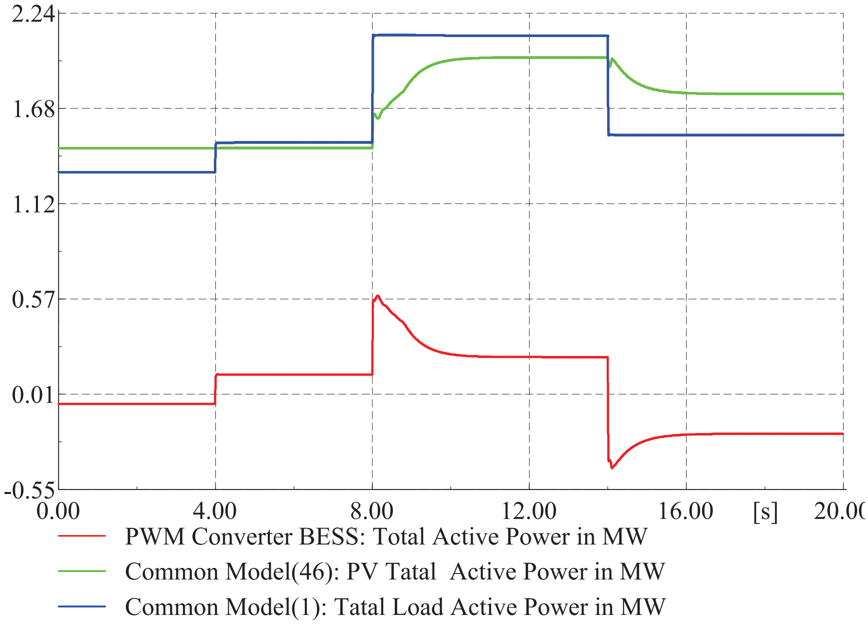

Figure 4.35: Active power trends with primary and secondary PV control.

On another hand, in grid connected mode, the PV generation plants provide the maximum active power available by the primary source as illustrated in figure 4.36. The surplus power is injected to the grid.

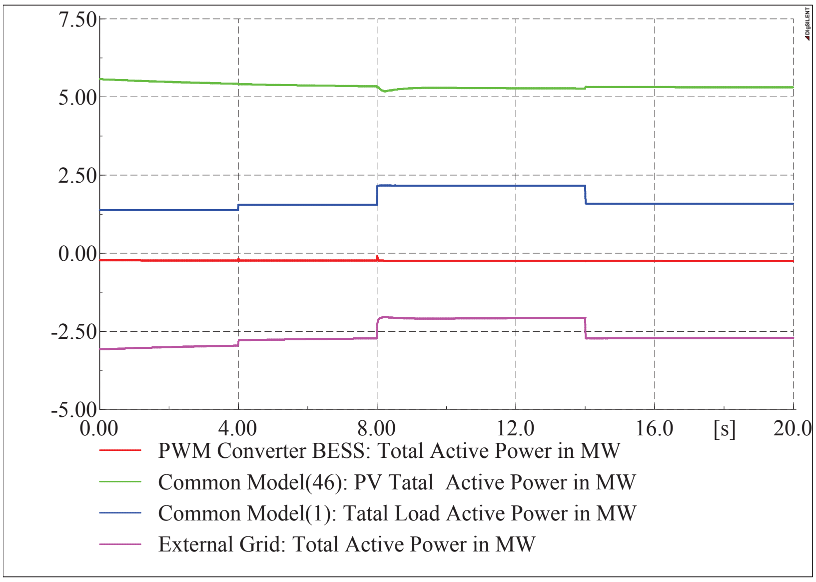

Figure 4.36: Active power trends in grid connected mode.

4.5.3.2 Voltage control and reactive power regulation.

The BESS provides rapidly the reactive power required by any load perturbation, as reported in figure 4.37, then the BESS modulates the voltage at its PCC to force the PVs to regulate their reactive power outputs aiming to reduce the reactive power of the BESS to zero and keeping the voltage levels close to $1p.u.$ as presented in figure 4.38. In this way, the PVs provide all reactive power network requirements. Consequently, the BESS inverter capability curve is not reduced by reactive power generation improving the BESS capacity of active power regulation and minimizing the power electronic converter losses.

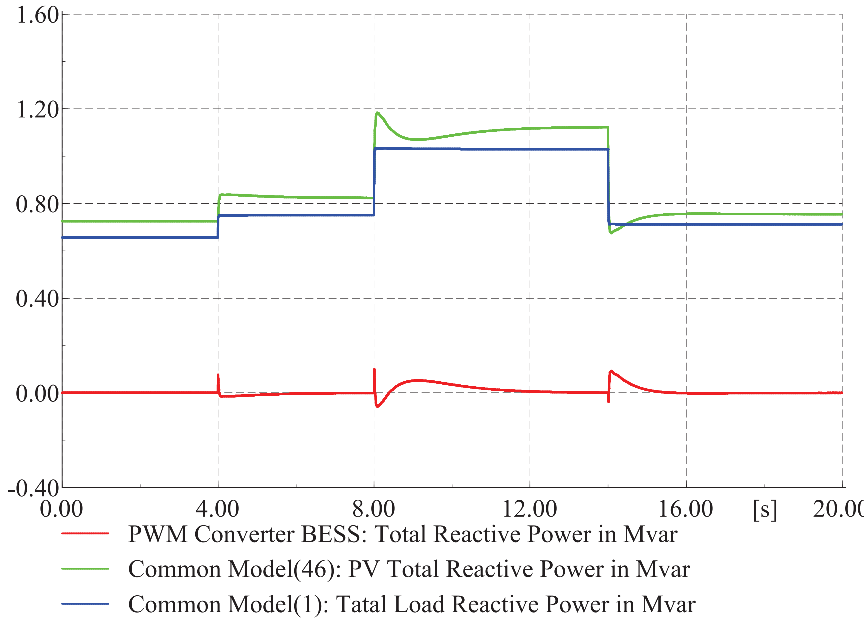

Figure 4.37: Reactive power trends in islanded mode.

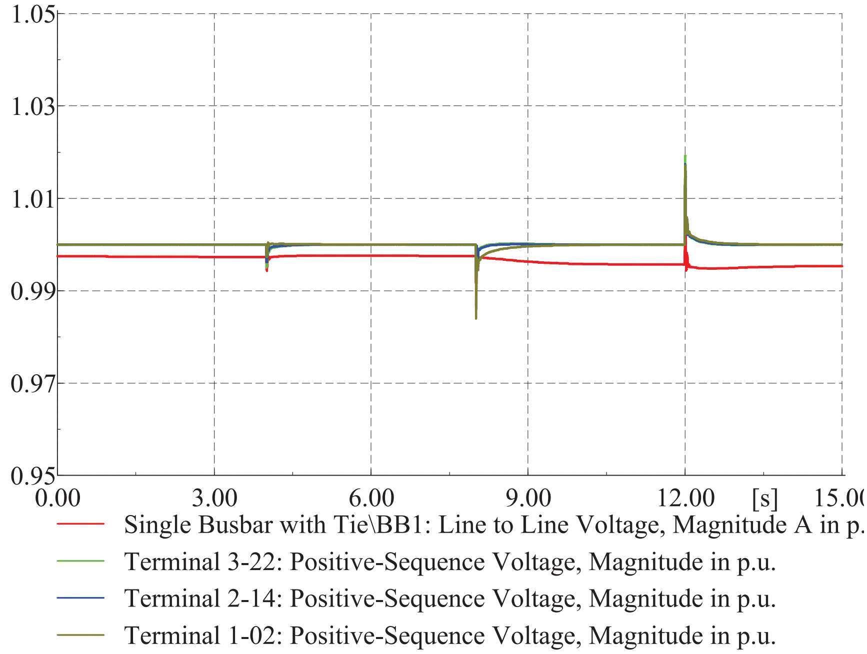

Figure 4.38: Voltage profile for selected strategic buses.

4.5.4 Energy balance.

In order to investigate system dynamic behavior in a span of 24 hours, a daily load curve of the distribution network (obtained from the sum of the variable demands within 24 hours of 20 typical loads) has been identified. For the daily equivalent load profile (blue line), illustrated in figure 4.39, a $10s$ interval represents an equivalent hour. The solar generation plants PV1, PV2, and PV3 rated at 2, 2, and 1MVA respectively are utilized to provide the renewable energy supply to the network. Thanks to the high solar radiation available in the considered geographic area, considering stable solar conditions, the generation profile reflects the typical solar radiation daily trend as reported in Figure 4.39 (green line).
A BESS is connected to the islanded network in order to preserve system stability and power balance between generation and load. Daytime overproduction is used to charge the storage plant, which supplies the load during evening and night figure 4.39 (red line). The proposed strategy is able to optimally manage both the BESS behavior and the

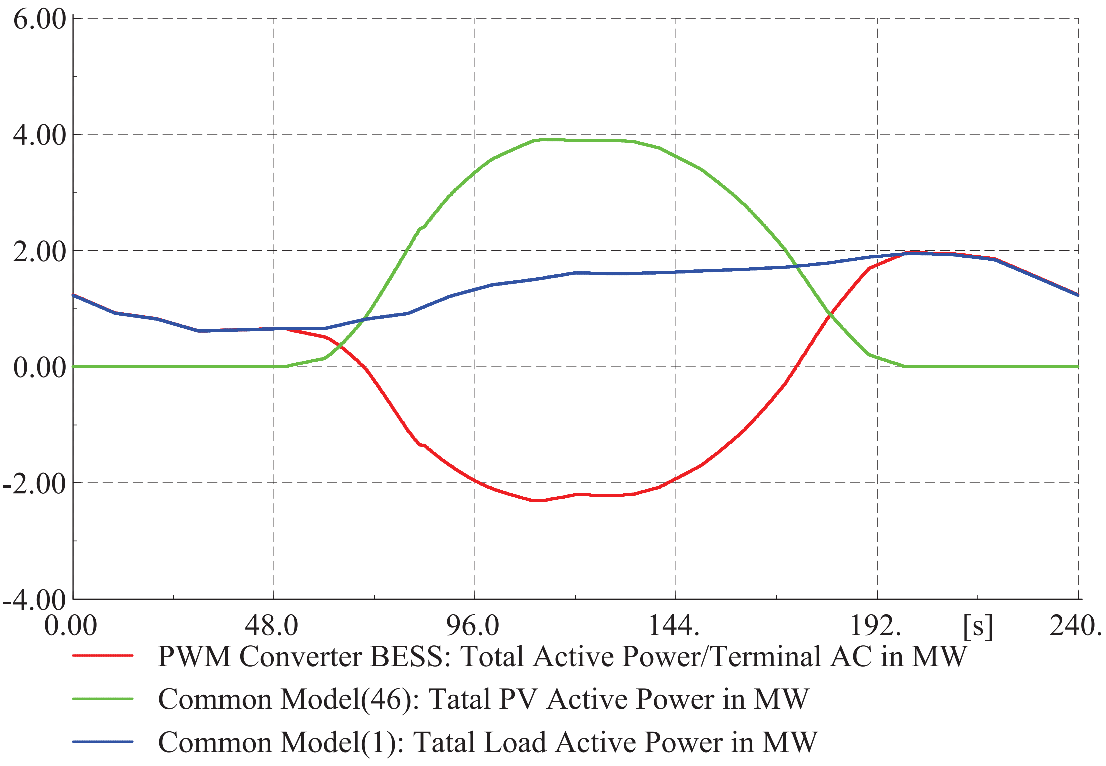

Figure 4.39: Load, BESS, and PV Active power in Islanded Mode.

PV source. In case the production overpasses the load, the BESS absorb power. If the overproduction excessed the BESS rated power, a positive frequency perturbation is intentionally introduced to modulate the PV generation and to preserve the islanded system stability. Vice-versa, when the generation is lower than the overall load, an under-frequency operating condition is forced to stimulate other DG plants, if there is any, otherwise load shedding technique or programmable load scheduling is implemented for keeping generation and load balance. The imposed frequency profile is reported in figure 4.40 and perfectly reflects the BESS active power exchange daily trend. Frequency is set at its rated value when the storage system active power exchange is within the BESS stability dead-band.

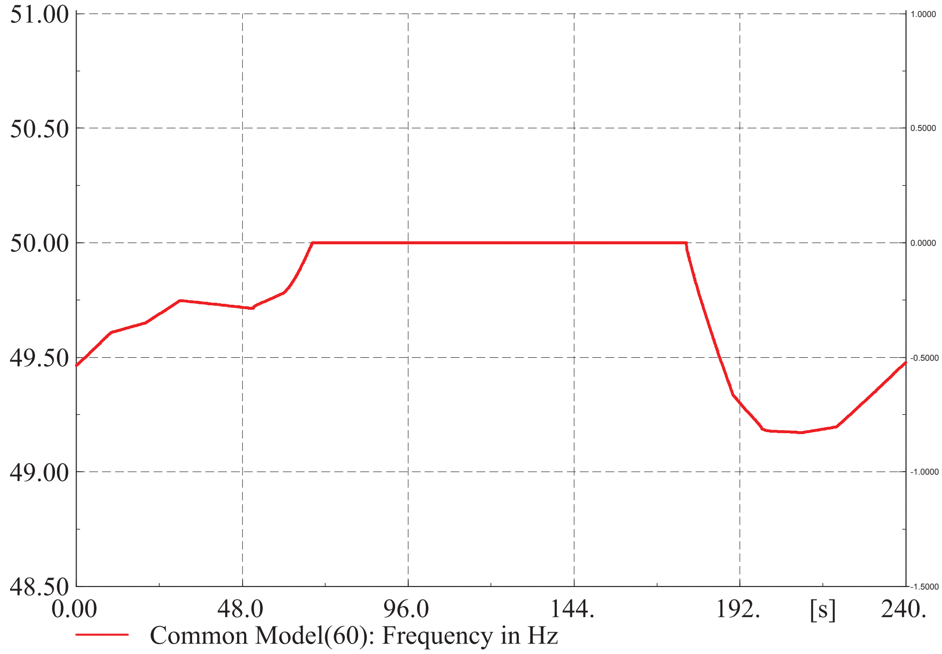

Figure 4.40: Frequency trend.

Chapter 5

BESS size minimizing and efficiency improvement

5.1 Implementation of Synchronous Generators

In MV islanded networks the size of BESS can be relatively large and have heavily impact on the total installation cost of the system. In particular, for islanded networks implementing BESS and PV, the longest period needs to be bridged by the BESS is from end of PV power availability at end of daytime to solar radiation starting on the next day, i.e. evening and night load requirements. Aiming to limit the overall installation cost, different strategies could be adopted for minimizing the size of the BESS:

1. Load-shedding techniques are able to reduce the night-time load with a disadvantage of affecting end user quality of supply;

2. Scheduling of programmable loads during daytime hours while availability of solar radiation;

3. Synchronous generators could be introduced as another group of DG units for supplying the base load, especially during night;

The third alternative, with no negative effects on end user quality of supply, has been adopted in the thesis. Synchronous generators are introduced in the developed control scheme as second slaves to supply the islanded loads during night in order to limit the required BESS size. All the control frames and models, required for the synchronous generators to operate according to the proposed control strategy, have been developed as would be described in next section.

5.1.1 Modelling of synchronous generator

In order to introduce synchronous generators as a second group of slaves according to the implemented control strategy, control composite and common models are developed in

DIgSILENT powerfactory environment considering the following characteristics:

- Synchronous generators work as slaves with secondary control;
- Synchronous generators are mainly implemented for supplying the islanded base load during evening and night periods;
- Synchronous generators active power outputs are regulated depending on the frequency deviation imposed by the BESS (master);
- Synchronous generators reactive power outputs are evaluated according to the voltage reference signal modulated by the by the BESS, at their PCC aiming BESS reactive power reaches zero at voltage steady-state condition;

In PowerFactory, a synchronous generator can be selected from the drag and drop items and added to the grid. From the edit windows, user can specify generator's type and data using specifications from global library, from other projects or new added specifications. Built in control frames and control models are also provided in global library standard models. A built in control frame (IEEE) from the global library, shown in figure 5.1, was originally adopted for this thesis. To implement the control frame for the developed

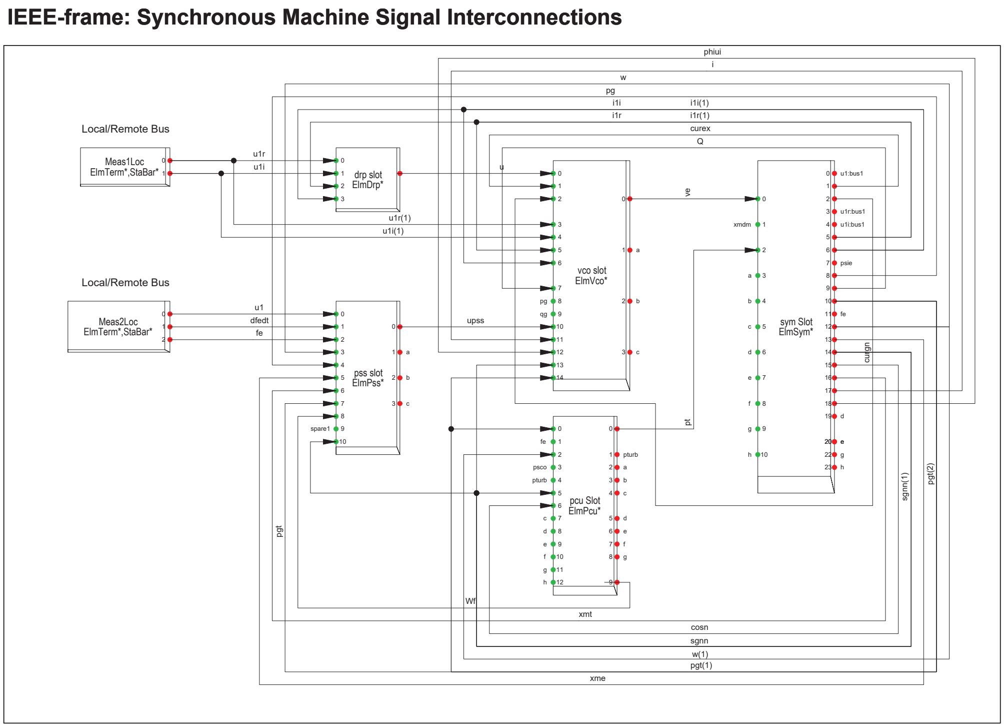

Figure 5.1: IEEE built in control frame from PowerFactory.

control strategy, as shown in figure 5.2, the following changes have been made on the built in control frame;

- Two control models which are active power control and reactive power control are added to the frame for providing respectively the active and reactive power references;

- Modifying the governor models by adding a reference signal provided by the active power control model, as shown in figure 5.4, to provide secondary control to the generator for regulating its active power depending on the frequency deviation imposed by the master (BESS). The parameters of the governor model are listed in table 5.3;

- The reference signal provided by the reactive power control is added to the voltage regulator models, as illustrated in figure 5.5, to evaluate the synchronous generators reactive power as required by the voltage modulated by the BESS. Table 5.4 lists the parameters for voltage regulator model.

- Adding of measured devices and modifying of signal flow;

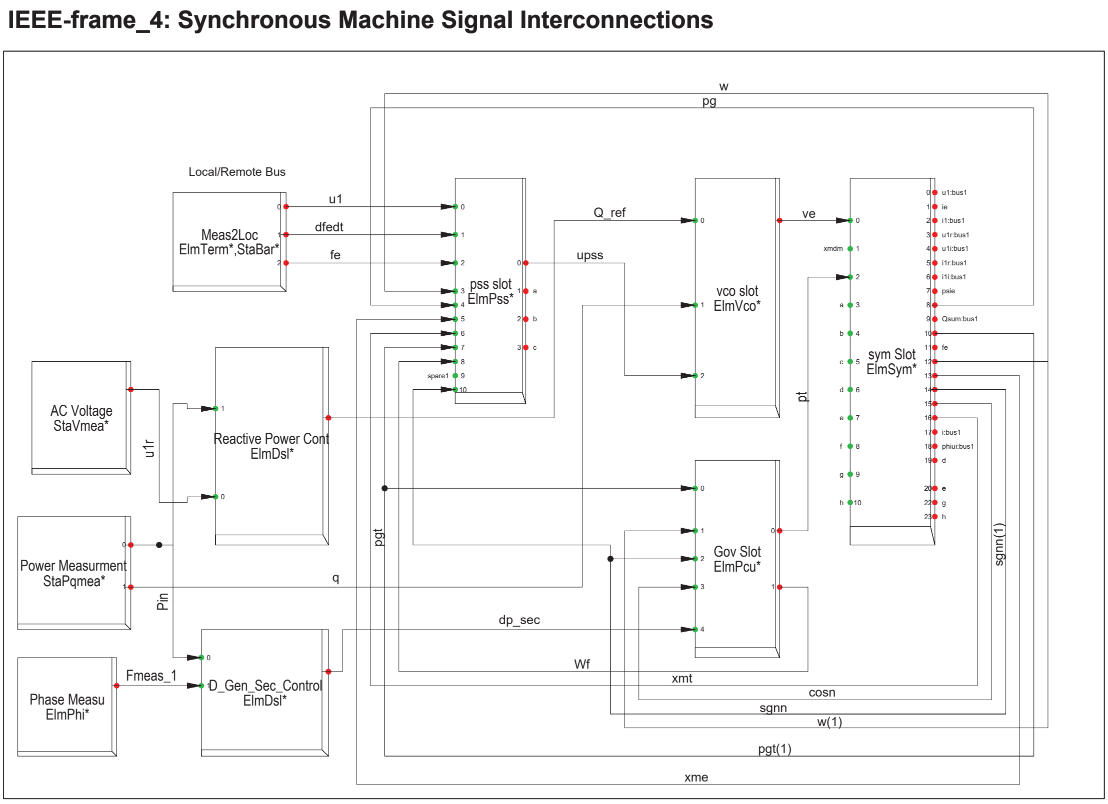

Figure 5.2: Synchronous generator control frame.

The synchronous generator control frame shown in figure 5.2 comprises the following control models.

- **Active power control model:** The blocks included in this model and theory of operation have been described in section 6.5 except additional two blocks for time delay and machine base as illustrated in figure 5.3. The scope of this model is to evaluate reference signal, depending on the frequency deviation imposed by the BESS, for the governor model to regulate the synchronous generator active power outputs. The parameters of this model are listed in table 5.1;

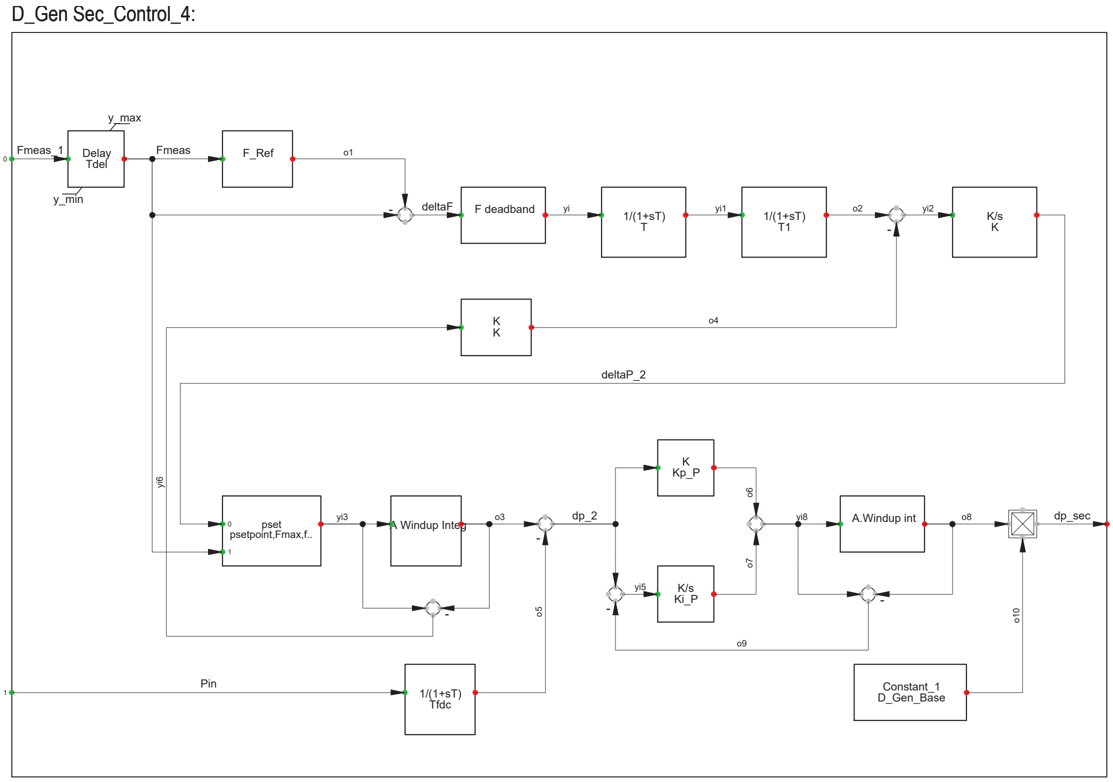

Figure 5.3: Active power control model.

Table 5.1: Parameters of active power control model.

Parameter	**Description**	**Value**
T_{fdc}	Filter time constant, act. power meas. path (s)	0.001
$P_{setpoint}$	Active power initial setpoint (pu)	0.1
F_{max}	Maximum frequency (Hz)	51
f_{DG-max}	DG stability dead band upper limit (Hz)	50.2
F_{min}	Minimum frequency (Hz)	49
f_{DG-min}	DG stability dead band lower limit (Hz)	49.8
K_{p-p}	Proportional gain of PI parallel controller (pu)	1
K_{i-p}	Integrator gain of PI parallel controller (pu)	10
T_1	Filter2 time constant (s)	0
K	Integrator gain (pu)	0.5
T	Filter1 time constant (s)	0
$D-Gen-Base$	Diesel generator rated power (MVA)	1
T_{del}	Delay time constant (s)	0.001
Y_{min}	Minimum limit of frequency measurment (Hz)	0
Y_{max}	Maximum limit of frequency measurment (Hz)	60

- **Reactive power control model:** This model has been described in section 6.5, for PV modeling, with the only changes in models parameters which are as listed in table 5.2. The reactive power control model provides the reference signal for the voltage regulator model to regulate the reactive power of the synchronous generator according to the voltage modulated by the BESS aiming to reduce to zero the BESS reactive power at steady state condition;

Table 5.2: Parameters of reactive power control model.

Parameter	**Description**	**Value**
T_u	Filter time constant (s)	0.01
$V_{setpoint}$	Volage set point (V)	1
K_{q1}	Integrator gaim (pu)	10
Q_{min}	Reactive power maximum limit (pu)	0
Q_{max}	Reactive power minimum limit (pu)	1

In order to regulate the active and reactive power outputs of the diesel generators according to the frequency and voltage modulated by the master (BESS), the diesel generators' governor and voltage control models are developed as shown in figures 5.4 and 5.5 respectively. The reference signals provided by the active control model (dp_sec) and that provided by the reactive control model (Q_ref) are added to the initial set points of the governor and voltage control models respectively to provide a secondary control to regulate the behavior of diesel generators power outputs depending on the frequency and voltage imposed by the BESS. The dispatcher blocks in the two models are used for simulation purposes, to be able to connect the diesel generators to supply the base load during night periods and disconnect them at solar availability during day time. Since there is no synchronizing unit in DIgSILENT software, the dispatcher blocks with (0 or 1) value are used as parameter events to be multiplied by the set points for connecting or disconnecting of the generators. The governor and the voltage regulator control models' parameters and their values are listed in tables 10.3 and 10.4 respectively.

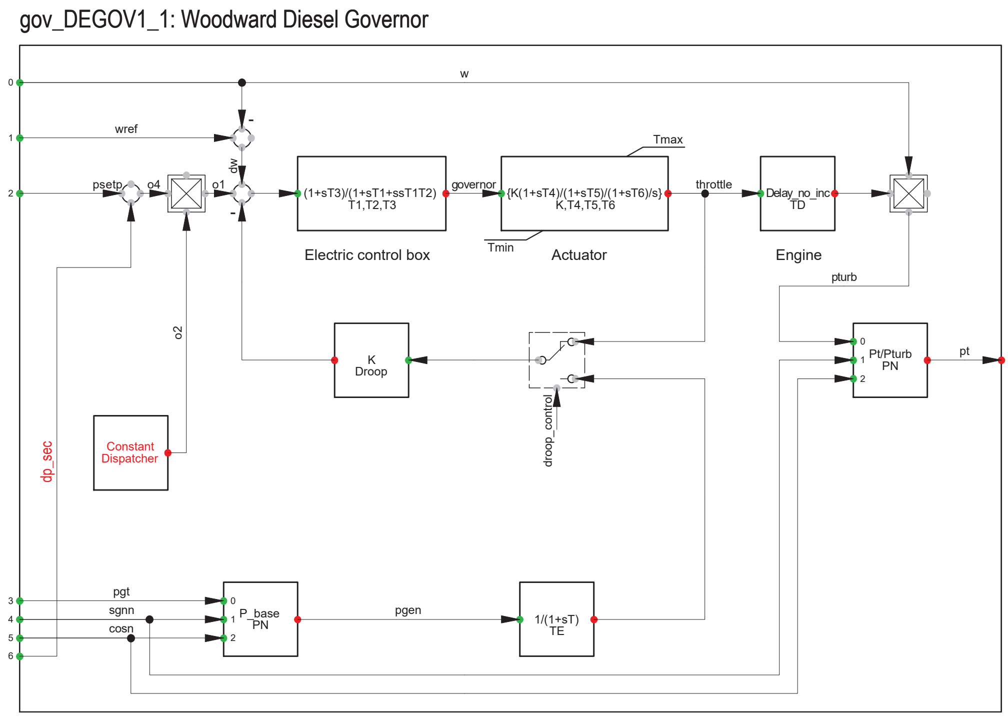

Figure 5.4: Synchronous generator governor control model.

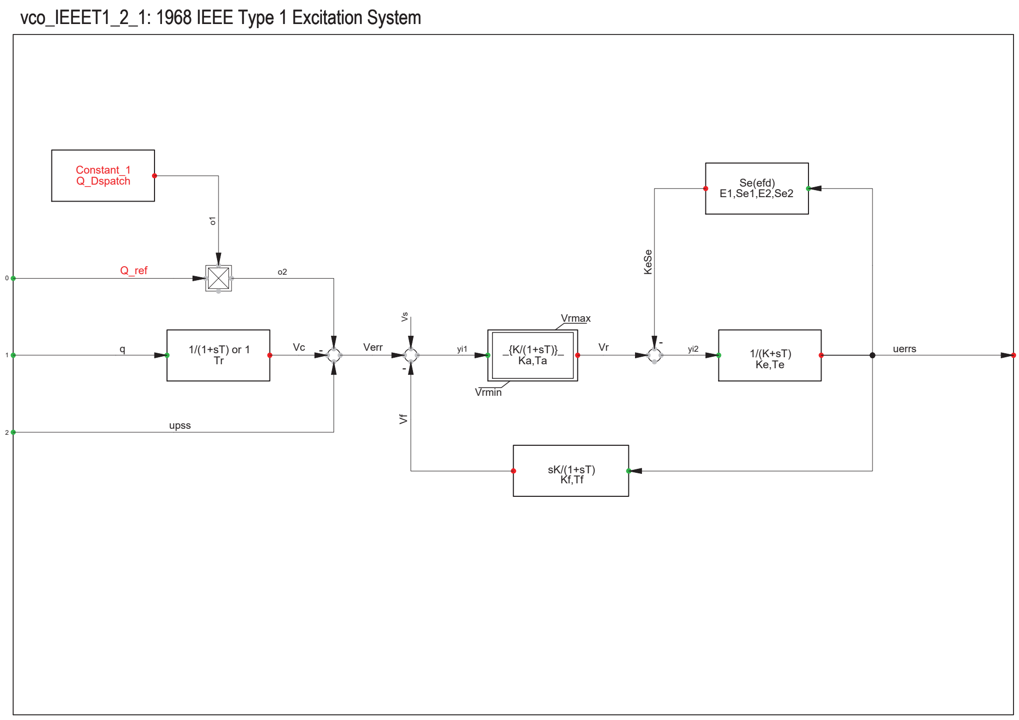

Figure 5.5: Synchronous generator voltage regulator control model.

Table 5.3: Parameters of Synchronous generator governor control model.

Parameter	Description	Value
K	Actuator Gain (pu/pu)	9
T_4	Actuator derative time constant (s)	1
T_5	Actuator first time constant (s)	0.002
T_6	Actuator second time constant (s)	0.005
T_D	Combustion Delay (s)	0.001
$Droop$	Droop (pu)	0.8
T_E	time constant fdbk (s)	0.5
T_1	Elec. cont. box first time constant (s)	0.005
T_2	Elec. cont. box second time constant (s)	0.001
T_3	Elec. cont. box derivative time constant (s)	0.1
$Droopcontrol$	(0=Throttle feedback, 1=Elec. Power feedback)	1
PN	Prime mover rated power (PN=Pgnn) (MW)	1
T_{min}	Minimum throttle (pu)	0
T_{max}	Maximum throttle (pu)	1.1

Table 5.4: Parameters of Synchronous generator voltage regulator control model.

Parameter	Description	Value
T_r	Measurement delay (s)	0.02
K_a	Controller gain (pu)	50
T_a	Controller time constant (s)	0.002
K_e	Excitor constant (pu)	1
T_e	Excitor time constant (s)	0
K_f	Stabilization path gain(pu)	0.0025
T_f	Stabilization path time constant (s)	1.5
E_1	Saturation factor 1 (pu)	6
S_{e1}	Saturation factor 2 (pu)	1.5
E_2	Saturation factor 3 (pu)	10
S_{e1}	Saturation factor 4 (pu)	2.46
V_{min}	Controller output minimum (pu)	-12
V_{max}	Controller output maximum (pu)	12

5.1.2 Simulation and results

For a purpose of minimizing the BESS size, three synchronous generators named (synch. Gen.1, synch. Gen.2, and synch. Gen.3) have been connected to busbars 2-14, 3-22, and 1-02 respectively as shown in figure 5.6. The proposed synchronous generators are to be implemented for supplying the base load during night periods to reduce the energy provided by BESS and consequently minimize its required size and cost. The control frames and models for the synchronous generators, to be introduced as a second group of slaves to the developed control strategy, have been described in section 8.1.1.

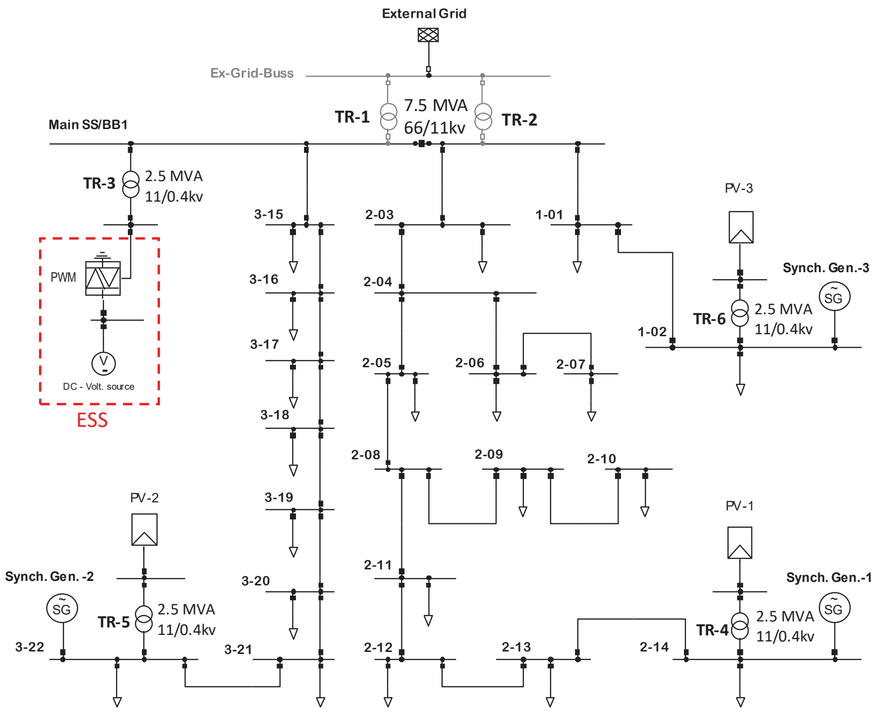

Figure 5.6: Single line presentation for system under study with proposed synchronous generators.

In order to investigate the dynamic behavior of the system and energy balance between generation and load, several simulation considering different scenarios have been carried out making use of DIgSILENT PowerFactory software.

5.1.2.1 Power, frequency and voltage dynamics

For validation of the developed control scheme, implementing BESS (master) and synchronous generators as slaves, the following load perturbations have been considered starting from a steady state condition.

1. At $t = 4s$, the overall load is step increased from $1.257MW$ to $1.434MW$ by switching on a couple of loads.

2. At $t = 8s$, the overall load is further step increased to $2.076MW$.

3. At $t = 12s$, some end-users are switched off to reduce the overall load to $1.502MW$.

- **Frequency control and active power regulation:** According to the developed control strategy, the active power outputs of the synchronous generators are regulated by secondary control with set point evaluated depending on the frequency deviation imposed by the master BESS. The frequency deviation imposed by the BESS can be either negative (reduced frequency), in case of BESS active power injected to the islanded system overpasses its stability dead-band, to force the synchronous generators to increase their active power outputs, or positive (increased frequency), in case of BESS active power absorbed overpasses its stability dead-band, to force the synchronous generators to reduce their active power outputs taking account of the batteries state of charge in both cases. Based on this control approach and considering the above mentioned load perturbations, the trend of the active power consumed by the load, that provided by the synchronous generators, and the active power injected or absorbed by the BESS are presented in figure 5.7. Figure 5.8 illustrates the frequency trend as measured at the BESS point of common coupling.

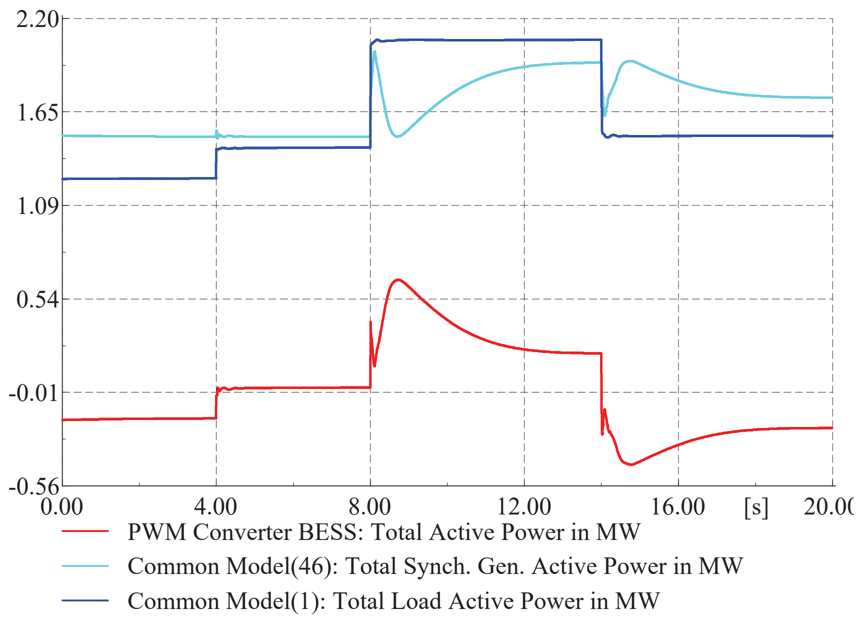

Figure 5.7: Active power trends in islanded mode.

It can be seen from the active power and frequency trends reported respectively in figures 5.7 and 5.8 that as a respond to the first load perturbation the BESS rapidly injects more active power, but still within its stability dead-band, so it does not impose any frequency deviation and no contribution is required from the

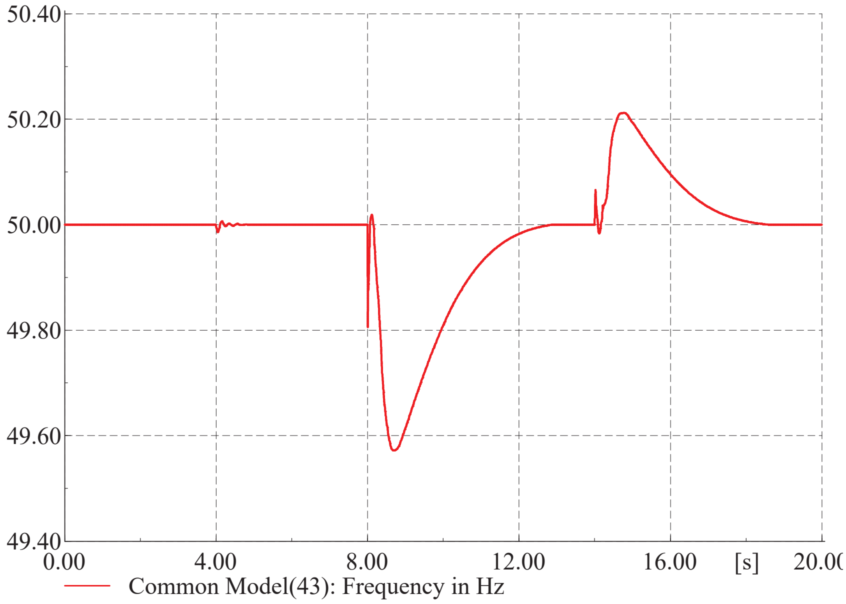

Figure 5.8: Frequency deviation.

synchronous generators. For the second load perturbation, the active power injected by the BESS overpasses its stability dead-band causing it to impose under frequency deviation forcing the synchronous generators to inject more active power to bring the frequency back to its rated value. Conversely, when the active power absorbed by the BESS violated its dead-band, the BESS imposed over frequency decreases the synchronous generators active power outputs to keep frequency at its rated value.

- **Voltage control and reactive power regulation:** For any load perturbation, the reactive power system requirements are rapidly provided by the BESS which modulates the voltage at its PCC to indirectly control the synchronous generators reactive power outputs behaviors as presented in figure 5.9. The synchronous generators regulate their reactive power injections aiming to keep the voltage levels at their PCC close to 1pu and to reduce the reactive power of the BESS to zero at steady state as illustrated in figures 5.10 and 5.9 respectively.

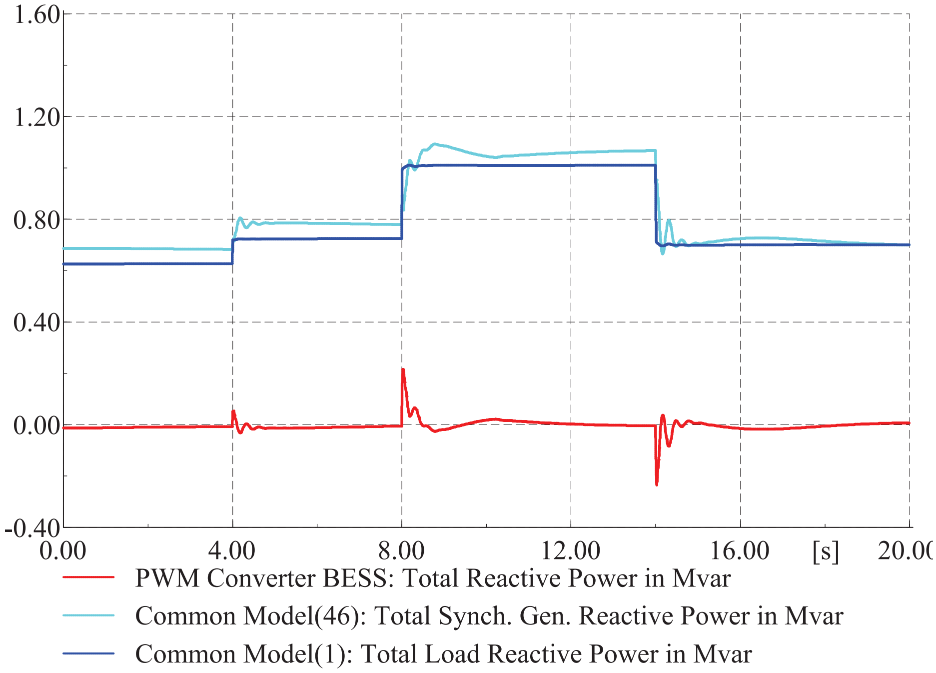

Figure 5.9: Reactive power trends in islanded mode.

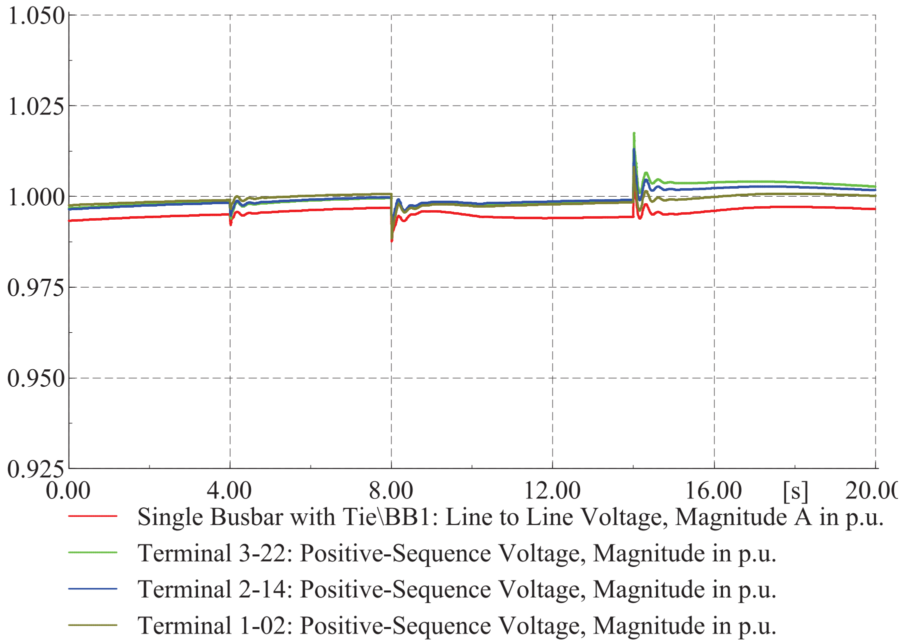

Figure 5.10: Voltage profile for selected strategic buses.

5.1.2.2 Energy balance

To enable studying of system dynamic behavior for a one-day period, a daily equivalent load profile, as shown in figure 5.11 (blue line), has been defined in which an interval of $10s$ represents an equivalent hour. The solar generation plants PV1, PV2, and PV3 rated at 1.5, 1.5, and $1MVA$ respectively are utilized to provide the renewable energy supply to the network during day with availability of solar radiation, as reported in figure 5.11 (green line), while the synchronous generators rated at 0.5MVA each are considered to feed the base load during night periods figure 5.11 (light blue line). A BESS is connected to the islanded network in order to preserve system stability and power balance between generation and load.

The developed strategy is able to optimally manage behavior of both the master (BESS)

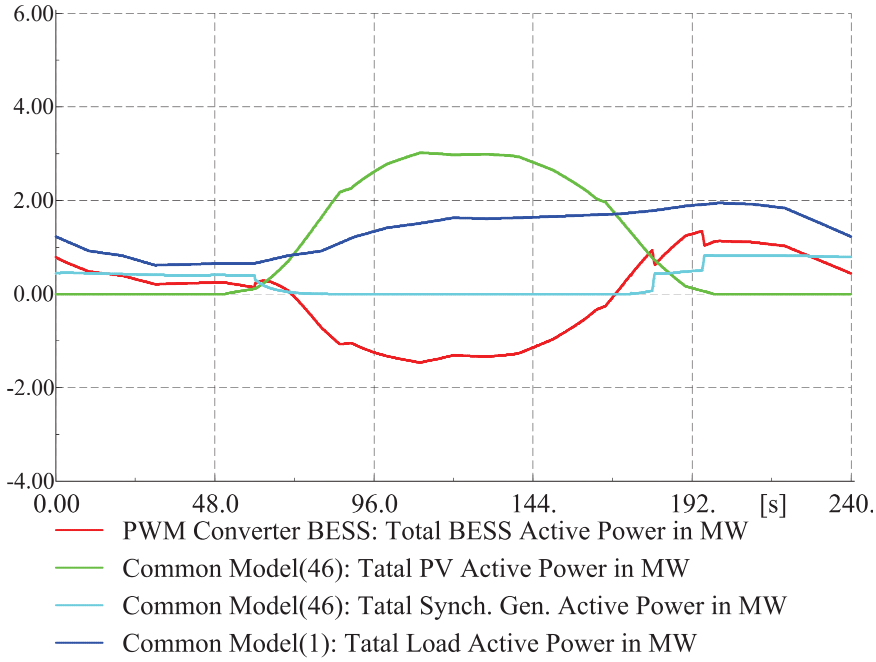

Figure 5.11: Load, BESS, PV and Synch. Gen. Active power in Islanded Mode.

and the slaves (PVs and synch. Generators). In case the production overpasses the load requirements, the BESS absorbs the surplus power for charging batteries bank. If the overproduction excesses the BESS rated power, the BESS forces the slave (PVs or synch. Generators) to reduce their active power generation to preserve the islanded system stability. On the other hand, when the generation is lower than the overall load, a negative frequency deviation is produced for modulating the slaves active power outputs and increase their production to keep system frequency at its rated value. Frequency trend is shown in figure 5.13 where the frequency is set at its rated value as far as the BESS active power exchange with the islanded system is within the stability dead-band. Figure 5.14 plots the state of charge of the batteries (SoC) which its value at the end of the day needs to be equal to or greater than its value at the beginning of the day for acceptable BESS size.

The synchronous generators are implemented for effectively reducing the size and consequently the total installation cost of the system.

In order to demonstrate the reduction in BESS size as an effect of introducing synchronous generators for supplying base load during night periods, the energy provided by BESS in the following two islanded mode scenarios were investigated.

1. Implementing BESS with PV generation plants as slave DG units.;
2. Implementing BESS with PV and synchronous generators as two groups of slave DG units.;

By comparing the energy provided by BESS in the first case as illustrated in figure 5.12, against that in the second case presented in figure 5.11, which are $15.00MWh$ and $8.6MWh$ respectively. The comparison clearly verifies the dramatic reduction in BESS size as a result of introducing synchronous generators in the developed control strategy.

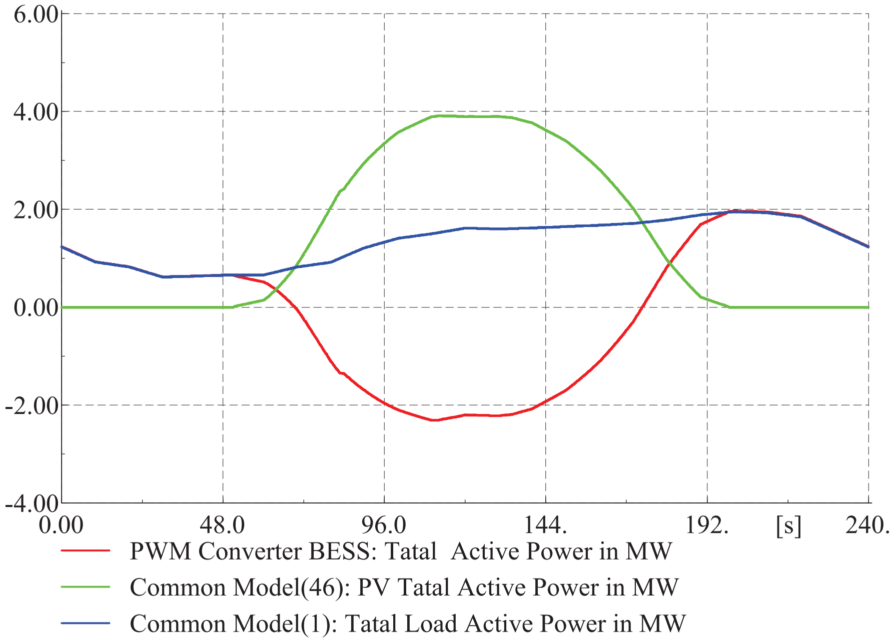

Figure 5.12: Load, BESS and PV Active power in Islanded Mode.

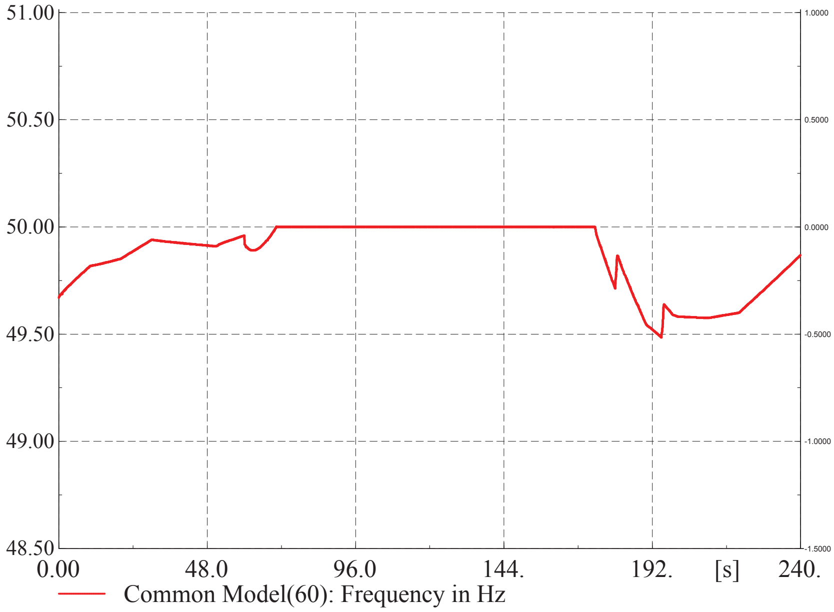

Figure 5.13: Frequency trend.

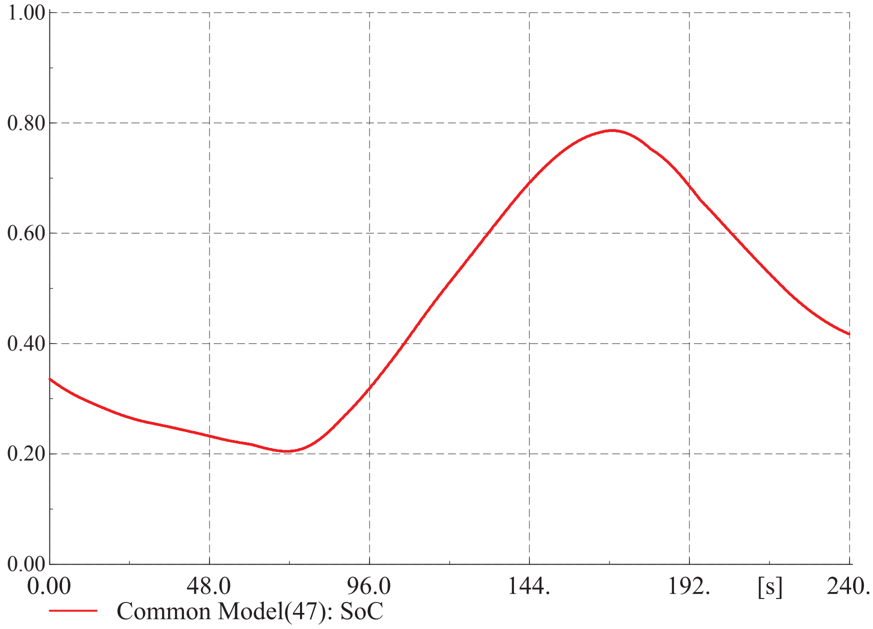

Figure 5.14: Batteries State of Charge (SoC).

Energy contributions of generation plants (PVs and Diesel Generators) to provide load requirements are illustrated in figure 5.15 where we can see that the PV generation plants provide the majority of the generated energy whereas the diesel generators are used to supply base loads during night periods. BESS store energy at generations surplus and release energy when generation is less than load requirements to preserve generation and load energy balance.

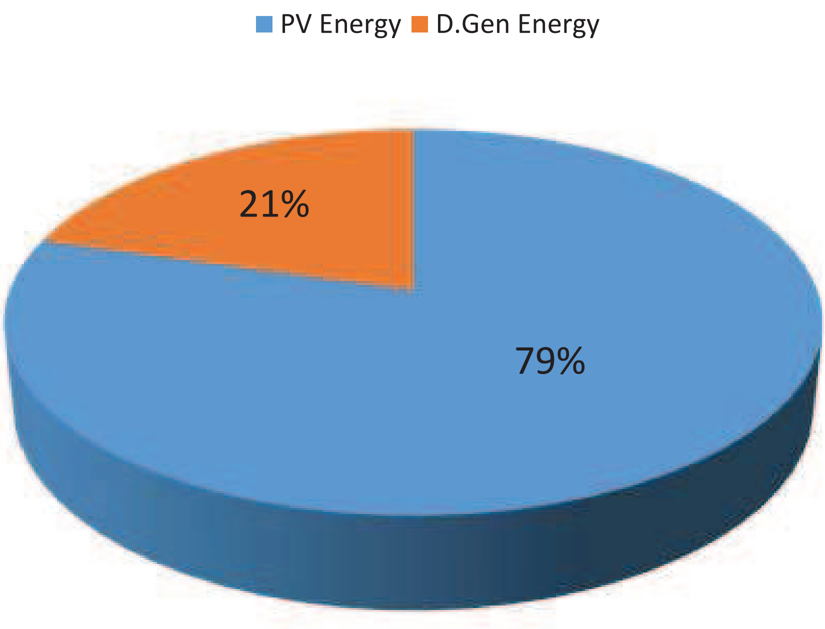

Figure 5.15: Energy contributions of generation plants.

5.2 Implementation of Battery-supercapacitor Hybrid ESS.

BESS and DGs in islanded systems have to be coordinated aiming to maximize the primary sources usage, to reduce losses and to preserve quality of supply, which primarily means frequency and voltage magnitude [119]. When more than one DG supply the islanded system, the total load should be shared between the DG units basing on their rated capacity to avoid over loading of single sources [120]. For stand-alone systems implementing PV generation plants, storage using Valve Regulated Lead Acid (VRLA) battery are the most commonly used technology, because of cost and availability point of view [124]. However, certain loads, e.g. motor starting, require high current for short period of time. Sizing the batteries to satisfy these load requirements may increase the cost dramatically. One of the alternatives which can be adopted is utilizing Battery Supercapacitor Hybrid energy storage system. The supercapacitor with its high power density provides peak load requirements for short period of time while batteries with their high energy density supply load continuous power. The use of battery supercapacitor hybrid ESS results in lower battery current and therefore a lower battery temperature, which are positively affecting battery lifetime [142].

5.2.1 Battery-supercapacitor Hybrid ESS modelling.

Ultracapacitors generally have high power density while in contrast batteries have high energy density. Battery-supercapacitor hybrid ESS has considerable effect on peak power enhancement and extended life of batteries. For further improvement to the implemented control strategy, especially under pulsed load conditions, a battery- supercapacitor hybrid ESS, as proposed in [142], has been implemented. A model for a battery supercapacitor hybrid ESS was developed in DIgSILENT environment as illustrated in figure 5.16. The supercapacitor is modelled by a capacitor C with an equivalent resistance R_{isc} and connected directly to the DC bus. The battery is modelled by a dc voltage source Vb with an internal resistance R_i and connected to the DC bus through a bidirectional DC/DC converter. Since the DIgSILENT software does not have a bidirectional DC/DC converter's model, a control frame with the required control models, as shown in figure 5.17, have been developed to utilize boost and buck converters for charge and discharge of the batteries.

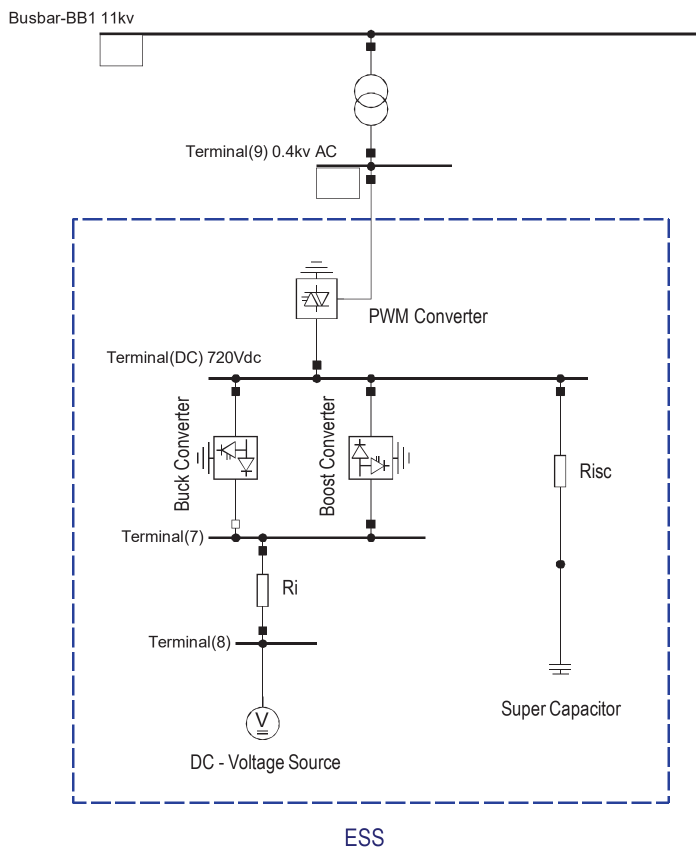

Figure 5.16: Battery- supercapacitor hybrid ESS modelled in DigSilent.

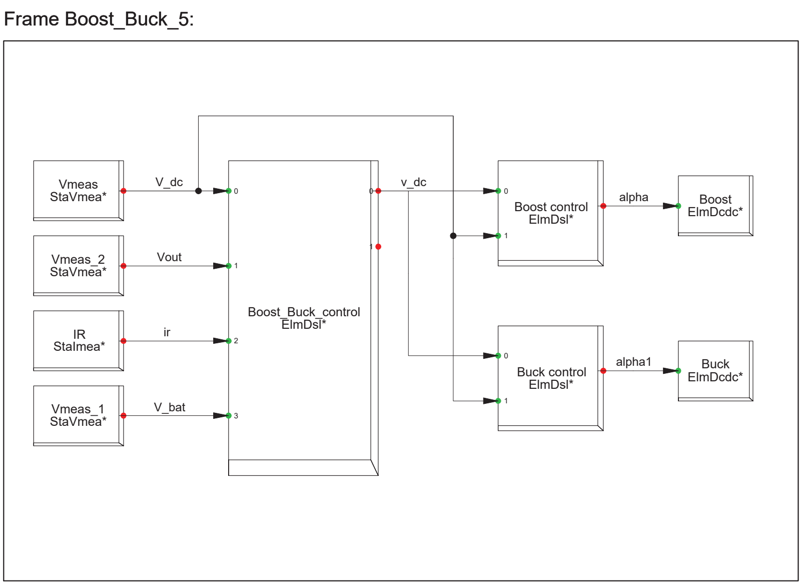

Figure 5.17: Boost-Buck control frame.

5.2.2 Simulation and results.

Each ESS technology has its own advantages for a specific application. Certain system requirements may not be satisfied by a single ESS technology. Utilizing Hybrid ESS can be an alternative to overcome this deficiency. A battery supercapacitor hybrid ESS may combine the advantages of high energy density in battery technology and high power density in supercapacitor technology to provide large power and energy capacities. A battery supercapacitor hybrid ESS has been implemented in the developed control scheme using a model proposed in [142]. Simulations are carried out applying load perturbations shown in figure 5.18. Figure 5.19 reports the active power contributed by the supercapacitor (green line) and that by the battery (blue line) to provide the total active power (red line) of the ESS. It can be seen from figure 5.19 that the supercapacitor supplies the major part of the peak load while the battery supplies the lower continuous power. In this way the battery's depth of discharge (DOD) is reduced and consequently its lifetime is improved. Researchers [142], [143], [144] have demonstrated several benefits achieved with the assistance of supercapacitor: battery's power rating, current and temperature are reduced resulting in battery reduced cost and improved overall efficiency of the ESS. However, the cost of supercapacitors still high but the prices are predicted to be decreased by advanced technologies. Economic studies for optimization of increasing the number of parallel batteries or utilizing supercapacitors may be carried out but it was not considered as one of the tasks of the thesis.

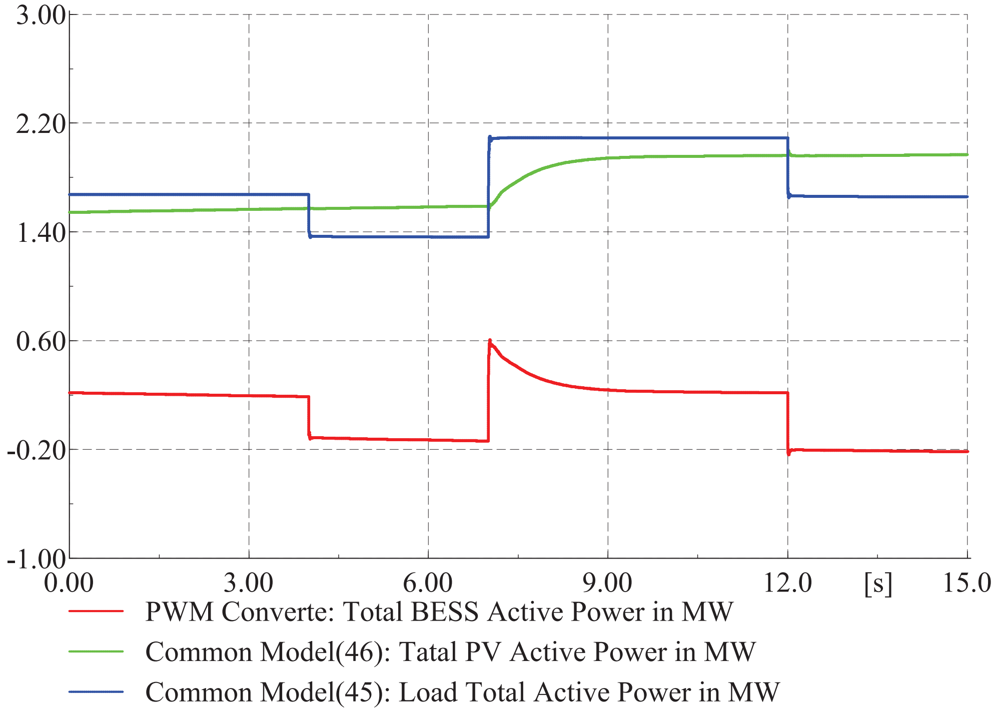

Figure 5.18: Load perturbation and active power trend.

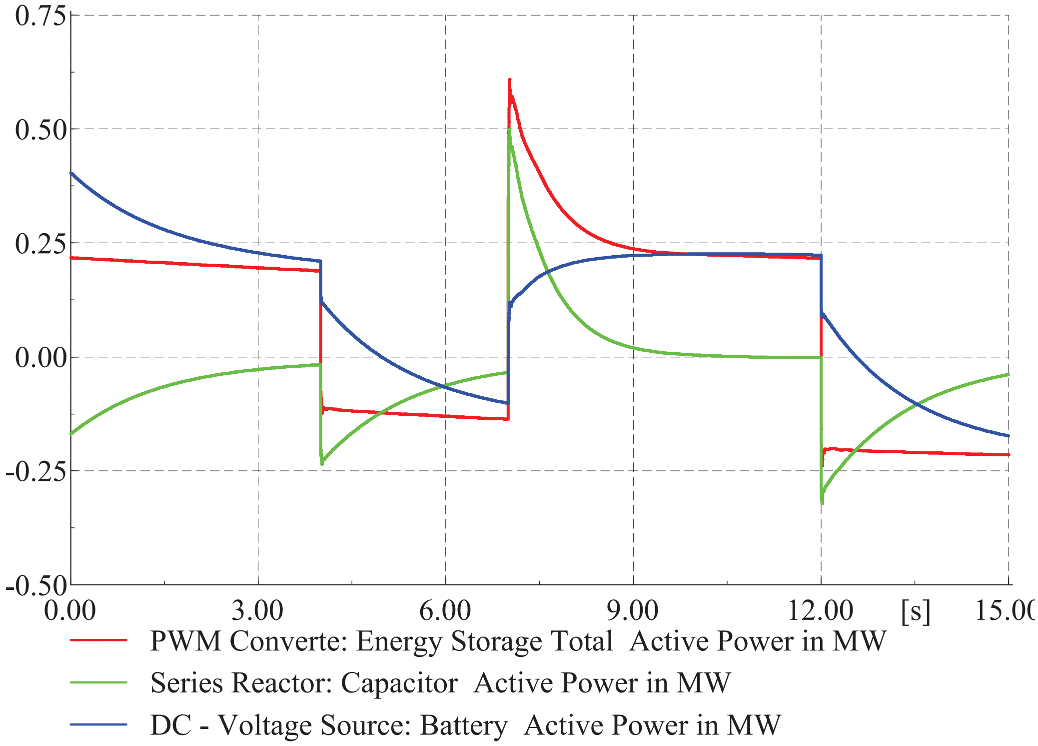

Figure 5.19: Batt.-Supercap. Hybrid ESS active power showing Batt. and supercap. contributions.

Chapter 6

Conclusions and Future works

Islanded systems making use of renewable energy sources becomes viable for supplying local networks with weak connection to main grid to preserve end-user power quality in case of temporary blackout. In Islanded systems, Energy Storage Systems (ESS) are essential to overcome PV output fluctuation nature and to preserve generation/load balance and system stability. Appropriate control strategies are key factors to coordinate energy storage systems and renewable energy resources in islanded network. The use of distributed generation technologies utilizing local renewable resources for electrification of a remote distribution network was investigated. A MV distribution network, corresponding in size to Libyan oasis-village, is assumed as a case study. Load flow simulation was carried out to illustrate improvement of the network power quality levels in both grid connected and islanded modes as a result of implemintation of distributed generation technologies. A (SMO) master/slave control strategy implementing PV and BESS was developed to regulate frequency and voltage in islanded mode. According to the developed control scheme, BESS operates as a slack node and modulates frequency and voltage at its PCC to indirectly control the PVs behavior while PVs are controlled as PQ generators with references depending on frequency and voltage imposed by the BESS.

The developed control strategy has the following characteristics:

1. BESS' active power exchange with the islanded system is minimized to maintain its ability to enhance system stability.

2. The reactive power of the BESS goes to zero at steady state while the PVs provide all reactive power network requirements. Consequently, the BESS inverter capability curve is not reduced by reactive power generation, improving the BESS capacity of active power regulation and minimizing the power electronic converter losses.

3. For implementing the developed control strategy no communication channels are required, since frequency and voltages are used for coordinating the role of both the solar generation and the energy storage system in facing active and reactive power requirements of the connected loads.

4. The number and the depth of batteries charge/discharge cycles are reduced to avoid impacts on batteries lifetime.

Dynamic simulations confirm the ability of implemented control schemes in providing load requirements in islanded mode with preserving system stability and power balance between generation and load along with the above mentioned characteristics. Whereas, in grid connected mode, the PV generation plants provide the maximum available active power with implementation of active power reduction signal to decrease PV active power output in over frequency transient while surplus power is injected to the grid.
System dynamic simulations in a span of 24 hours demonstrate that the proposed strategy is able to optimally manage both the BESS behavior and the PV source. However, exploiting solely PVs in MV islanded networks, with energy production just during daytimes, as integrated DGs units with the BESS results in a large size of the BESS is required providing islanded network requirements during evening and night periods. So alternative solutions such as; load shedding, programmable load scheduling, or introducing other DG units to cover load requirements during evening and night periods, are to be adopted to minimize the BESS size.
Focusing on the last alternative, synchronous generators were introduced in the developed control strategy to supply the load during night period in order to minimize the size of the battery storage system. The reduction in BESS size was illustrated by comparing the energy provided by BESS in case of using PV only to that implementing PV and synchronous generators which were $15.00MWh$ and $8.6MWh$ respectively. The comparison clearly verifies the dramatic reduction in BESS size as a result of introducing synchronous generators in the developed control strategy.
For storage system efficiency improvement and further reduction of batteries size, battery supercapacitor hybrid ESS is proposed to the developed control strategy. Dynamic simulations demonstrate that, from the total ESS active power, the supercapacitor supplies the major part of the peak load while the battery supplies the lower continuous power. This reduces the depth of discharge of the batteries (DOD) and consequently improves their lifetimes and moreover reduces batteries size and improves overall efficiency of the ESS. However, the cost of supercapacitors still relatively high but the prices may be decreased by advanced technologies. Economic studies for optimization of increasing the number of parallel batteries or utilizing supercapacitors may be carried out but it was not considered as one of the tasks of the thesis.

For future works, different types of energy storages can be investigated to evaluate the most suitable type for this application. Also other DGs technologies can be analyzed to integrate PV and energy storage for supplying base load during evening and night periods to find out better alternatives from technical, environmental, and economic points of view.

Economic studies can be carried out to evaluate an optimum selection for either using larger size of battery energy storage (BESS) or battery-supercapacitor hybrid ESS. Strategical study for installation of utility scale PV system can be performed to get benefits of the high availability of solar radiation in the area under study.

Appendix A

Appendix

A.1 PowerFactory (DIgSILENT) Software

This appendix gives a concise description of the main power systems components modelling available in the selected simulation software library.

A.1.1 DIgSILENT PF software environment

DIgSILENT PowerFactory is an advanced power system simulation software package for studying and analyzing of industrial, utility and commercial electrical power systems. Its name DIgSILENT stands for Digital SimuLation and Electrical NeTwork simulation program. It combines reliable and flexible system modeling capabilities, with state-of-the-art solution algorithms and a unique database management concept. It presents methodological approaches for modelling of system components used in generation, transmission and distribution systems. Thse features allow the user to create detailed power system models, simulate and analyze power systems for optimum operation and expansion planning. PowerFactory comprises a list of simulation functionality including [136]:

- Balanced and unbalanced power flow.
- Fault analysis;
- Harmonics, Frequency scans.
- RMS Stability.
- EMT simulations for three, two and single phase AC systems and DC systems.
- Protection simulation and co-ordination.
- Distribution, transmission and generation reliability.
- Small signal analysis (eigenvalues).
- Static and dynamic voltage stability.

- Active and reactive power dispatch.
- State estimation.
- Open tie optimization, optimal capacitor placement, cable sizing.
- Built-in automation interface (DPL).
- ODBC driver, interfaces for GIS and SCADA integration, PSS/E compatibility.

Library: DIgSILENT PowerFactory provides global libraries and user libraries with respective access and modification rights. Global library contains a comprehensive model library, powerful built-in functions and equipment types such as transformers, cables, generators, motors, conductors, tower configurations, controllers, etc. The user can define and organize his own integrated libraries for all kind of data, grids, output definitions, forms, user-written models, frames, etc.
Graphical Editor: DIgSILENT PowerFactory also provides a fully integrated graphical editing environment, which enables the user to:

- Draw and modify electrical grids for integrated network and area diagrams, classic single line and substation configuration diagrams, with a configurable multi-layer network viewing and plotting capability.
- Utilize a comprehensive "drag and drop" power system element library containing transformers, generators, HVDC systems, etc., which the user is free to expand to include new elements for both devices and types.
- Initiate calculation events directly within the graphical environment.
- Display calculation results immediately in result boxes within the single line diagram.

Modeling Flexibility: Although DIgSILENT PowerFactory contains a comprehensive model library and powerful built-in functions, the user may define additional control models and calculation functionality (user defined models). This can be done by using DIgSILENT Simulation Language (DSL). DSL allows the creation of any kind of static or dynamic multi-input/multi-output model.

A.1.2 Modeling of PV Generation Plant

PV generation plants can be represented in PowerFactory either by implementing a PWM converter or Static Generator. In case of using PWM converter the PV model is represented with a DC current source and a DC link capacitor connected to the DC bus as shown in figure A.1.

Implementing a static generator for representing the PV is the more common way used in PowerFactory. The static generator can be dragged and dropped from elements

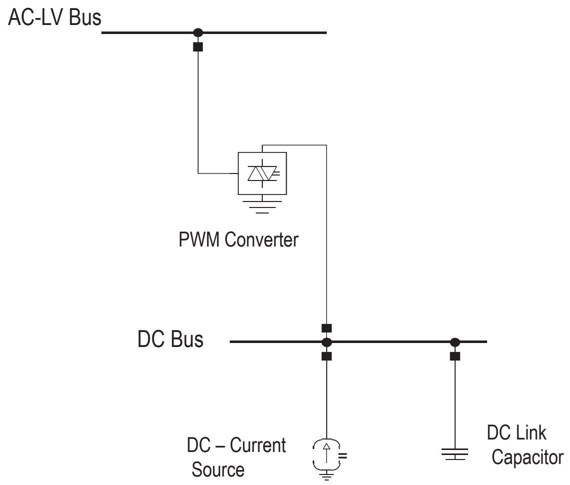

Figure A.1: PV presentation in PowerFactory using PWM converter

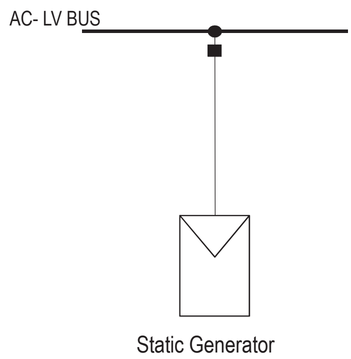

Figure A.2: PV presentation in PowerFactory using static generator

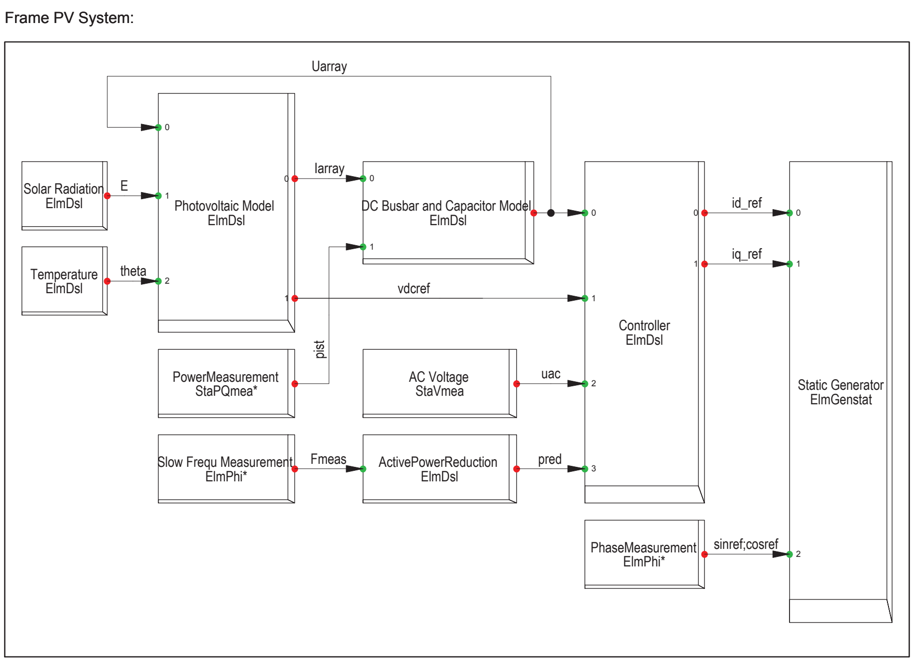

Figure A.3: Built-in PV frame or composite model in PowerFactory library and connected to the LV AC bus as shown in figure A.2. No interfacing converter is required since the static generator represents the PV array and the converter.

A built-in template using static generator is provided in PowerFactory library. Figure A.3 [145] illustrates the system control frame (composite model) showing the different common models, measurement devices and signals flow. The included common models are briefly described as following:

- **Solar Radiation:** Limited time integrator to integrate the accumulated change of irradiance per second and send its output as the solar radiation E in (W/m^2) to the photovoltaic model.;
- **Temperature model:** Limited time integrator for integrating the accumulated change in temperature per second and send its output as ambient temperature (theta in $(^{\circ}C)$) to the photovoltaic model.;
- **Photovoltaic model:** The model as shown in figure A.4 [145] has 3 inputs, Uarray , E, and Theta. After Uarray is filtered and divided by the number of series modules to get voltage of one module, the three inputs are used in PV Module, based on equations written in DSL, to calculate string current I and a module voltage in the maximum power point Vmmp. In order to obtain the array's current and voltage, I and Vmmp are multiplied by the number of parallel modules and the number of series modules respectively, which are the output of the photovoltaic model (Iarray and Vmmp array).;

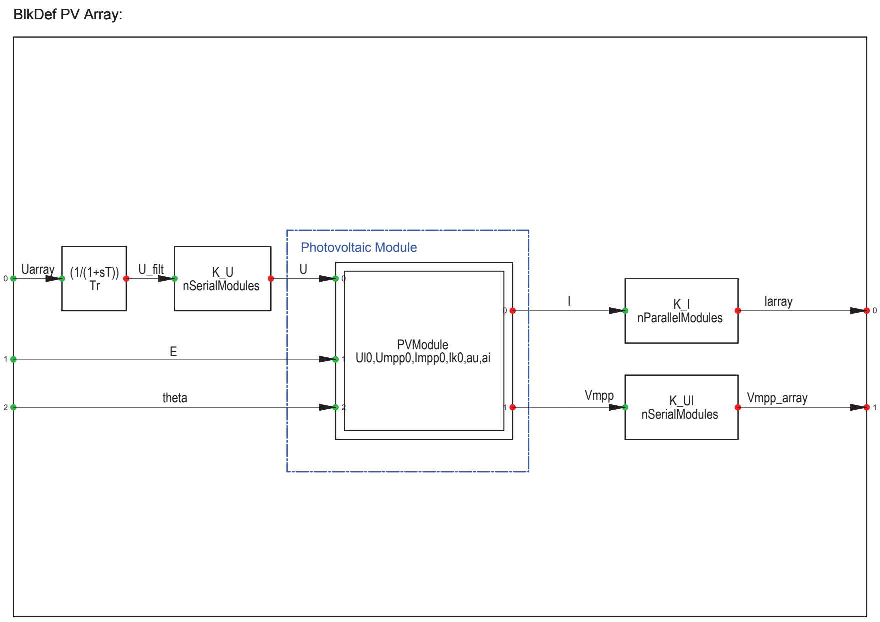

Figure A.4: Photovoltaic model.

- **DC Busbar and Capacitor model:** The two inputs to this model are the array current from the photovoltaic model and the measured PV active power while the output is the DC voltage across the capacitor which considered as the actual DC voltage as shown in figure A.5 [145]. In this block the measured active power is divided by the DC voltage to get the DC current, the difference between the array current and the DC current gives the differential current in the capacitor. The resultant current is converted to p.u. integrated and then multiplied by base voltage to get the output DC voltage.

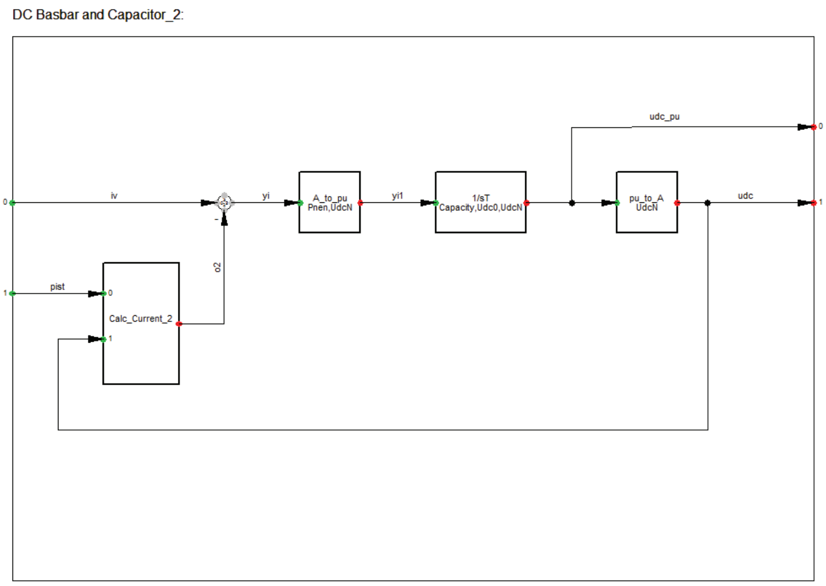

Figure A.5: DC Busbar and Capacitor.

- **Active Power Reduction model:** This model has the measured frequency as an input to provide an output signal (pred), as shown in figure A.6 [145], to force the controller to reduce the active power output of the static generator in case of over frequency. It functions when the frequency goes upper than 50.2Hz and reduces the active power by 40% per Hz. If the frequency falls below 50.05Hz, the controller can increase the PV delivered active power;

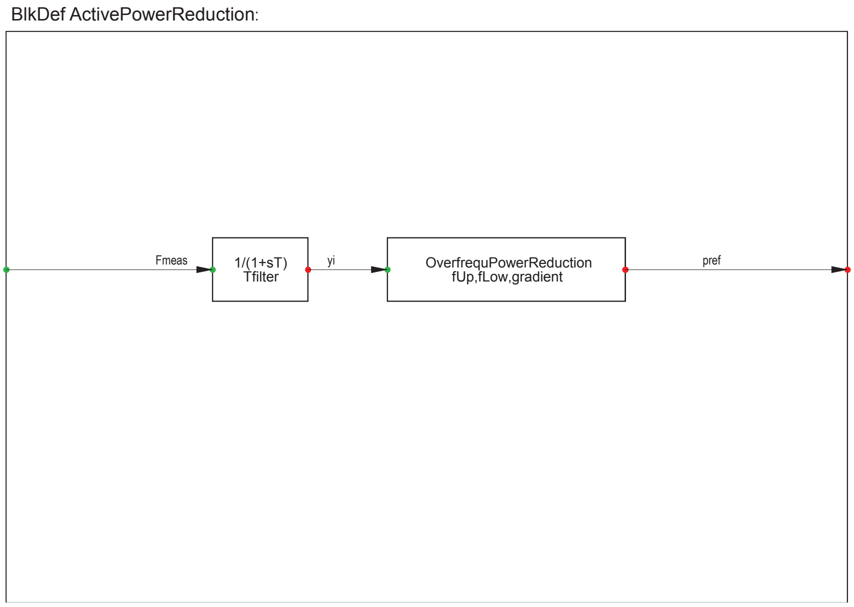

Figure A.6: Active Power Reduction.

- **PV Controller:** It can be considered as the main controller in the PV system control frame. Its aim is to regulate the PV system active and reactive power outputs based on reference signals provided from the DC side of the PV system;

  As illustrated in figure A.7 [145], the active power is regulated according to the reference signal ($vdcref$) from photovoltaic model which compared with ($vdcin$) from DC busbar and capacitor model, the difference (dp) injected to PI controller with ($pred$) signal from active power reduction model to prevent over frequency. The output of the PI (i_d), with upper and lower limits (i_{dmax}) and (i_{dmin}), passed through the current limiter to provide the d-axis component of the reference current (i_{dref}) which regulate the active power output of the static generator. On the other hand, the reactive power is regulated according to AC voltage measurement of the LV bus, this value is compared with the steady state reference value and the difference is injected to the reactive power support block. The equations in this block are written with a deadband and droop control. The deadband and droop are denoted as parameters and can be changed according to the implemented standard recommendations. The output of the reactive power support block (i_q), with upper and lower limits (i_{qmax}) and (i_{qmin}), passed through the current limiter to provide the q-axis component of the reference current (i_{qref}) which regulate the reactive power output of the static generator;

- **Static Generator:** Astatic generator is a power source with no rotating parts. The active and reactive power outputs of the static generator are respectively regulated by the real and imaginary parts of its current which are defined by i_{dref} and i_{qref}

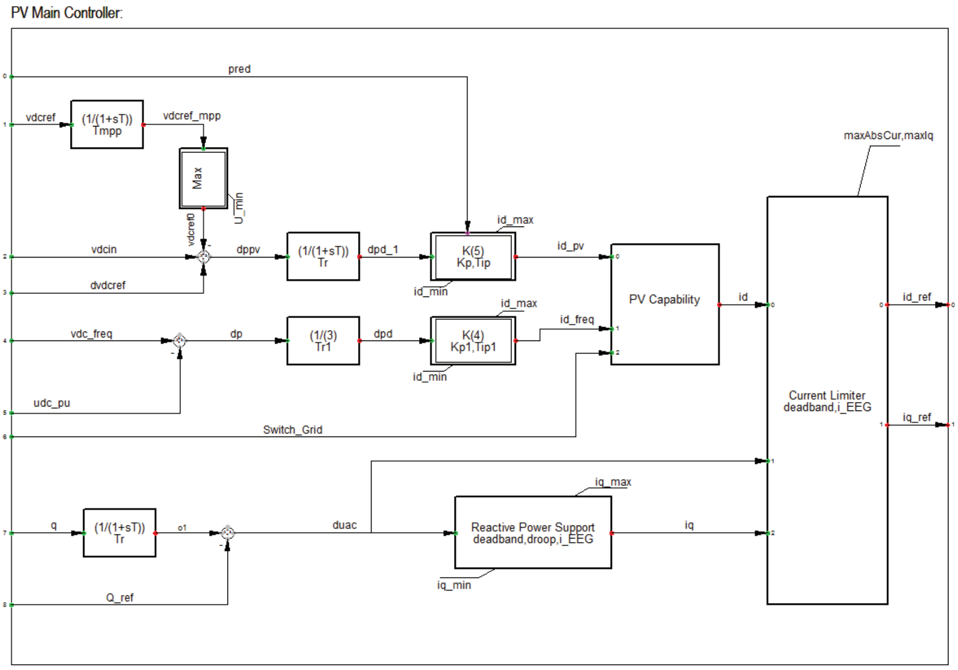

Figure A.7: Main PV Controller.

provided by the PV controller. In Power Factory, static generator can be selected from the "drag and drop", generator data is specified using the edit data windows. Figure A.8 shows static generator edit data window 'Basic data'. From this window the following data can specified;

1. The connected terminal 'busbar'.
2. Type of generator can be selected from a category list which comprises (Photovoltaic, Wind Generator, Other Renewable Generators, Fuel Cell, Other Static Generators).
3. Machine rating in MVA and power factor.
4. Number of machines in parallel.

Furthermore, from the data window 'load flow', shown in figure A.9, the following data can be specified:

1. The machine can be selected as a reference machine or not.
2. Local Voltage Controller can be selected from the list as; Power Factor, Voltage, or Droop.
3. The Corresponding Bus Type can be defined as a SL or PQ based upon if the machine is a reference machine or not.

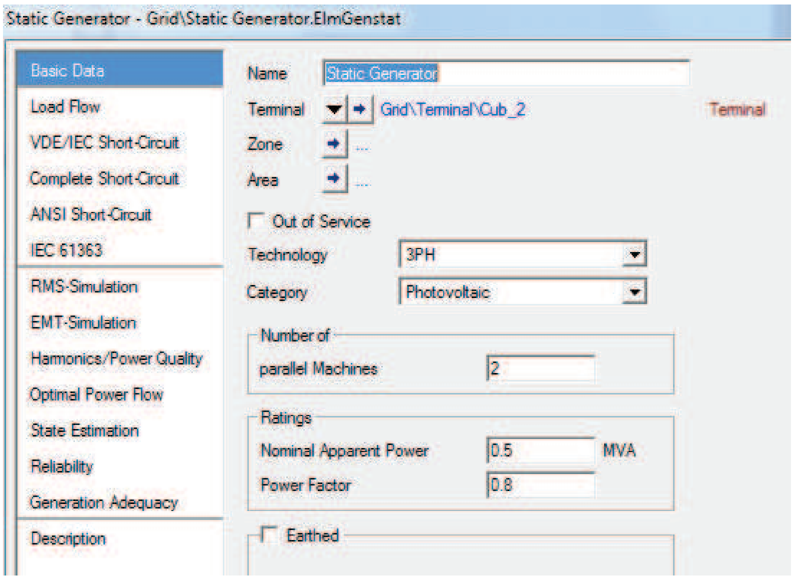

Figure A.8: Static generator's edit data window 'Basic data'.

4. The dispatched active and reactive powers.

5. Reactive Power Operational Limits can be specified either manually by setting the value in the related place, or according to the capability curve.

6. Capability curve as illustrated in figure A.9 shows the active and reactive power limits of the static generator in per unit values. The blue curve defines the power limits of the inverter. The active power limit specified on the y-axis depending on the power factor value while the reactive power limits are defined as Q_{min} and Q_{max} on the x-axis.

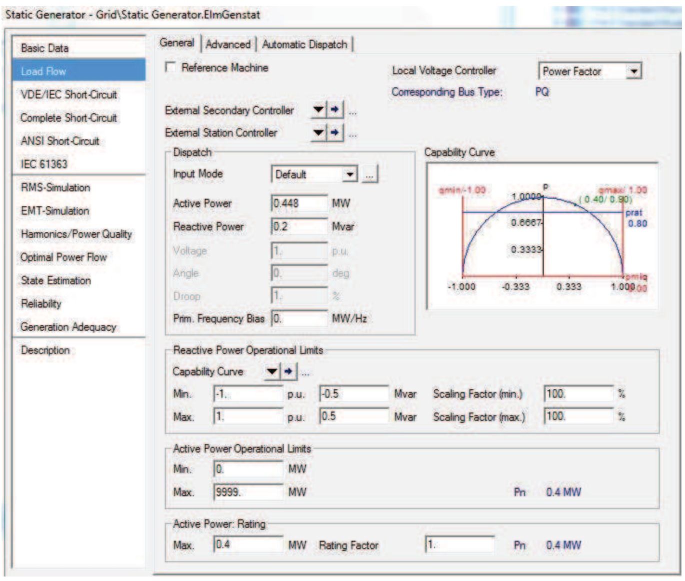

Figure A.9: Static generator's edit data window 'load flow'.

A.1.3 Modeling of BESS

Battery Energy Storage System (BESS) is represented in PowerFactory by a DC voltage source and a PWM converter as shown in figure A.10. The nominal voltage of the DC voltage source is defined using the data window 'Basic data'. For PWM, as shown in figure A.11 and figure A.12, edit data window 'Basic data' is used to set:

1. The rated voltages of the connected AC and DC terminals in kv.

2. PWM rated power in MVA.

While edit data window 'load flow' is used for defining:

1. Control mode (Vac-phi, Vdc-phi, PWM- phi, Vac-P, P-Q, Vdc-Q, or Vac-Vdc).

2. Reactive power limits.

3. Active power setpoint.

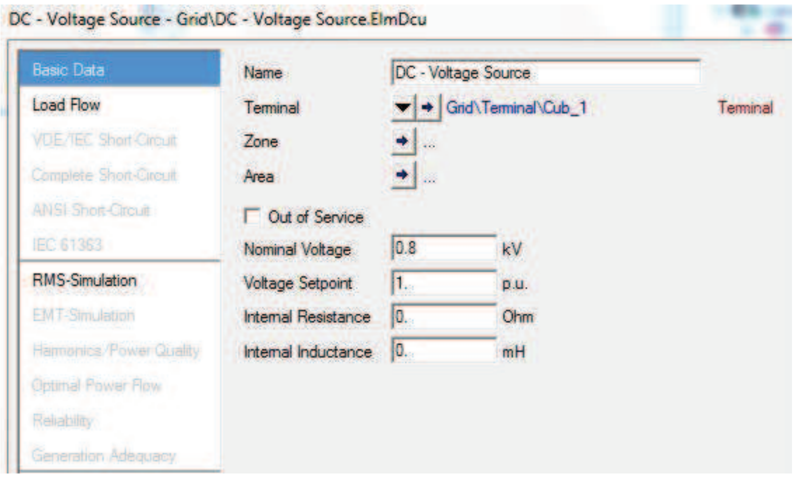

Figure A.10: Representing of BESS in PowerFactory..

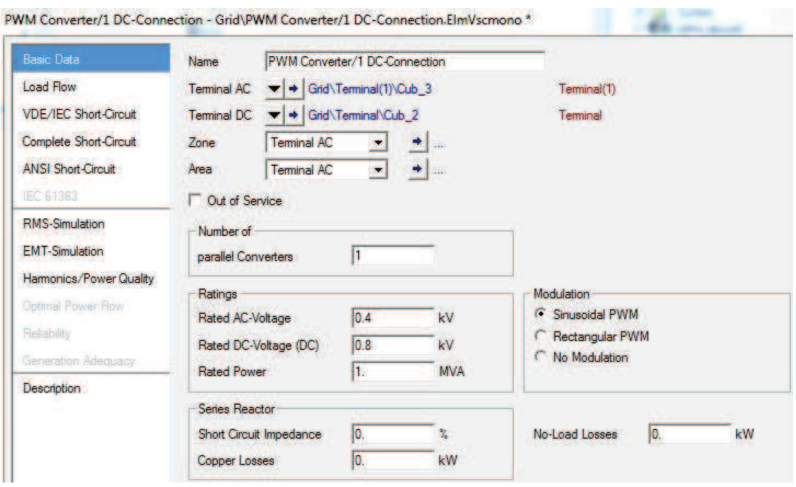

Figure A.11: PWM's edit data window 'Basic data'.

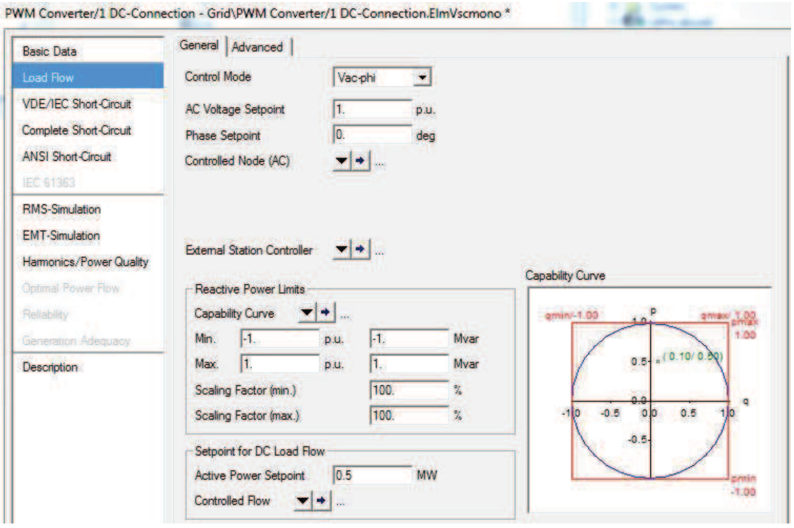

Figure A.12: PWM's edit data window 'load flow'.

A BESS built-in model is provided in PowerFactory library. Figure A.13 shows the control frame of the BESS model (composite model) which comprises Battery composite model, frequency control, PQ control , charge control, PWM converter model, measuring devices and flow signals. These models are only briefly described in the following part because the built-in model is not implemented in the thesis.

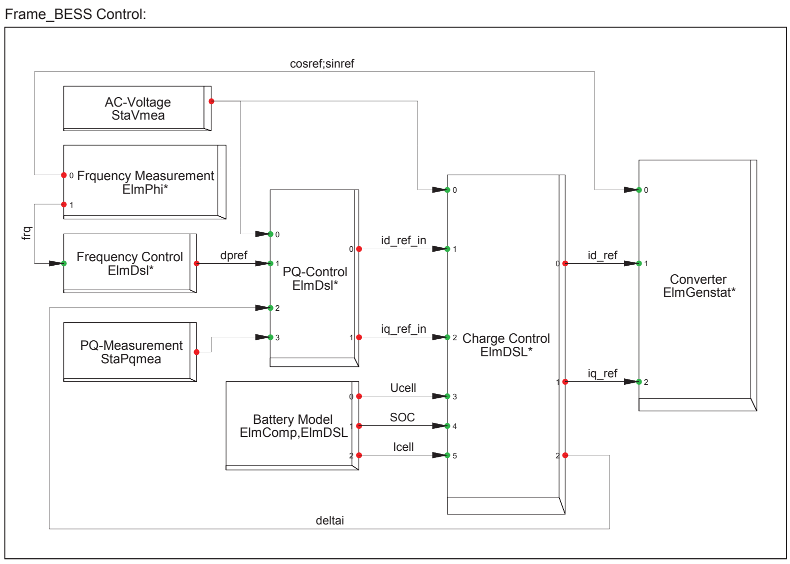

Figure A.13: Built-in control frame (composite model) of the BESS in powerfactory [146].

1. **Battery Composite model:** The battery composite model as shown in figure A.14 [146] includes: simple battery model, DC current measurement, and DC voltage source model. In the simple battery model, as illustrated in figure A.15 [146], the DC input current is used to evaluate the cell's current and voltage, the battery voltage and the state of charge (SoC).

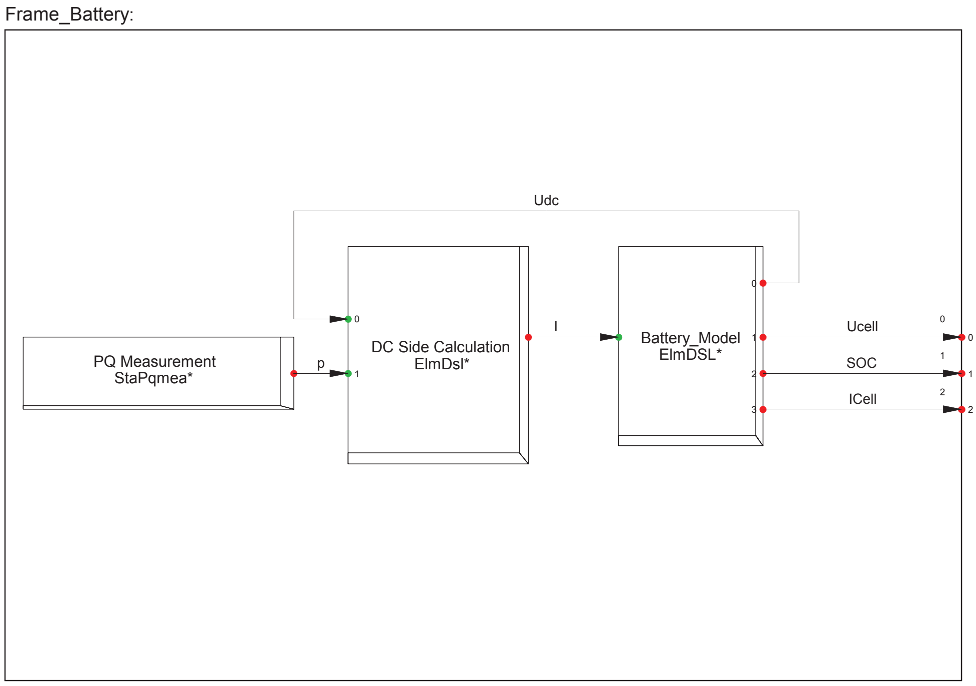

Figure A.14: Battery composite model in PowerFactory.

2. **Frequency Control model:** This model, as shown in figure A.16, compares the measured frequency against frequency reference and implements deadband and (f-p) droop control blocks to provide the active power reference to PQ control model.

3. **PQ Control model:** This model, as illustrated in figure A.17, provides id_ref and iq_ref for regulating active and reactive powers respectively. The upper part compares the measured active power with the reference power from frequency control model, the difference dp is filtered and used as an input of PI controller to get id_ref. The lower part also compares the measured voltage with reference voltage and the difference dv after filtered used as an input to a proportional with a deadband and an integrator to provide iq_ref.

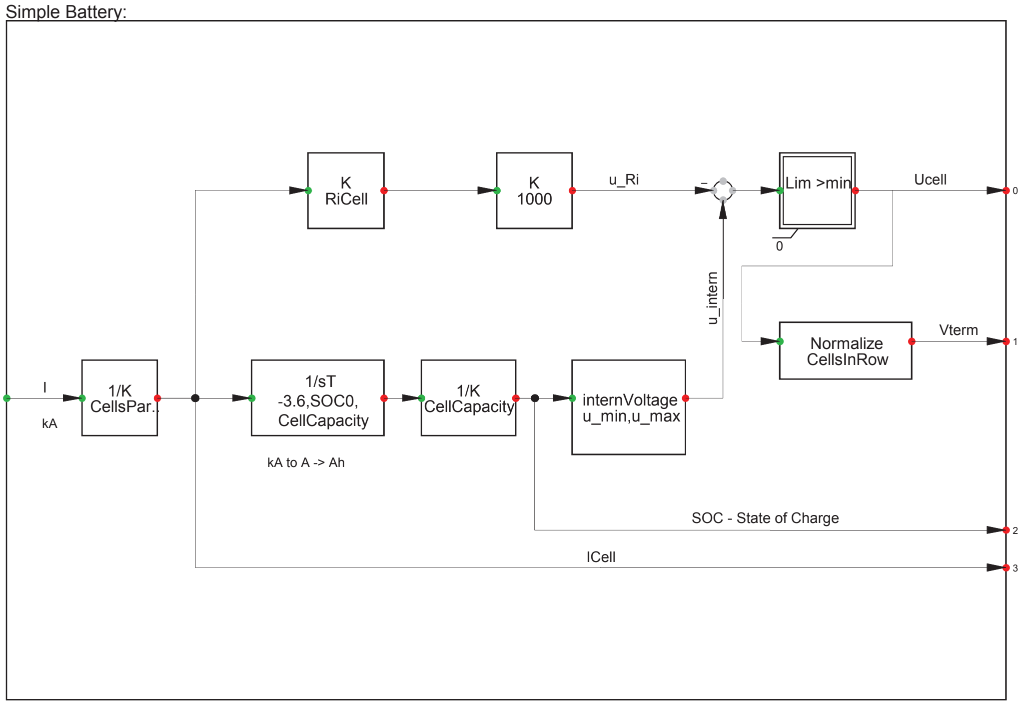

Figure A.15: Simple battery model in PowerFactory.

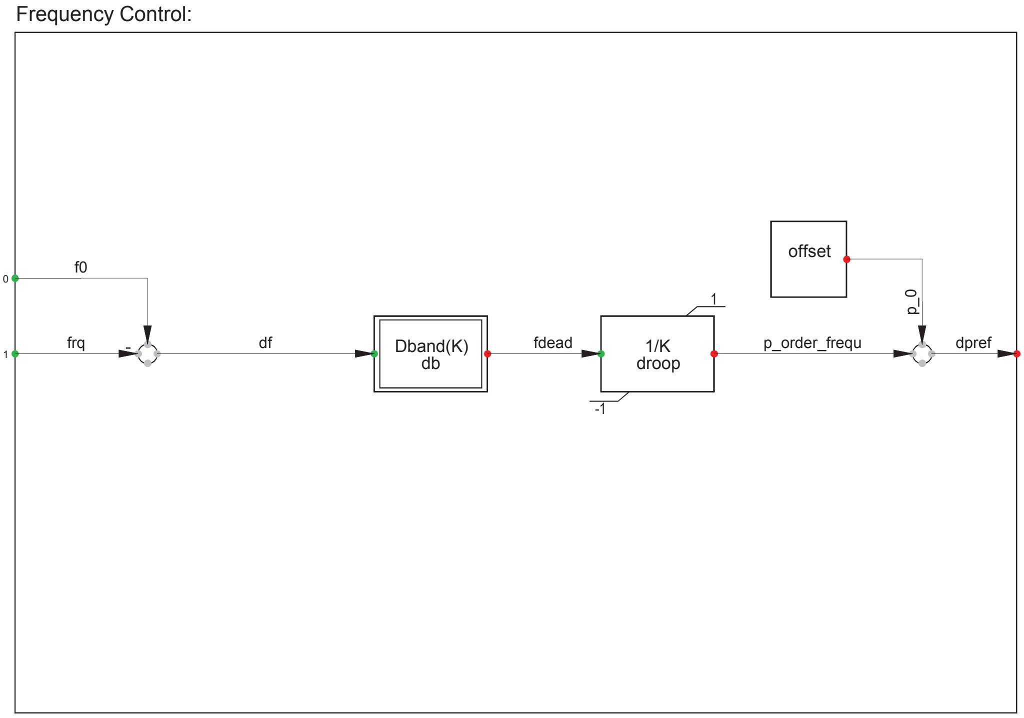

Figure A.16: Frequency control model.

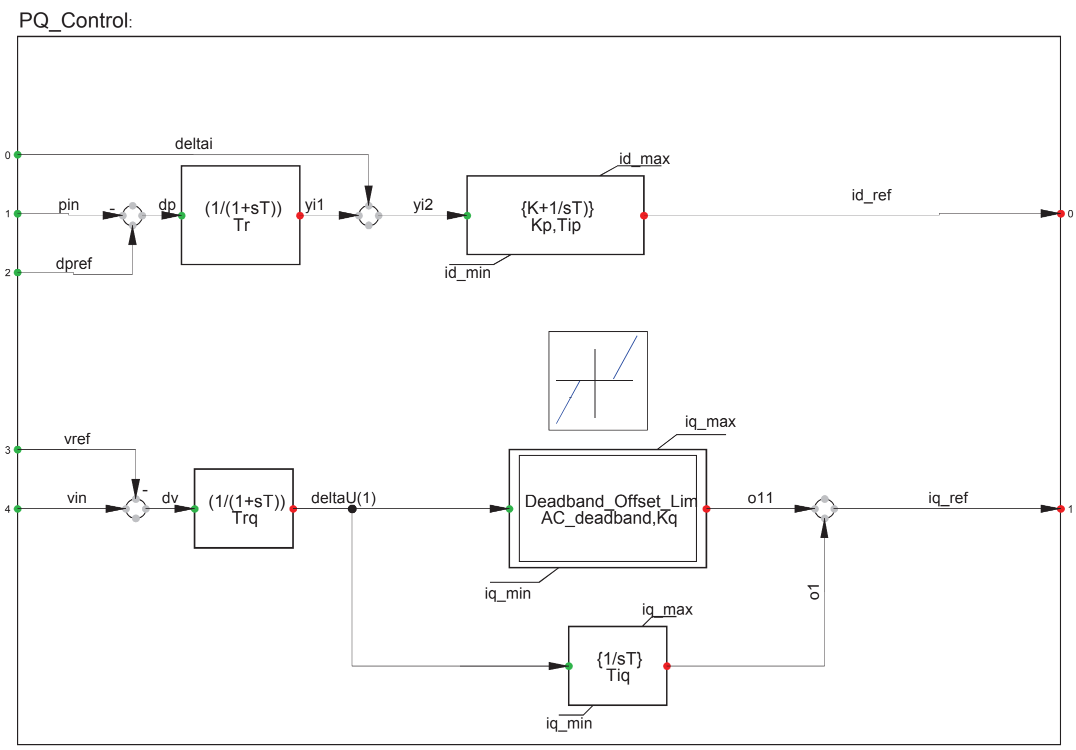

Figure A.17: PQ Control model.

4. **Charge Control model:** This model, as shown in figure A.18, has two bocks; charge control for controlling charging based on SOC, and current limiter to limit d and q axis currents based upon parameter values.

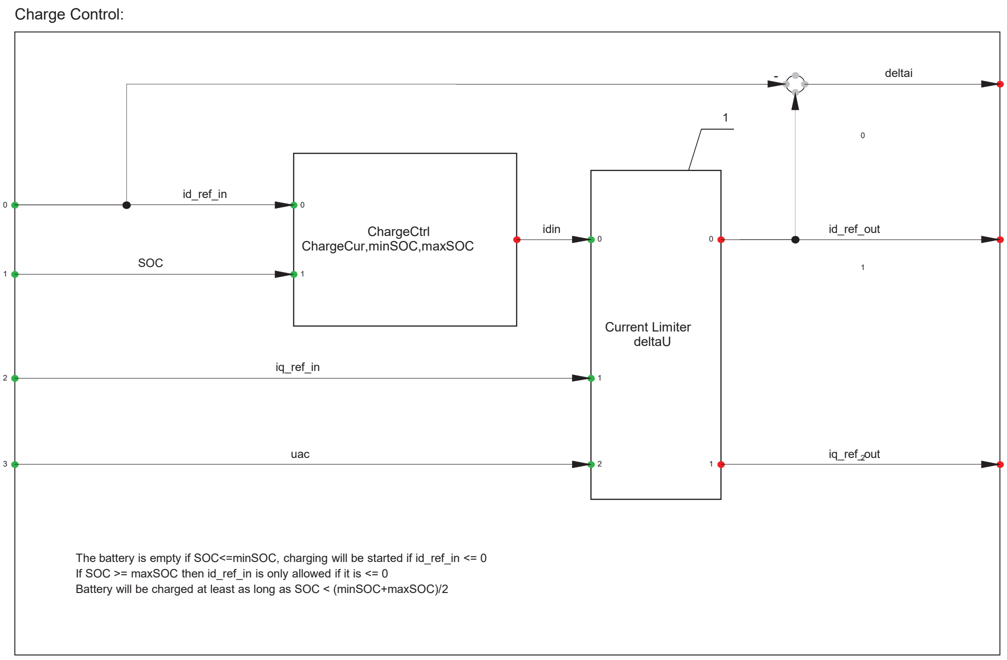

Figure A.18: Charge Control model.

5. **PWM Converter model:** The inputs to this model are id_ref and iq_ref for regulating respectively the active and reactive powers provided by the PWM. In powerfactory, PWM is available at the drag and drop library and its data can be specified using the edit data windows as previously illustrated in figures A.11 and A.12.

A.1.4 Modeling of Synchronous Generators

Synchronous generator can be selected from drag and drop library in PowerFactory panel and its data can be defined using basic data and load flow windows shown in figures A.19 and A.22 respectively.
The following data can be defined using Basic data window:

1. Machine type can be selected from global library or from a project or a new type can be created.

2. Connected terminal.

3. Generator /motor.

4. Internal grounding impedance.

The horizontal arrow beside 'Type' can be clicked to open 'Type basic data and load flow windows' as shown respectively in figures A.20 and A.21.

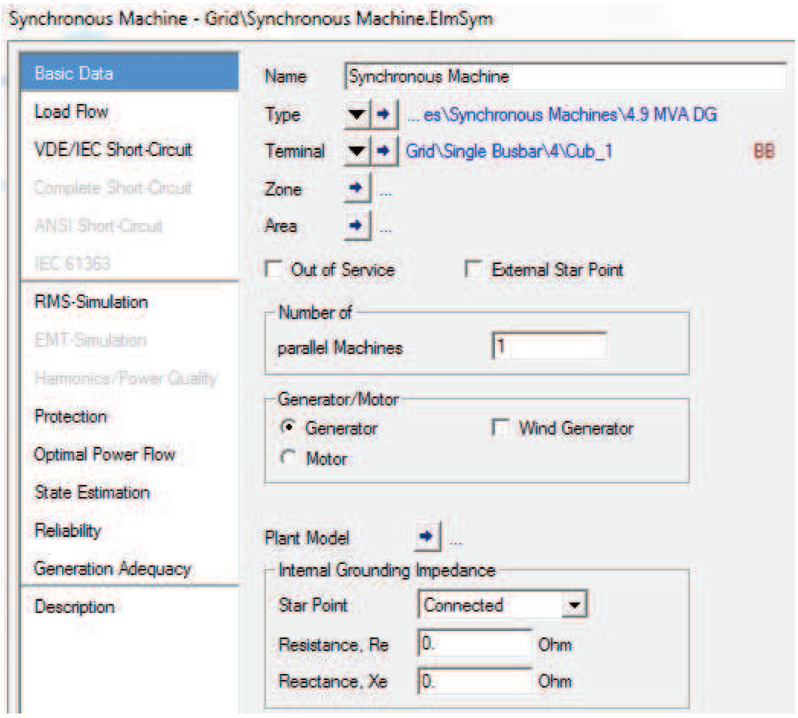

Figure A.19: Synchronous generator's edit data window 'Basic data'.

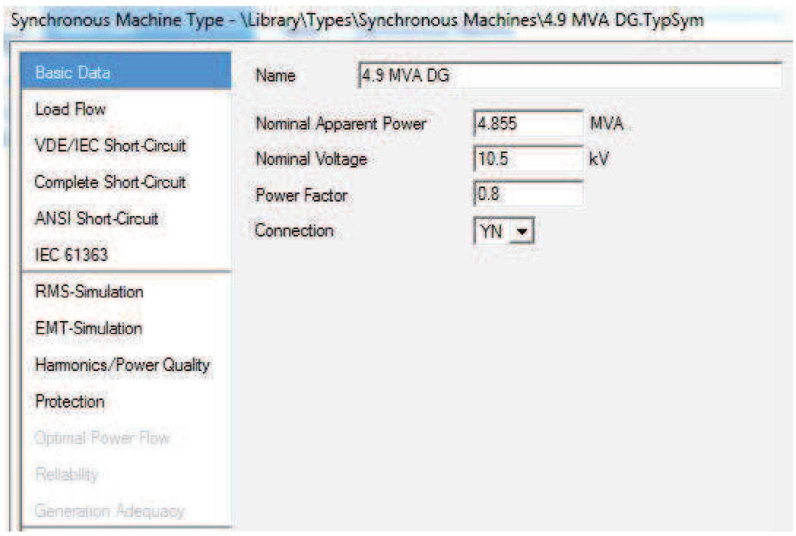

Figure A.20: Synchronous Generator's Type edit data window 'Basic data'.

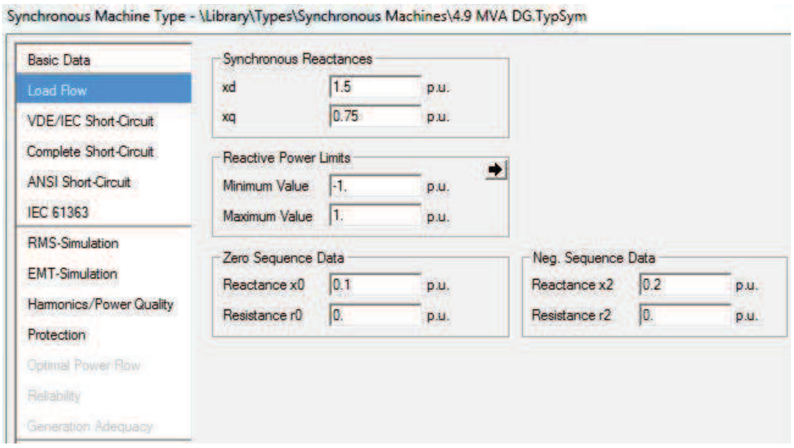

Figure A.21: Synchronous Generator's Type edit data window 'load flow'.

On the other hand, from the load flow window, shown in figure A.22, the following data can be defined:

- Whether the machine is a reference machine or not and consequently the corresponding bus is SL or PQ.
- Mode of local voltage control (power factor or voltage).
- Dispatched active and reactive power.
- Active and reactive powers operational limits.

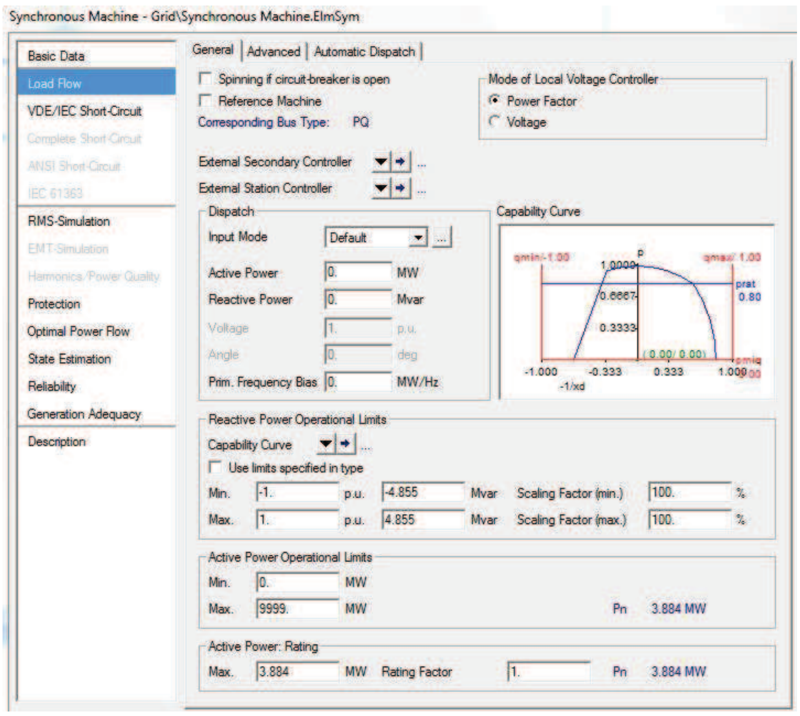

Figure A.22: Synchronous generator's edit data window 'load flow'

Bibliography

[1] X. Luo, J. Wang, M. Dooner, and J. Clarke, "Overview of current development in electrical energy storage technologies and the application potential in power system operation," *Applied Energy*, vol. 137, pp. 511–536, 2015.

[2] H. Farhangi, "The path of the smart grid," *IEEE power and energy magazine*, vol. 8, no. 1, pp. 18–28, 2010.

[3] Report to Congressional Requesters prepared by the United States General Accounting Office, "Air Pollution, Meeting Future Electricity Demand Will Increase Emissions of Some Harmful Substances," October 2002, Retrieved August 2009. [Online]. Available: http://www.gao.gov/new.items/d0349.pdf

[4] Y. Aldali, D. Henderson, and T. Muneer, "A 50 mw very large-scale photovoltaic power plant for al-kufra, libya: energetic, economic and environmental impact analysis," *International Journal of Low-Carbon Technologies*, p. ctr015, 2011.

[5] G. A. Center *et al.*, "Concentrating solar power for the mediterranean region," *German Aerospace Center (DLR) Institute of Technical Thermodynamics, Section Systems Analysis and Technology Assessment, Stuttgart*, 2005.

[6] I. M. Saleh, "Prospects of renewable energy in libya," in *Solar Physics and Solar Eclipses (SPSE 2006)*, vol. 1, 2006, pp. 153–161.

[7] General Electric Company of Libya (GECOL), "Annual report 2012-statistics 2012." [Online]. Available: http://www.gecol.ly

[8] M. Ekhlat, I. Salah, and N. Kreama, "Energy efficiency and renewable energy. libya–national study," *Sophia Antipolis: UNEP, Plan Bleu, Regional Activity Centre*, 2007.

[9] A. E. A Dagroum, A Assnousi, "Integration of renewable energy into libyan electrical grid," *Tunis, Tunisia*, 9th of October 2014.

[10] I. of Electrical Engineers and N. Jenkins, *Embedded Generation (IEE power and energy series; 31)*. Institution of Engineering and Technology-IET, 2000.

[11] S. Galli, A. Scaglione, and Z. Wang, "For the grid and through the grid: The role of power line communications in the smart grid," *Proceedings of the IEEE*, vol. 99, no. 6, pp. 998–1027, 2011.

[12] J. Jin, "Transformational relationship of renewable energies and the smart grid," *Clark WW II (Editor and Author) Sustainable communities design handbook. Elsevier Press, New York, NY*, pp. 217–232, 2010.

[13] [Online]. Available: http://osceolaenergy.com/wp-content/uploads/2015/06/distributed-power-generation-diagram.png

[14] Palo Alto, CA: EPRI., "Engineering guide for integration of distributed generation and storage into power distribution systems," December 2012. [Online]. Available: http://www.epri.com/abstracts/Pages/ProductAbstract.aspx?ProductId=000000000001000419

[15] V. Techn, "Distributed generation, education modules," *2007 Consortium on Energy restructuring, Virginia Tech. Available at www. dg. history. vt. edu/ch1/introduction. html*, 2007.

[16] A. Thornton and C. R. Monroy, "Distributed power generation in the united states," *Renewable and Sustainable Energy Reviews*, vol. 15, no. 9, pp. 4809–4817, 2011.

[17] P. P. Barker and R. W. De Mello, "Determining the impact of distributed generation on power systems. i. radial distribution systems," in *Power Engineering Society Summer Meeting, 2000. IEEE*, vol. 3. IEEE, 2000, pp. 1645–1656.

[18] G. Pepermans, J. Driesen, D. Haeseldonckx, R. Belmans, and W. D'haeseleer, "Distributed generation: definition, benefits and issues," *Energy policy*, vol. 33, no. 6, pp. 787–798, 2005.

[19] F. L. Alvarado, "Locational aspects of distributed generation," in *Power Engineering Society Winter Meeting, 2001. IEEE*, vol. 1. IEEE, 2001, pp. 140–vol.

[20] L. Coles and R. Beck, "Distributed generation can provide an appropriate customer price response to help fix wholesale price volatility," in *Power Engineering Society Winter Meeting, 2001. IEEE*, vol. 1. IEEE, 2001, pp. 141–143.

[21] J. EIA, "International energy outlook. us energy information administration," DOE/EIA-0484 (2013) Edition, Tech. Rep., 2013.

[22] J. Dong, T.-t. Feng, H.-x. Sun, H.-x. Cai, R. Li, and Y. Yang, "Clean distributed generation in china: Policy options and international experience," *Renewable and Sustainable Energy Reviews*, vol. 57, pp. 753–764, 2016.

[23] R. Passey, T. Spooner, I. MacGill, M. Watt, and K. Syngellakis, "The potential impacts of grid-connected distributed generation and how to address them: A review of technical and non-technical factors," *Energy Policy*, vol. 39, no. 10, pp. 6280–6290, 2011.

[24] J. R. Fanchi, *Energy: technology and directions for the future.* Academic Press, 2004.

[25] I. A. Kateeb, M. Bikdash, and P. Chopade, "Back to the future renewable energy sources and green smart grid," in *Southeastcon, 2011 Proceedings of IEEE.* IEEE, 2011, pp. 147–152.

[26] T. Ackermann, G. Andersson, and L. Söder, "Distributed generation: a definition," *Electric power systems research*, vol. 57, no. 3, pp. 195–204, 2001.

[27] W. El-Khattam and M. Salama, "Distributed generation technologies, definitions and benefits," *Electric power systems research*, vol. 71, no. 2, pp. 119–128, 2004.

[28] H. L. Willis, *Distributed power generation: planning and evaluation.* CRC Press, 2000.

[29] [Online]. Available: https://online.platts.com/PPS/P=m&e=1092414376228.-3902959445184628128/Power-Jun04-GM_6.jpg

[30] A. Borbely and J. Kreider, "Distributed generation: A new paradigm for the new millenium"," 2001.

[31] G. W. Massey, *Essentials of distributed generation systems.* Jones & Bartlett Learning, 2010.

[32] [Online]. Available: http://me1065.wikidot.com/local--resized-images/microturbines/Figure_9/medium.jpg

[33] P. Fraser, "Distributed generation in liberalised electricity markets," in *International symposium on distributed generation: power system and market aspects*, 2002, pp. 1G–12.

[34] M. Suter, "Active filter for a microturbine," in *Telecommunications Energy Conference, 2001. INTELEC 2001. Twenty-Third International.* IET, 2001, pp. 162–165.

[35] A. M. B. a. J.F.Kreider., "Distributed generation (2001 ed.)." 2001.

[36] M. Boyce, "Handbook for cogeneration and combined cycle power plants. 2004," *New York: The American Society of Mechanical Engineers.*

[37] [Online]. Available: http://www.fzjuelich.de/SharedDocs/Bilder/PORTAL/EN/EnergyEnvironment/brennstoffzelle-aufbau.jpg?__blob=poster

[38] Department of Energy (DOE)., "DOE 2003 Fuel Cell Report to Congress ," Feb. 2003. [Online]. Available: https://www.hydrogen.energy.gov/pdfs/fc_report_congress_feb2003.pdf

[39] M. Farooque and H. C. Maru, "Fuel cells-the clean and efficient power generators," *Proceedings of the IEEE*, vol. 89, no. 12, pp. 1819–1829, 2001.

[40] DOE/NETL Brochure., "Distributed Generation," June 2003. [Online]. Available: https://www.netl.doe.gov/File%20Library/Publications/brochures/Dist_Gen_brochure_final_1.pdf

[41] S. Said, A. Massoud, M. Benammar, and S. Ahmed, "A matlab/simulink-based photovoltaic array model employing simpowersystems toolbox," *Journal of Energy and Power Engineering*, vol. 6, no. 12, p. 1965, 2012.

[42] [Online]. Available: http://www.alternative-energy-news.info/images/technical/solar-power.jpg

[43] S. Heier, "Wind power [a review of grid integration of wind energy conversion systems (s. heier; 2006); book review]," *IEEE Power and Energy Magazine*, vol. 6, no. 3, pp. 95–97, May 2008.

[44] [Online]. Available: http://www.energizect.com/sites/default/files/uploads/Energy101/WindDiagram.jpg

[45] International Energy Agency (IEA)., "Renewables for Power Generation: Status and Prospects," 2004. [Online]. Available: http://www.antoniolima.web.br.com/arquivos/renewpower_2003.pdf

[46] IEA., *Renewable Energy: Market and Policy Trends in IEA Countries.* OECD Publishing, 2004.

[47] D. of Energy and C. C. (DECC), "Energy from waste including anaerobic digestion," 2013. [Online]. Available: http://www.decc.gov.uk/en/content/cms/meeting_energy/bioenergy/waste/waste.aspx

[48] S. Gopiya Naik, D. Khatod, and M. Sharma, "Planning and operation of distributed generation in distribution networks," 2012.

[49] E. Martinot, J. L. Sawin *et al.*, "Renewables 2012 global status report," *Renewable Energy Policy Network for the 21st Century*, 2012.

[50] G. Masson, M. Latour, M. Rekinger, I.-T. Theologitis, and M. Papoutsi, "Global market outlook for photovoltaics 2013-2017," *European Photovoltaic Industry Association*, pp. 12–32, 2013.

[51] M. Rekinger and F. Thies, "Global market outlook for solar power 2015–2019," *SolarPower Europe*, 2015.

[52] Michael Schmela, SolarPower Europe, "Solar Market Report and Membership Directory – 2016 Edition," 2004. [Online]. Available: http://www.antoniolima.web.br.com/arquivos/renewpower_2003.pdf

[53] E. Lorenzo, *Solar electricity: engineering of photovoltaic systems.* Earthscan/James & James, 1994.

[54] M. G. Villalva, J. R. Gazoli, and E. Ruppert Filho, "Comprehensive approach to modeling and simulation of photovoltaic arrays," *IEEE Transactions on power electronics*, vol. 24, no. 5, pp. 1198–1208, 2009.

[55] M. Gilbert, "Masters, renewable and efficient electric power systems," *Wiley-Interscience, John Wiley & Sons, Inc, New Jersey*, vol. 75, p. 76, 2004.

[56] R. Ramaprabha and B. L. Mathur, "Matlab based modelling to study the influence of shading on series connected spva," in *2009 Second International Conference on Emerging Trends in Engineering & Technology.* IEEE, 2009, pp. 30–34.

[57] M. M. Begovic, I. Kim, D. Novosel, J. R. Aguero, and A. Rohatgi, "Integration of photovoltaic distributed generation in the power distribution grid," in *System Science (HICSS), 2012 45th Hawaii International Conference on.* IEEE, 2012, pp. 1977–1986.

[58] T. Yetayew and T. Jyothsna, "Improved single-diode modeling approach for photovoltaic modules using data sheet," in *2013 Annual IEEE India Conference (INDICON).* IEEE, 2013, pp. 1–6.

[59] N. M. A. A. Shannan, N. Z. Yahaya, and B. Singh, "Single-diode model and two-diode model of pv modules: A comparison," in *Control System, Computing and Engineering (ICCSCE), 2013 IEEE International Conference on.* IEEE, 2013, pp. 210–214.

[60] D. Sera, R. Teodorescu, and P. Rodriguez, "Photovoltaic module diagnostics by series resistance monitoring and temperature and rated power estimation," in *Industrial Electronics, 2008. IECON 2008. 34th Annual Conference of IEEE.* IEEE, 2008, pp. 2195–2199.

[61] [Online]. Available: http://www.itacanet.org/wp-content/uploads/2011/05/cell1-600x497.jpg

[62] [Online]. Available: http://www.itacanet.org/wp-content/uploads/2011/05/cell2-600x375.jpg

[63] J. Dunlop, "National joint apprenticeship and training committee for the electrical industry. photo-voltaic systems. orland park, ill," 2010.

[64] [Online]. Available: http://www.seawardsolar.com/userfiles/image/landing-pages/curve-tracing/irradiance-affect-i-v-curves-2.jpg

[65] [Online]. Available: http://www.pvresources.com/img/solarcells/solarcells4.png

[66] H. Rauschenbach, *Solar cells array design handbook: the principles and technology of photovoltaic energy conversion*. Van Nostrand Reinhold, 1980.

[67] A. H. ALQahtani, M. S. Abuhamdeh, and Y. M. Alsmadi, "A simplified and comprehensive approach to characterize photovoltaic system performance," in *Energytech, 2012 IEEE*. IEEE, 2012, pp. 1–6.

[68] [Online]. Available: http://cdn2.bigcommerce.com/server5500/hfd09/product_images/uploaded_images/hsl60-poly-iv-curve.jpg

[69] [Online]. Available: http://www.pvresources.com/img/solarcells/solarcells2.png

[70] T. Esram, P. L. Chapman *et al.*, "Comparison of photovoltaic array maximum power point tracking techniques," *IEEE Transactions on Energy Conversion EC*, vol. 22, no. 2, p. 439, 2007.

[71] V. Ćuk, P. F. Ribeiro, J. F. Cobben, W. L. Kling, F. R. Isleifsson, H. W. Bindner, N. Martensen, A. Samadi, and L. Söder, "Considerations on the modeling of photovoltaic systems for grid impact studies," in *1st International Workshop on the Integration of Solar Power into Power Systems*, 2011.

[72] W. Wu, N. Pongratananukul, W. Qiu, K. Rustom, T. Kasparis, and I. Batarseh, "Dsp-based multiple peak power tracking for expandable power system," in *Eighteenth Annu. IEEE Appl. Power Electron. Conf. Expo*, 2003, pp. 525–530.

[73] Dezso Sera, "Maximum Power Point Tracking (MPPT) for PV systems." [Online]. Available: http://www.et.aau.dk

[74] Havard Breisnes Vika, "Modelling of Photovoltaic Modules with Battery Energy Storage in Simulink/Matlab," 2005.

[75] A. Tariq and M. J. Asghar, "Development of an analog maximum power point tracker for photovoltaic panel," in *2005 International Conference on Power Electronics and Drives Systems*, vol. 1. IEEE, 2014, pp. 251–255.

[76] Paraskevi Breza, "Modelling and simulation of a PV generator for applications on distributed generation systems," 2013.

[77] [Online]. Available: http://www.invertergo.com/Content/Images/uploaded/solar%20power%20system2.gif

[78] [Online]. Available: http://www.greenrhinoenergy.com/solar/technologies/images/pv_system_blocks-02.jpg

[79] H. Chen, T. N. Cong, W. Yang, C. Tan, Y. Li, and Y. Ding, "Progress in electrical energy storage system: A critical review," *Progress in Natural Science*, vol. 19, no. 3, pp. 291–312, 2009.

[80] I. Hadjipaschalis, A. Poullikkas, and V. Efthimiou, "Overview of current and future energy storage technologies for electric power applications," *Renewable and sustainable energy reviews*, vol. 13, no. 6, pp. 1513–1522, 2009.

[81] H. Ibrahim, A. Ilinca, and J. Perron, "Energy storage systems—characteristics and comparisons," *Renewable and sustainable energy reviews*, vol. 12, no. 5, pp. 1221–1250, 2008.

[82] ISGF India Smart Grid Knowledge Portal , "Electric-Energy-Storage-(EES)." [Online]. Available: http://www.indiasmartgrid.org/Electric-Energy-Storage-(EES).php?m=4&y=2016

[83] A. Oberhofer and P. Meisen, "Energy storage technologies & their role in renewable integration," *Global Energy Network Institute*, 2012.

[84] [Online]. Available: http://www.ourworldofenergy.com/images/other-renewables-energy/vignette_image_10_1.jpg

[85] M. Beaudin, H. Zareipour, A. Schellenberglabe, and W. Rosehart, "Energy storage for mitigating the variability of renewable electricity sources: An updated review," *Energy for Sustainable Development*, vol. 14, no. 4, pp. 302–314, 2010.

[86] S. Succar, R. H. Williams *et al.*, "Compressed air energy storage: theory, resources, and applications for wind power," *Princeton environmental institute report*, vol. 8, 2008.

[87] [Online]. Available: http://www.intechopen.com/source/html/42268/media/image2_w.jpg

[88] A. Cavallo, "Controllable and affordable utility-scale electricity from intermittent wind resources and compressed air energy storage (caes)," *Energy*, vol. 32, no. 2, pp. 120–127, 2007.

[89] [Online]. Available: http://storage4.eu/wp-content/uploads/Battery_Charge_Discharge-620x541.png

[90] R. Walawalkar and J. Apt, "Market analysis of emerging electric energy storage systems," *National Energy Technology Laboratory*, pp. 1–118, 2008.

[91] F. Rahman, S. Rehman, and M. A. Abdul-Majeed, "Overview of energy storage systems for storing electricity from renewable energy sources in saudi arabia," *Renewable and Sustainable Energy Reviews*, vol. 16, no. 1, pp. 274–283, 2012.

[92] IEC-International Electrotechnical Commission , "White Paper-Electrical Energy Storage." [Online]. Available: http://www.iec.ch/whitepaper/energystorage/

[93] F. Díaz-González, A. Sumper, O. Gomis-Bellmunt, and R. Villafáfila-Robles, "A review of energy storage technologies for wind power applications," *Renewable and Sustainable Energy Reviews*, vol. 16, no. 4, pp. 2154–2171, 2012.

[94] [Online]. Available: https://www.researchgate.net/figure/220037284_fig6_NaS-battery-6566[accessedOct4,2016]

[95] P. Taylor, R. Bolton, D. Stone, X.-P. Zhang, C. Martin, and P. Upham, "Pathways for energy storage in the uk," *Report for the centre for low carbon futures, York*, 2012.

[96] D. H. Doughty, P. C. Butler, A. A. Akhil, N. H. Clark, and J. D. Boyes, "Batteries for large-scale stationary electrical energy storage," *The Electrochemical Society Interface*, vol. 19, no. 3, pp. 49–53, 2010.

[97] A. Evans, V. Strezov, and T. J. Evans, "Assessment of utility energy storage options for increased renewable energy penetration," *Renewable and Sustainable Energy Reviews*, vol. 16, no. 6, pp. 4141–4147, 2012.

[98] [Online]. Available: http://s1.q4cdn.com/674549448/files/images/Projects/redoxbattery_diagram.jpg

[99] Z. Yang, J. Zhang, M. C. Kintner-Meyer, X. Lu, D. Choi, J. P. Lemmon, and J. Liu, "Electrochemical energy storage for green grid," *Chemical reviews*, vol. 111, no. 5, pp. 3577–3613, 2011.

[100] F. Rahman and M. Skyllas-Kazacos, "Optimization of supersaturated vanadium electrolyte for high energy density vanadium redox battery," in *4th international conference and exhibition on chemistry in industry*, 2000.

[101] A. Gonzalez, B. Ó. Gallachóir, E. McKeogh, and K. Lynch, "Study of electricity storage technologies and their potential to address wind energy intermittency in ireland," *Sustainable Energy Ireland*, 2004.

[102] ecofys , "Energy Storage Opportunities and Challenges." [Online]. Available: http://www.ecofys.com/en/publication/energy-storage-opportunities-and-challenges/

[103] [Online]. Available: http://pubs.rsc.org/services/images/RSCpubs.ePlatform.Service.FreeContent.ImageService.svc/ImageService/Articleimage/2015/EE/c4ee04041d/c4ee04041d-f1_hi-res.gif

[104] S. Mekhilef, R. Saidur, and A. Safari, “Comparative study of different fuel cell technologies,” *Renewable and Sustainable Energy Reviews*, vol. 16, no. 1, pp. 981–989, 2012.

[105] S. G. Chalk and J. F. Miller, “Key challenges and recent progress in batteries, fuel cells, and hydrogen storage for clean energy systems,” *Journal of Power Sources*, vol. 159, no. 1, pp. 73–80, 2006.

[106] H. Chen, Y. Ding, T. Peters, and F. Berger, “Method of storing energy and a cryogenic energy storage system,” Feb. 25 2016, uS Patent App. 15/053,840.

[107] S. C. Smith, P. Sen, and B. Kroposki, “Advancement of energy storage devices and applications in electrical power system,” in *Power and Energy Society General Meeting-Conversion and Delivery of Electrical Energy in the 21st Century, 2008 IEEE*. IEEE, 2008, pp. 1–8.

[108] X. Fang, N. Kutkut, J. Shen, and I. Batarseh, “Analysis of generalized parallel-series ultracapacitor shift circuits for energy storage systems,” *Renewable Energy*, vol. 36, no. 10, pp. 2599–2604, 2011.

[109] [Online]. Available: https://www.researchgate.net/profile/Xing_Luo3/publication/267048009/figure/fig9/AS:267873708933123@1440877477998/Schematic-diagram-of-a-SMES-system.png

[110] C. Naish, I. McCubbin, O. Edberg, and M. Harfoot, “Outlook of energy storage technologies,” *European Parliament’s committee on Industry, Research and Energy*, 2008.

[111] K. Honghai and W. Zhengqiu, “Research of super capacitor energy storage system based on dg connected to power grid,” in *2009 International Conference on Sustainable Power Generation and Supply*. IEEE, 2009, pp. 1–6.

[112] EESI Environmental and Energy Study Institute , “Energy Storage .” [Online]. Available: http://www.eesi.org/papers/view/issue-brief-energy-storage?/issue-brief-energy-storage-06-aug-2013

[113] B. Wang, B. Zhang, and Z. Hao, “Control of composite energy storage system in wind and pv hybrid microgrid,” in *TENCON 2013-2013 IEEE Region 10 Conference (31194)*. IEEE, 2013, pp. 1–5.

[114] K. Le Dinh and Y. Hayashi, “Centralized bess control to minimize demand of pv-supplied micro-grid under voltage constraints,” in *Power and Energy (PECon), 2012 IEEE International Conference on*. IEEE, 2012, pp. 864–869.

[115] A. Ghazanfari, M. Hamzeh, H. Mokhtari, and H. Karimi, "Active power management of multihybrid fuel cell/supercapacitor power conversion system in a medium voltage microgrid," *IEEE Transactions on Smart Grid*, vol. 3, no. 4, pp. 1903–1910, 2012.

[116] F. Bignucolo, A. Raciti, and R. Caldon, "Coordinating active and reactive energy balances in islanded networks supported by renewables and bess," in *Renewable Power Generation Conference (RPG 2014), 3rd*. IET, 2014, pp. 1–6.

[117] A. R. Jordehi, "Allocation of distributed generation units in electric power systems: A review," *Renewable and Sustainable Energy Reviews*, vol. 56, pp. 893–905, 2016.

[118] E. Reihani, S. Sepasi, L. R. Roose, and M. Matsuura, "Energy management at the distribution grid using a battery energy storage system (bess)," *International Journal of Electrical Power & Energy Systems*, vol. 77, pp. 337–344, 2016.

[119] M. Shao, R. Liu, and D. Lv, "Control strategy of voltage and frequency for islanded microgrid," in *Power Electronics and Motion Control Conference (IPEMC), 2012 7th International*, vol. 3. IEEE, 2012, pp. 2085–2089.

[120] H. Karimi-Davijani and O. Ojo, "Dynamic operation and control of a multi-dg unit standalone microgrid," in *Innovative Smart Grid Technologies (ISGT), 2011 IEEE PES*. IEEE, 2011, pp. 1–7.

[121] X. Li, D. Hui, and X. Lai, "Battery energy storage station (bess)-based smoothing control of photovoltaic (pv) and wind power generation fluctuations," *IEEE Transactions on Sustainable Energy*, vol. 4, no. 2, pp. 464–473, 2013.

[122] J.-Y. Kim, J.-H. Jeon, S.-K. Kim, C. Cho, J. H. Park, H.-M. Kim, and K.-Y. Nam, "Cooperative control strategy of energy storage system and microsources for stabilizing the microgrid during islanded operation," *IEEE Transactions on Power Electronics*, vol. 25, no. 12, pp. 3037–3048, 2010.

[123] S. Teleke, M. E. Baran, A. Q. Huang, S. Bhattacharya, and L. Anderson, "Control strategies for battery energy storage for wind farm dispatching," *IEEE Transactions on Energy Conversion*, vol. 24, no. 3, pp. 725–732, 2009.

[124] M. Glavin, P. K. Chan, S. Armstrong, and W. Hurley, "A stand-alone photovoltaic supercapacitor battery hybrid energy storage system," in *Power Electronics and Motion Control Conference, 2008. EPE-PEMC 2008. 13th*. IEEE, 2008, pp. 1688–1695.

[125] N. Hajilu, G. Gharehpetian, S. Hosseinian, M. Poursistani, and M. Kohansal, "Power control strategy in islanded microgrids based on vf and pq theory using droop control of inverters," in *Electric Industry Automation (ICEIA), 2015 International Congress on*. IEEE, 2015, pp. 37–42.

[126] D. Wu, F. Tang, J. M. Guerrero, and J. C. Vasquez, "Autonomous control of distributed generation and storage to coordinate p/q sharing in islanded microgrids-an approach beyond droop control," in *Energy Conference (ENERGYCON), 2014 IEEE International*. IEEE, 2014, pp. 983–988.

[127] D. Wu, F. Tang, T. Dragicevic, J. C. Vasquez, and J. M. Guerrero, "Autonomous active power control for islanded ac microgrids with photovoltaic generation and energy storage system," *IEEE Transactions on Energy Conversion*, vol. 29, no. 4, pp. 882–892, 2014.

[128] T. L. Vandoorn, B. Renders, L. Degroote, B. Meersman, and L. Vandevelde, "Active load control in islanded microgrids based on the grid voltage," *IEEE Transactions on Smart Grid*, vol. 2, no. 1, pp. 139–151, 2011.

[129] D. Wu, F. Tang, T. Dragicevic, J. C. Vasquez, and J. M. Guerrero, "Coordinated primary and secondary control with frequency-bus-signaling for distributed generation and storage in islanded microgrids," in *Industrial Electronics Society, IECON 2013-39th Annual Conference of the IEEE*. IEEE, 2013, pp. 7140–7145.

[130] J. P. Lopes, C. Moreira, and A. Madureira, "Defining control strategies for analysing microgrids islanded operation," in *Power Tech, 2005 IEEE Russia*. IEEE, 2005, pp. 1–7.

[131] R. Caldon, M. Coppo, A. Raciti, and R. Turri, "Dynamic control of inverter-connected generators for intentionally islanded mv distribution networks," in *Power Engineering Conference (UPEC), 2013 48th International Universities'*. IEEE, 2013, pp. 1–6.

[132] D. Wu, F. Tang, J. M. Guerrero, J. C. Vasquez, G. Chen, and L. Sun, "Autonomous active and reactive power distribution strategy in islanded microgrids," in *2014 IEEE Applied Power Electronics Conference and Exposition-APEC 2014*. IEEE, 2014, pp. 2126–2131.

[133] K. Ilango, A. Bhargav, A. Trivikram, P. Kavya, G. Mounika, and M. G. Nair, "Power quality improvement using statcom with renewable energy sources," in *2012 IEEE 5th India International Conference on Power Electronics (IICPE)*. IEEE, 2012, pp. 1–6.

[134] D. E. Olivares, C. A. Cañizares, and M. Kazerani, "A centralized optimal energy management system for microgrids," in *2011 IEEE Power and Energy Society General Meeting*. IEEE, 2011, pp. 1–6.

[135] A. Tuladhar, H. Jin, T. Unger, and K. Mauch, "Control of parallel inverters in distributed ac power systems with consideration of line impedance effect," *IEEE Transactions on Industry Applications*, vol. 36, no. 1, pp. 131–138, 2000.

[136] G. DIgSILENT GmbH Gomaringen, "Digsilent powerfactory-version 15, user's manual," August 2013.

[137] R. Kabiri, D. Holmes, and B. McGrath, "Digsilent modelling of power electronic converters for distributed generation networks," 2013.

[138] G. DIgSILENT GmbH Gomaringen, "Digsilent powerfactory-version 15, user manual-technical reference-battery," August 2013.

[139] M. Chamana and S. B. Bayne, "Modeling, control and power management of inverter interfaced sources in a microgrid," in *2011 IEEE 33rd International Telecommunications Energy Conference (INTELEC)*. IEEE, 2011, pp. 1–7.

[140] G. E. C. of Libya (GECOL).www.gecol.ly, "Alkufra distribution networks."

[141] A. Kalankul, P. Jirapong, P. Saraisuwan, and S. Premrudeepreechacharn, "Development of distributed generation assessment tool considering multi-system constraints for evaluating initial grid connection," in *Utility Exhibition on Power and Energy Systems: Issues & Prospects for Asia (ICUE), 2011 International Conference and*. IEEE, 2011, pp. 1–7.

[142] L. Gao, R. A. Dougal, and S. Liu, "Power enhancement of an actively controlled battery/ultracapacitor hybrid," *IEEE Transactions on Power Electronics*, vol. 20, no. 1, pp. 236–243, 2005.

[143] R. A. Dougal, S. Liu, and R. E. White, "Power and life extension of battery-ultracapacitor hybrids," *IEEE Transactions on components and packaging technologies*, vol. 25, no. 1, pp. 120–131, 2002.

[144] W. Li and G. Joos, "A power electronic interface for a battery supercapacitor hybrid energy storage system for wind applications," in *2008 IEEE Power Electronics Specialists Conference*. IEEE, 2008, pp. 1762–1768.

[145] G. DIgSILENT GmbH Gomaringen, "Digsilent powerfactory-version 15, library-built-in pv models," 2013.

[146] ——, "Digsilent powerfactory-version 15, library-built-in bess models," 2013.